PERFORMANCE EVALUATION OF HIGH STRENGTH ALLOY STEEL CAST CONNECTOR UNDER QUASI-STATIC LOAD

by

Sharad Dangol

A thesis submitted to the faculty of
The University of Utah
in partial fulfillment of the requirements for the degree of

Master of Science

Department of Civil and Environmental Engineering

The University of Utah

May 2013

The University of Utah Graduate School

STATEMENT OF THESIS APPROVAL

The thesis of **Sharad Dangol**

has been approved by the following supervisory committee members:

Luis F. Ibarra	, Chair	**03/07/2013** Date Approved
Chris P. Pantelides	, Member	**03/07/2013** Date Approved
Janice J. Chambers	, Member	**03/07/2013** Date Approved

and by **Chris P. Pantelides** , Interim Chair of the Department of **Civil and Environmental Engineering**

and by Donna M. White, Interim Dean of The Graduate School.

ABSTRACT

High strength alloy steel cast connector refers to a bracing system to be used in **James L. Greene Science Center, Columbia University** in New York. The cast connectors, as the name suggests, are the connection elements in a bracing system that uses stainless steel rods as the braces instead of traditional steel sections.

The bracing system was designed to support lateral wind load. The cast connector material is A148 GR. 115/95 (ASTM A958, 2006). The nominal yield strength is f_y = 95 ksi, whereas the nominal ultimate strength is f_u = 115 ksi. Although the material has very high yield strength, its ductility is rather limited. Hence, limiting the use of the connectors in a quasi-static load like wind load.

This study evaluates cast connector performance under monotonic and cyclic loading. Experimental results are validated by a finite element (FE) model created in ANSYS (Chapter 4).

Initial proposed tests on the cast connector specimens showed linear performance. For loads of 2 and 2.5 times the design load (P = 275 kip), the test specimens exhibited linear behavior. Further tests with increased load were performed on a second specimen (Cast Connector 2) to obtain nonlinear behavior and connector failure modes. The non-linear portion of the curve was not well developed as one would expect for steel, which demonstrated the brittleness of the material.

TABLE OF CONTENTS

LIST OF FIGURES

LIST OF TABLES

ACKNOWLEDGMENTS

I would like to express my sincere gratitude towards my advisor, Assistant Prof. Luis Ibarra for all the mentoring and support he provided through each and every step. Special thanks go to the other members of supervisory committee, Prof. Chris Pantelides and Associate Prof. Janice Chambers.

I am also thankful for all the help provided by Mark Bryant and Wade Stinson during instrumentation of the cast connector subassemblies and to Justin Page for the fabrication of the subassembly. Dr. Scott Adan, principal of Adan Engineering, needs special mention for providing valuable and necessary information necessary to carry out the experimental tests and to complete this thesis.

Fellow graduate students and friends also deserve a vote of thanks. Help and support from Joel Parks, Esra Hasanbas, Birhanu Bishaw and Kalen Wilson are much appreciated. Last but not the least: I owe huge thanks towards my mom, sister and brother.

Any opinions, finding and conclusions or recommendations expressed in this thesis are mine. Comments, constructive criticism and any recommendations are heartily welcomed.

CHAPTER 1

INTRODUCTION

1.1 Background

The cast connector is a part of a new bracing system to be used in the James L. Greene Science Center at Columbia University in New York (NY). The bracing system provides lateral stability to the building under wind load. Each cast connector has to withstand a design load (P) of 275 kip. This bracing system was tested for the first time at full-scale in this experiment.

Each specimen of cast connector (Cast Connector 1 and 2, see Section 1.2) was subjected to monotonic and cyclic tests. The monotonic test followed the procedure for testing notch bracing casting connection assembly of the New York City Building Code (NYCBC, 2012; Section 1714.3.1). The cyclic test included tensile loading and unloading cycles, but no compression loading cycles due to the nature of the bracing system. The connectors performed within the linear interval during the above tests. Hence further tests were performed on Cast Connector 2 (section 1.3).

The results from the experiments are presented in this thesis along with results from Finite Element (FE) analysis. Experimental tests were carried out on two connectors under quasi-static loading. The experimental test results reproduced in FE analysis to

determine the main parameters controlling the performance of cast connectors under quasi-static loading.

1.2 Objectives

The main objective of this study is to evaluate the performance of a novel cast connector under quasi-static tensile loading using experimental tests and numerical simulations. The numerical analyses are used to identify the parameters controlling the cast connector response.

CHAPTER 2

LITERATURE REVIEW

2.1 Introduction

In recent years, the usage of steel castings has increased in frequency of use and variety of applications. Steel castings became increasingly popular, especially in Europe, after they were used in the main stadium at the 1972 Olympics Games in Munich, Germany. However, the use of steel cast components remained limited to special applications. Lack of sufficient research data is one of the main reasons behind the limited applications.

Traditional methods connect multiple members by using complex connection details, a complexity that can be reduced by using cast members or cast connectors. Steel casting connections use members formed by pouring molten metal into a mold, which is then connected to other structural members. This facilitates the fabrication process and enhances the system's aesthetics because the casting can be molded into any geometry. This allows designer flexibility in selecting a bracing system that meets load carrying capacity requirements as well as an attractive aesthetic appearance. Despite these

apparent benefits the development of steel castings as structural elements has not been satisfactory.

Conventional connections tend to include complex details leading to constructability problems, such as misalignment, incorrect drawing interpretation, lack of available information, high fabrication and assemblage costs, among others. Steel castings are capable of overcoming these requirements, but there are no sufficient research studies on the performance of steel casting connectors. Moreover designers, fabricators and erectors are unaware of the benefits of steel casting components.

2.2 Cast Steel vs. Milled Steel

The term "cast steel" refers to steel castings of high strength alloy steel. It is a specialized form of casting that is used when normal (milled) steel cannot deliver enough strength or the required geometry. Cast steel is produced by pouring molten steel mixture into a preformed mold of the required geometry. Whereas, "milled steel" refers to steel that is manufactured by steel mills using traditional methods, and it is available only in fixed forms or shapes.

The use of cast or milled steel has pros and cons. Cast steel can be formed to required dimensions or geometry, and has higher strength than milled steel. However, such high strength cast steel has low ductility compared to milled steel. Also, the structural behavior of cast steel is not very well known. On the other, hand milled steel is a ductile material has been used and studied for a long time now. On the down side, milled steel strength is lower compared to cast steel. Sometimes, strength requirement dictates the complexity joint and size for elements to be used. Heavy joint detailing

required when using such steel can be easily simplified using cast steel connections. Hence, cast steel can be a good alternative to tradition steel design provided proper study has been conducted.

2.3 Factors Governing the Steel Casting Design

Chen et al. (2010) conducted studies of two types of steel cast connectors and concluded that the design and performance of cast steel joints are governed primarily by the geometric configuration, casting process and joint structural behavior. Usually, the cast steel connectors have higher strength than the members they connect. They found that in some cases, aesthetic and casting process control the design rather than the functional requirement of steel casting joint.

Chen et al. found that stresses in the steel casting are usually lower than those predicted by analytical formulations. This discrepancy pointed out, that the exact prediction of stress distribution and stress flow routine in the cast steel joint is very difficult using simple computations.

Monroe and Poweleit (2003) performed cast steel connector tests, concluding that although the functional requirements are the primary factors governing the connector design, geometric complexities and the casting process play a vital role. They also found that the connected members usually fail before the steel cast connectors, as expected from the applied design philosophy.

Their study also provided insights on the effect of strength, ductility, weldability of materials used for the casting on the overall connectors' performance. Increasing the

strength of steel normally reduces its ductility, toughness and weldability. Hence, it is often desirable to use lower strength grade steel and increase the section size.

Bjorhovde (2010) pointed that limited deformation capacity of high strength steel could be problematic, in part because knowledge data base are very limited. Response characteristics of high strength steel are still not fully known. This presents challenges as well as opportunities to engineers and designers to investigate more into application of such materials.

2.4 Use of Cast Connectors in Bracing System

Steel castings are broadly used in industrial equipments as connectors or component parts. Steel casting applications in structures have been limited to compression members, although recently their use is gaining popularity in other areas as well. Their use in the main stadium at 1972 Olympic Games in Munich increased their popularity. Cast connectors are used commonly in bridge applications to replace complicated welded connections. In buildings, castings have mostly been used for architecturally exposed connections, particularly bracing connections.

Casting connectors are used in many large-span spatial structures and high-rise buildings (e.g., the "Bird's Nest" stadium for Beijing Olympics) because they can be fabricated in a large variety of geometrical shapes and with high strength steel.

Bracing systems are mostly designed to take tensile load. According to Bjorhovde (2010), high strength materials give major advantage in tension members and connection applications. Full advantage of higher strength of materials could be taken because

slenderness, local or overall buckling and rotation capacity are rarely considered for tension members.

Monroe and Poweleit (2003) mentioned that, "steel castings are expensive sources of steel but cheap suppliers of geometry" to indicate that high steel casting costs can be easily compensated by savings achieved by fabricating and assembling less parts, and optimization of material and system geometry.

Engineers and designers are currently working to establish pre-engineered connection design and fabrication for hollow structural section connections. Studies are focused on using cast connectors to modify standard fabrication practices for seismic-resistant and aesthetic pin connections for hollow structural section. Oliveira et al. (2008) evaluated the seismic performance of a proprietary cast connector design. They identified cases where the use of mass produced cast steel components could provide significant advantages over standard fabrication practices. Their study focuses on development of seismic-resistant and aesthetic pin connections for hollow structural sections using standardized cast steel connectors developed at the University of Toronto.

The cast connectors evaluated in this study are part of a bracing system designed to withstand tensile stress caused by lateral wind loads. The steel castings connect solid stainless steel rods as braces, unlike other system used for connecting HSS bracing. This is rather new concept compared to traditional bracing systems.

2.5. Analysis Techniques for Cast Connectors' Structural Performance

The flexibility to fabricate castings of complex geometry presents engineers and designers with a tough task of analyzing their performance. In general structural design, the connection behavior can be computed using standard equations for joint capacity.

Numerical, analytical and/or experimental techniques are necessary to predict the behavior cast connectors with complicated geometry. However, information on structural design methods of cast connectors is sparse. Most of the available data refers to the mechanical properties of weldable steel castings (Herrion et al. 2007). The studies on the developments and applications of casting connections are limited and focused on the mechanical properties of casting, casting design, and quality control, rather than the structural design (Poweleit 2006 and Puthli 2008).

Unlike other steel components, steel casting manufacturing processes involved are not standardized. The casting process, including pouring into cast, cooling and heat treatment, may vary widely for different cases. This variation in casting processes affects the casting behavior. For these reasons standard methods for cast connector design are not available, and experimental tests and FE analyses are needed to validate new connector designs

Experimental tests can provide insights into strain distributions and failure modes, but there are limitations on the number of tests that can be performed, as well as in measuring techniques. In addition, for full scale specimens, it is usually difficult to obtain plastic deformations, or reach final failure due to loading capacity limitations. To overcome these limitations, FE analyses are performed to complement experimental tests.

CHAPTER 3

TEST SETUP AND DESCRIPTION OF CAST CONNECTORS

3.1 Cast Connector Description

The two cast connector specimens tested in this study are the two-halves of a single connector. The steel casting connections are welded to the column. To facilitate the testing of the connector, the tested specimens were cast as two separate halves. Figure 3.1 shows the tested two cast connectors. Both connectors have two circular legs 2.25 in. in diameter, coming out from 2 in. thick base. The orientation of the two legs and the geometry of the two connectors vary as shown in Figure 3.1.

A subassembly was fabricated to support the tension loads applied to the cast connector. Figure 3.2 shows the test assembly elevation used for fabrication. Figure 3.3 presents the subassembly for Cast Connector 2, as installed in the tower frame at the structural laboratory of the University of Utah. This tower frame has a 2000 kip-actuator, and it is capable of withstanding more than two times the factored design loads applied to the cast connectors.

The components and joints of the subassembly and top assembly plate (Figures 3.2 and 3.3) were analyzed using SAP 2000 (CSI, 2009). The structural components'

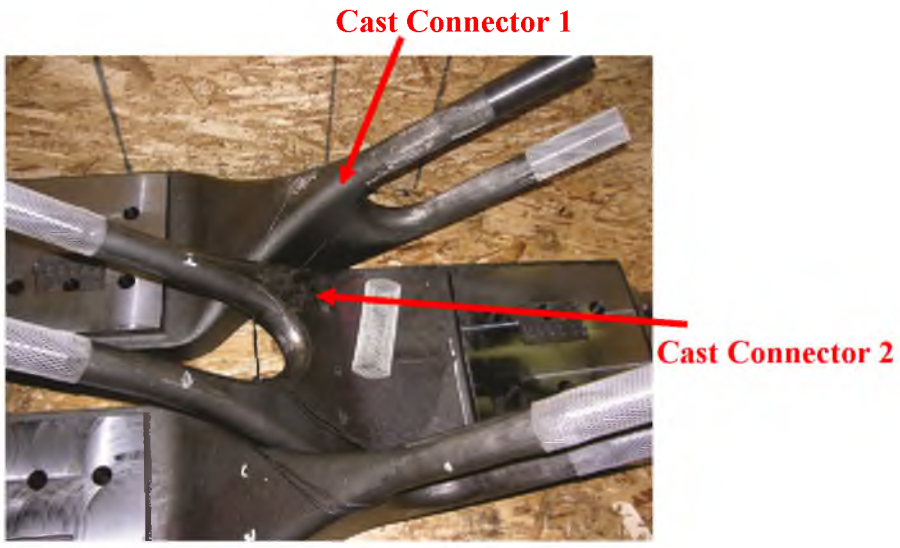

Fig 3.1: Steel Cast Connectors Used in the Experimental Tests

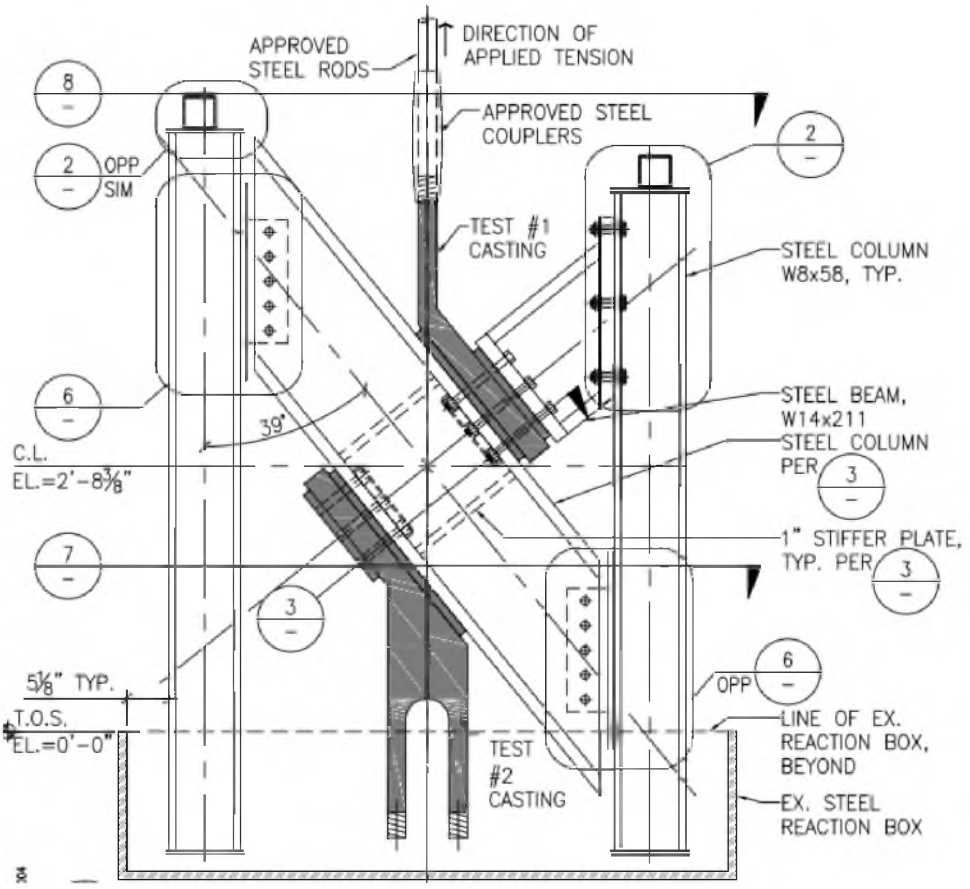

Fig 3.2: Test Assembly Elevation
(Reprinted with permission from Adan Engineering, LLC, 2012)

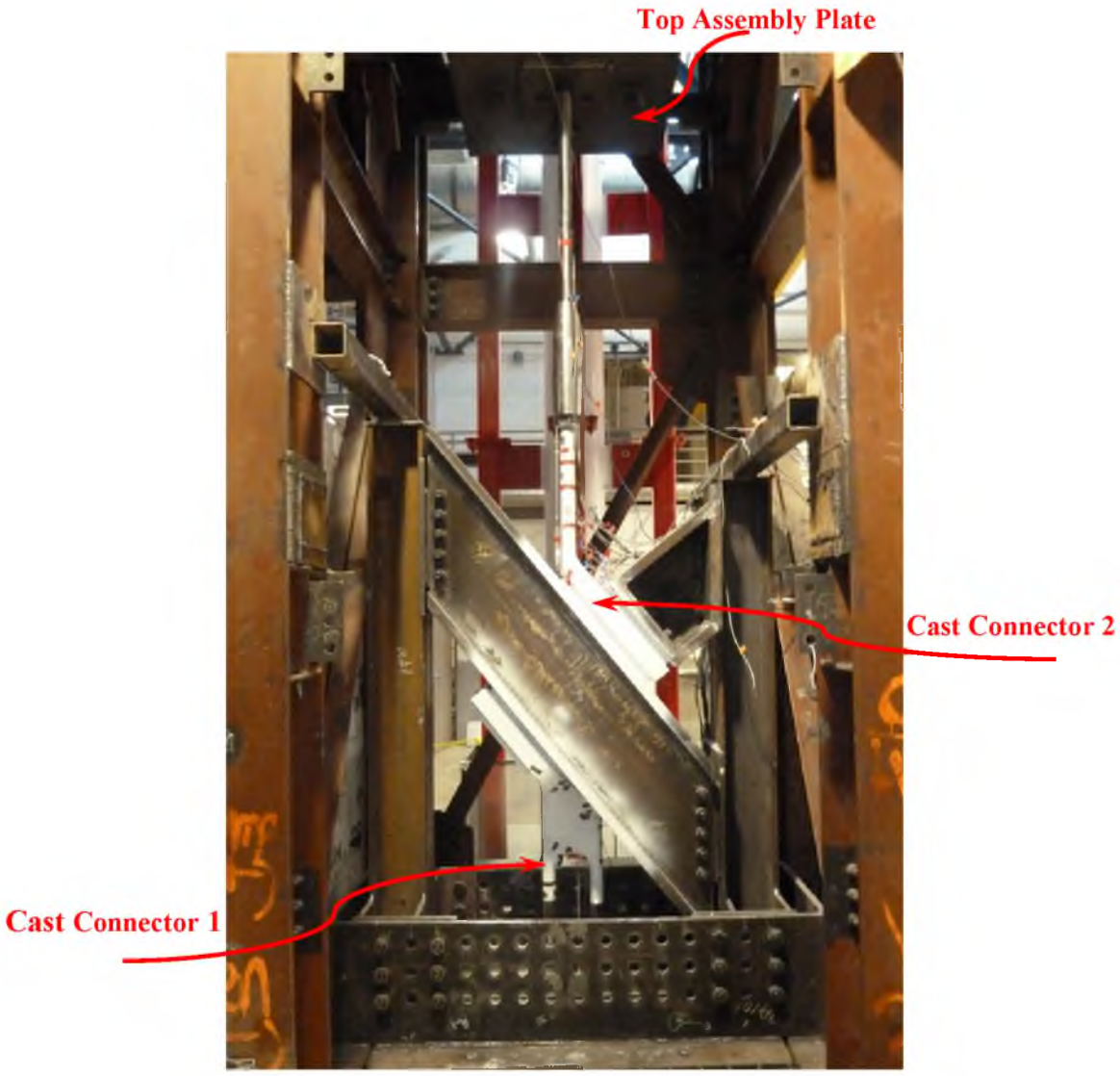

Fig 3.3: Subassembly for Cast Connector for Experimental Tests

strength capacity and deflection limits were evaluated for a maximum load of 2.5P = 688 kips (Appendix A).

3.2 Description of Test Performed

ASTM A 370-05, Standard Test Methods and Definitions for Mechanical Testing of Steel Products, describes several tests applicable to wrought and cast steels, stainless steels and related alloys. These tests include tension test, bend test, hardness test, and charpy impact testing.

Tension test is related to the mechanical testing of steel products subjected to a measured load sufficient to cause rupture. Main properties sought are yield point, yield strength, tensile strength, elongation and reduction of area.

Generally the loading of the test specimen is done by two loading systems, mechanical (screw power) and hydraulic. The essential requirement is that the load should be transmitted axially. Any convenient speed of testing may be used up to 0.5 yield point or yield strength. If the machine is equipped with a device to indicate rate of loading, the rate of loading from 0.5 yield point or yield strength through the yield point or strength should not exceed 100,000 psi/min. However the minimum rate of stressing shall not be less than 10,000 psi/min.

3.2.1 Force vs. Displacement Controlled Loading

The tension test can be categorized as per the method of loading to control speed of testing. The speed of testing is important because mechanical properties are a function of strain rate (Davis, 2004). Generally, a slow speed test results in lower strength values

and larger ductility than a fast speed test. A test's speed can be determined by one of the following methods:

a) Strain (displacement) rate

b) Stress (load) rate

c) Cross-head separation rate during the test

d) Elapsed time

These methods are listed in order of decreasing precision. The most common methods of testing are strain (displacement) rate and stress (load) rate. **Strain (displacement) rate** is expressed as the change in strain per unit time. As strain is a dimensionless value, it is expressed as a ratio of change in length per unit length. Generally, a strain rate between 10^{-5} and 10^{-1} is preferable for quasi-static tensile tests. **Stress (load) rate** is expressed as the change in stress per unit of time. This is usually determined by defining the load rate. ASTM A 370-05 "Standard Test Methods and Definitions for Mechanical Testing of Steel Products," requires that stress rate not exceed 100 ksi/min. This number corresponds to an elastic strain rate of about 5×10^{-5} s^{-1} for steel.

It is important to compare displacement (strain) controlled and load (stress) controlled loading. For elastic behavior, the stain and stress methods are identical. Once the elastic limit is exceeded, the strain rate increases when a constant stress rate is applied. Alternatively, the stress rate decreases when a constant strain rate is specified.

Experimental tests performed for this study employed stress controlled or load controlled loading. This method was chosen as New York City Building Code (NYCBC) recommends load based tension tests for such connectors. It was also difficult to control

the strain or displacement rate of the test setup, which included several components that could displace. Load controlled loading is usually not preferable for testing beyond elastic limit, however, the strain rate for any given load rate was found to be within the recommended values for load controlled tests (Appendix B). Moreover, the load rate was reduced for large load levels.

3.2.2 Test Procedures

3.2.2.1 Monotonic Test

The monotonic test followed the procedure for testing notch bracing casting connection assembly is based on the New York City Building Code (NYCBC, 2012), Section 1714.3.1. The test tensile load for the monotonic test is 2 times the superimposed design load of 275 kips (i.e., 550 kips). The cast connectors were loaded according to the following stages:

Stage 1. 0% of the load on the assembly, deflection gage readings set to read 0.000"

Stage 2. 25% of the test load on the assembly, deflection gage readings recorded.

Stage 3. 50% of the test load on the assembly, deflection gage readings recorded.

Stage 4. 75% of the test load on the assembly, deflection gage readings recorded.

Stage 5. 100% of the test load on the assembly, deflection gage readings recorded.

Stage 6. 100% of the test load on the assembly shall be left for 24 hours, deflection gage readings recorded.

Stage 7. 0% of the test load on the assembly, deflection gage readings recorded.

NYCBC also recommends the passing criteria for monotonic test under quasi-static tensile loading. The passing criteria given in the NYCBC states that, the test

assembly has to recover more than 75% of the maximum deflection within 24 hours after removal of the test load.

3.2.2.2 Cyclic Test

After visual inspection of the specimen, the cast connectors were reloaded and subjected to a superimposed load of 2.5 times the design load. Because of the nature of the braced system, the loading protocol for cyclic tests only included reloading and unloading cycles in tension.

3.2.2.3 Additional Tests

Five additional tests were performed in Cast Connector 2 after the completion of proposed monotonic and cyclic tests which showed the linear behavior of the connectors. These tests were done as attempts to obtain nonlinear behavior or failure. The load was applied in quasi-static manner in all the additional tests.

The last two additional tests were performed by loading only one leg of the Cast Connector 2. Each test was performed on a different leg. The load was applied only on one leg because of failure of the nut connecting the rod to the top assembly plate, after the third test. Testing only one leg had another benefit. The load applied could be reduced by half of the load that should have been applied if both legs were loaded. This meant that the subassembly and its connections were prevented from reaching failure (Section 3.6).

3.3 Material Characteristics

Material used for casting of the cast connectors is A148 GR. 115/95 (ASTM A958, 2006). The nominal yield strength is f_y = 95 ksi, whereas the nominal ultimate strength is f_u = 115 ksi. However, tests on two different heats used in the fabrication of the cast connectors showed that the material mechanical properties-exhibit overstrength (Appendix C). The yield strength obtained for the two heats was f_y = 115.8 and 121.8 ksi, and the ultimate strength was f_u = 130.8 and 137.3 ksi. Therefore, the yield and ultimate strength are on average 25 and 17% larger than the nominal specification, respectively. The rest of the mechanical properties of the material used in the cast connectors are presented in Appendix C.

Figure 3.4 shows the stress-strain for the material compared to that for typical ASTM Gr. 60 mild steel and ASTM Gr. 75 (Gr. 520) steel (used for stainless steel rods). As observed, the casting material is a lot less ductile compared to typical mild steel and stainless steel used for rods. The curve for the stainless steel material is as recorded in lab and does not extend up to failure unlike the other three curves shown in the figure.

3.4 Experimental Results for Tests Performed on Cast Connector 1

Cast connector 1 was first tested under monotonic load. After reaching the maximum load of 550 kip (2P), the specimen was loaded at the maximum load for 24 hours. Then the specimen was tested under cyclic load. The cast connector deformations were recorded with 12 strain gages (SG # 6 was out of order) and 5 LVDTs (Figures 3.5 and 3.6). See Appendix D for LVDTs and strain gage characteristics.

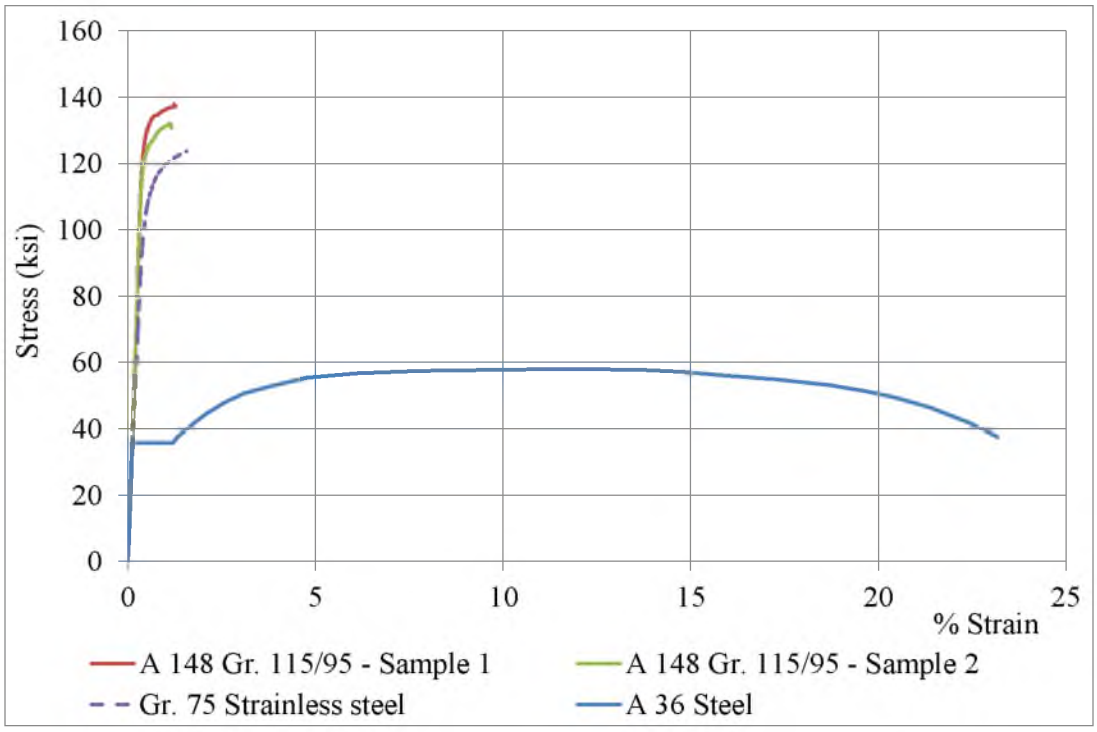

Fig 3.4: Stress-Strain Curves for Different Steel Materials

Fig 3.5: LVDTs and Strain Gages Location on Cast Connector 1 (View I)

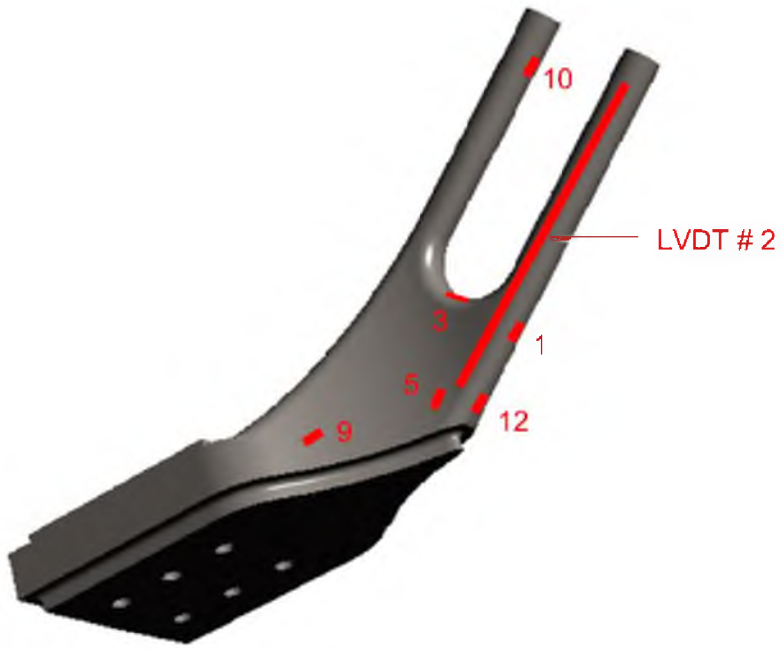

Fig 3.6: LVDTs and Strain Gages Location on Cast Connector 1 (View II)

3.4.1 Monotonic Test: Maximum Applied Load 2P = 550 kips (CC1-T1)

The load protocol for the monotonic test was divided into four stages based on the fraction of total load (2P) applied at the end of each stage (see Section III). The load rate was 5 kips/min for Stage 2 (0.25 × 2P), 4 kips/min for Stages 3 (0.5 × 2P) and 4 (0.75 × 2P), and 3 kips/min for Stage 5 (2P). There were 10-minute pauses between different stages.

Table 3.1 provides cast connector's vertical deformations recorded by the five LVDTs installed in the subassembly. Deformations and strains are presented at the stages specified by Section 1714.3.1 of NYCBC, 2012. LVDTs # 2 and 3 measure the deformation at each side of one of the cast connector legs. Also, a comparison of

Table 3.1: LVDT Deflection Reading for CC1-T1. Maximum Load = 2.0 P = 550 kips.

				On Cast Connector Leg			
Stage	Load (% 2P)	Load (kips)	LVDT # 1 (in.)	LVDT # 2 (in.)	LVDT # 3 (in.)	LVDT # 4 (in.)	LVDT # 5 (in.)
1	0%	0.0	0.00000	0.00000	0.00000	0.00000	0.00000
2	25%	137.5	0.01989	0.00615	0.00640	-0.01137	0.01712
3	50%	275.0	0.03598	0.01083	0.01152	-0.02135	0.03318
4	75%	412.5	0.05624	0.01812	0.01839	-0.04454	0.06537
5	100%	550.0	0.06979	0.02254	0.02300	-0.07097	0.11741
6	100%*	550.0	0.07104	0.02250	0.02336	-0.07097	0.11936
7	0%	0.0	0.00659	-0.00004	-0.00150	-0.02901	0.05171
* The second reading at 100% was taken 24 hours after the maximum load was reached.							

deformations when the maximum load is reached (Stage 5) and after 24 hours of sustained load (Stage 6) indicates that the cast connector material did not exhibit creep effects. Also, the residual deformation after the load was withdrawn (Stage 7) is practically null. This indicates that the cast connector did not experience plastic deformations, and performed in the elastic interval. This behavior easily meets the passing criterion for the monotonic test, which requires the assembly to recover more than 75% of the maximum deflection within 24 hours after removal of the test load.

The rest of LVDTs were installed to track the subassembly components' performance. LVDT # 1 recorded the relative displacement of top assembly plate with respect to the actuator plate. The residual deformation in LVDT # 1, though small, was caused by the rearrangement of the bolts and nuts connecting the top assembly plate and the actuator plate. LVDT # 4 recorded the lateral displacement of the subassembly with respect to the tower frame. The readings from LVDT # 4 were constantly monitored to prevent contact of the subassembly with the brace of the tower frame. These

deformations were caused by stiffness asymmetry of the subassembly frame that caused a slight lateral deformation to the right hand side of the test (Figure 3.4).

LVDT # 5 measured the vertical deflection from the subassembly with respect to the steel floor (Figure 3.3).The residual deformation of LVDT # 5 was mainly caused by slip of the frame at the connection of steel reaction box and the subassembly (see "Slip of Column – Steel Box Connection", Section 3.4.2.1).

Tables 3.2 and 3.3 present the strain gage readings at the fork and legs of the cast connector, and the lower half of the connector, respectively. In addition, Figure 3.7 presents the maximum strains recorded at each strain gage. The results show that strains at the lower half of the connector are significantly lower than those recorded at the legs and fork of the specimen. Strain gages 1, 2, 10 and 11 exhibited the largest tensile strain, whereas strain gage 3 showed maximum compressive strain. Strain gage 3 recorded large compressive strains at the saddle, but these strains rapidly decrease, as can be seen on the reading for strain gage 13, which is located right below strain gage 3.

The strain gage readings in Tables 3.2 and 3.3 confirm that the cast connector was capable of sustaining 2 times the superimposed design loads for a period of 24 hours, without exhibiting creep effects (compare strains at Stages 5 and 6). Stage 7 in Tables 3.2 and 3.3 show strain readings close to zero after the specimen was unloaded, indicating that creep effects and permanent plastic deformations did not occur. Therefore, the NYCBC (2012, Section 1714.3.1) criterion is satisfied.

Table 3.2: Strain Gage Reading (μ strain) for CC1-T1 (Fork and Leg Locations). Maximum Load = 2.0 P = 550 kips.

			End of Legs		Fork Section		Saddle	
Stage	Load (% 2P)	Load (kips)	SG # 10 μ strain	SG # 11 μ strain	SG # 1 μ strain	SG # 2 μ strain	SG # 3 μ strain	SG # 13 μ strain
1	0%	0.0	0	0	0	0	0	0
2	25%	137.5	735	585	836	580	-566	-156
3	50%	275.0	1362	1114	1373	1098	-993	-267
4	75%	412.5	2281	1806	2137	1800	-1578	-426
5	100%	550.0	2913	2192	2652	2217	-1951	-528
6	100%*	550.0	2937	2204	2576	2229	-1951	-521
7	0%	0.0	172	-200	-90	-44	49	18
* The second reading at 100% was taken 24 hours after the maximum load was reached								

Table 3.3: Strain Gage Reading (μ strain) for CC1-T1 (Base Locations). Maximum Load = 2.0 P = 550 kips.

Stage	Load (% 2P)	Load (kips)	SG # 4 μ strain	SG # 5 μ strain	SG # 6 † μ strain	SG # 7 μ strain	SG # 8 μ strain	SG # 9 μ strain	SG # 12 μ strain
1	0%	137.5	0	0	-	0	0	0	0
2	25%	137.5	113	130	-	20	26	86	200
3	50%	275.0	190	214	-	50	47	147	329
4	75%	412.5	298	327	-	99	79	231	502
5	100%	550.0	373	401	-	130	100	285	615
6	100%*	550.0	383	409	-	133	102	267	622
7	0%	0.0	3	3	-	23	7	-36	-11
* The second reading at 100% was taken 24 hours after the maximum load was reached.									
† The reading of SG # 6 could not be retrieved because of faulty wire.									

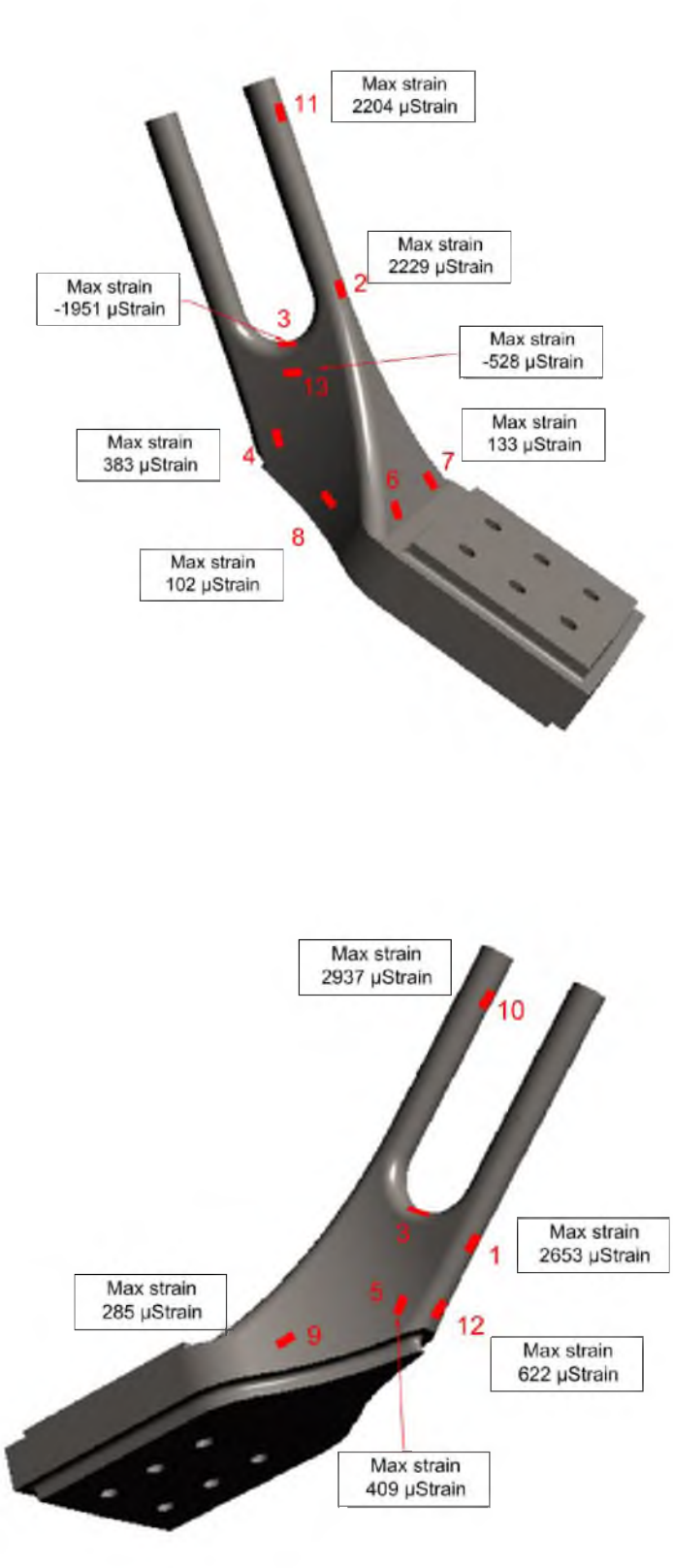

Fig 3.7: Maximum Strains for Monotonic Test of Cast Connector 1

3.4.1.1 Stress-Strain Behavior under Monotonic Loading

The stress-strain curves for all the cast connector strain gages were linear under a maximum monotonic load 2P = 550 kip, even after 24 hours of sustained loading. Figure 3.8 shows the strain versus time curves for the specimen at representative strain gages 10, 11 and 7. The curves showed that the increase in strain was linear, as it should be expected for linear materials subjected to a constant load application increase. The plots also show that the load was sustained during 24 hours without significant changes in the strain level.

The stress levels reached at the locations of SGs # 10, 11, and 7 are shown on the stress-strain curves of Figure 3.9, which were obtained based on an elastic modulus of elasticity E = 29 × 10^6 psi. The maximum computed stress for this test (SG # 10) is approximately 89.2 ksi, which is smaller than the nominal yield stress f_y = 95 ksi, and the average recorded stress from the heat tests (f_y = 118.8, Appendix C).

3.4.2 Cyclic Test: Maximum Applied Load 2.5P = 688 kips (CC1-T2)

Six cycles were performed for the cyclic test based on a maximum load equivalent to 2.5P = 688 kips (Figure 3.10). The protocol is adapted from the study performed by Krawinkler et al. (2001). The load rates were 30 kips/min for the first four cycles, 20 kips/min for the fifth cycle, and 10 kips/min for the sixth cycle.

Tables 3.4, 3.5 and 3.6 show LVDT deformations and strain gage readings of the cast connector under the last cycle of the loading protocol. The stages presented in these tables correspond to the load levels recorded during the monotonic test, but the load percentage changes because it is based on 2.5P. The NYCBC (Section 1714.3.1) criterion

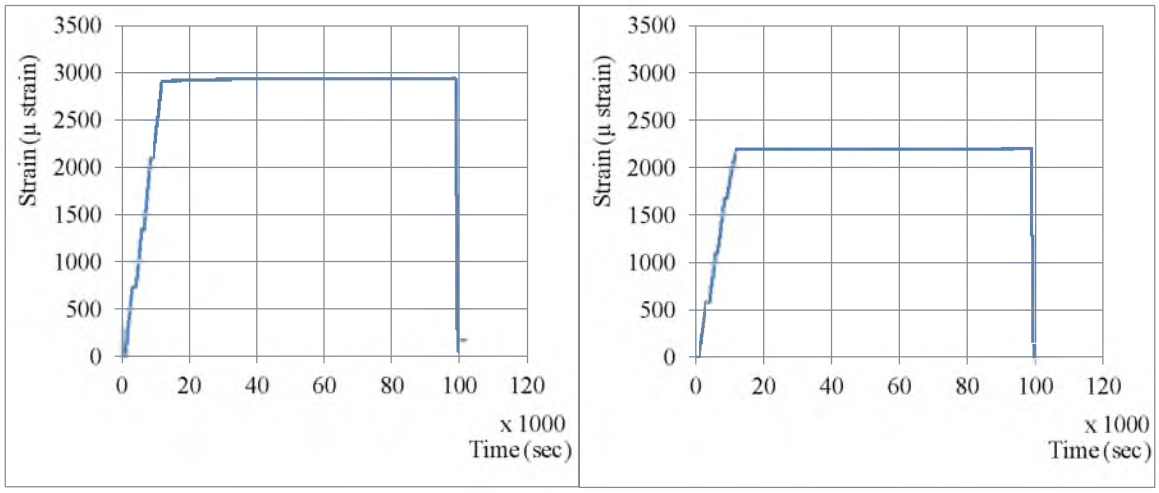

(a) (b)

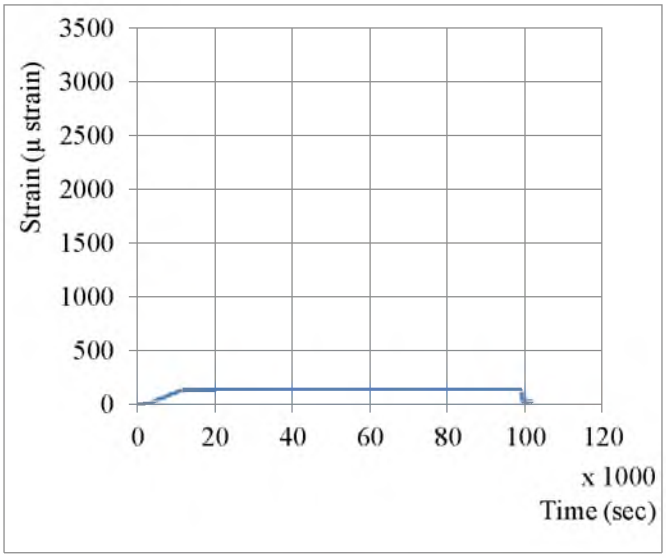

(c)

Fig 3.8: Strain Variation with Time: (a) SG # 10; (b) SG #11; (c) SG # 7

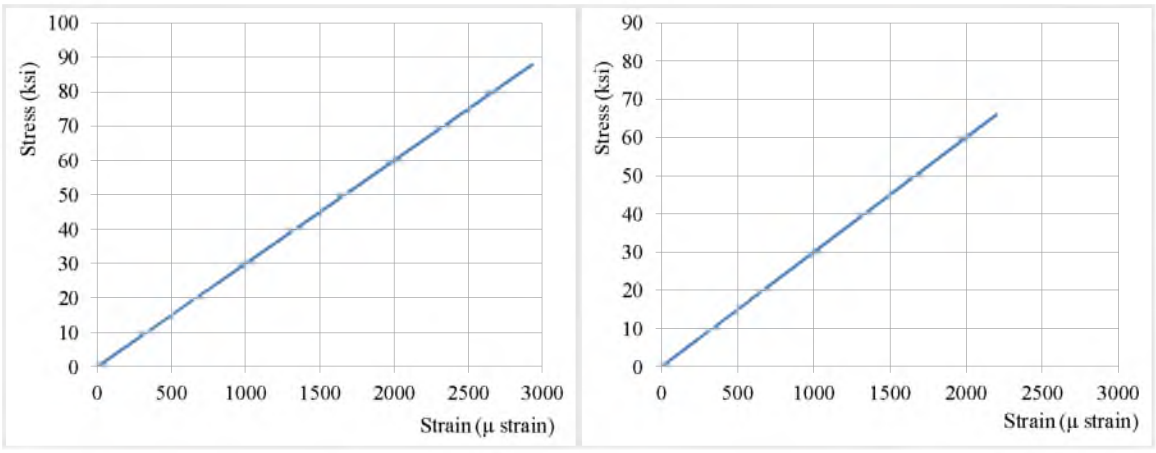

(a) (b)

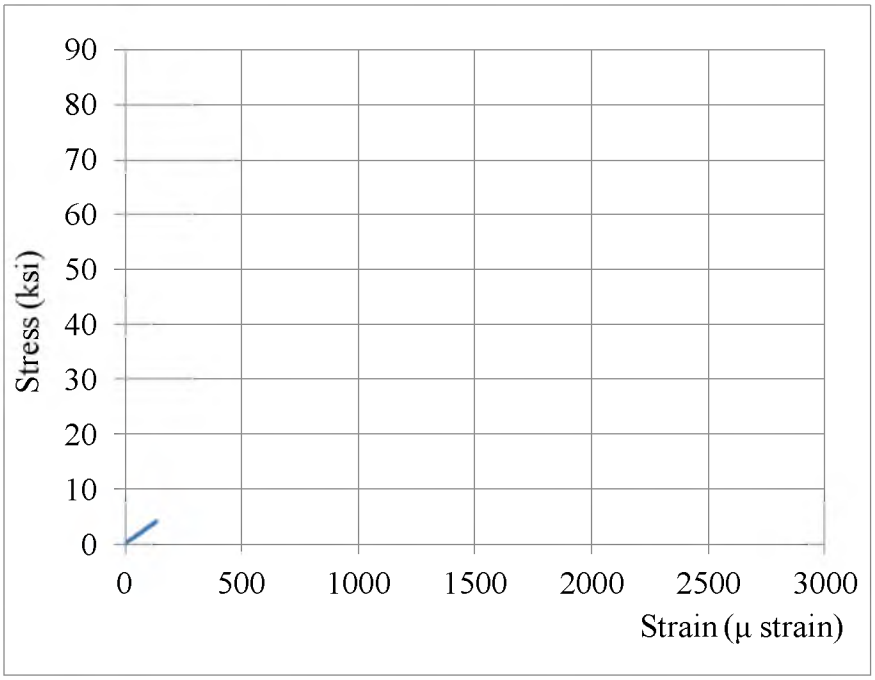

(c)

Fig 3.9: Stress-Strain Curves (Monotonic test): (a) SG # 10; (b) SG # 11; (c) SG # 7

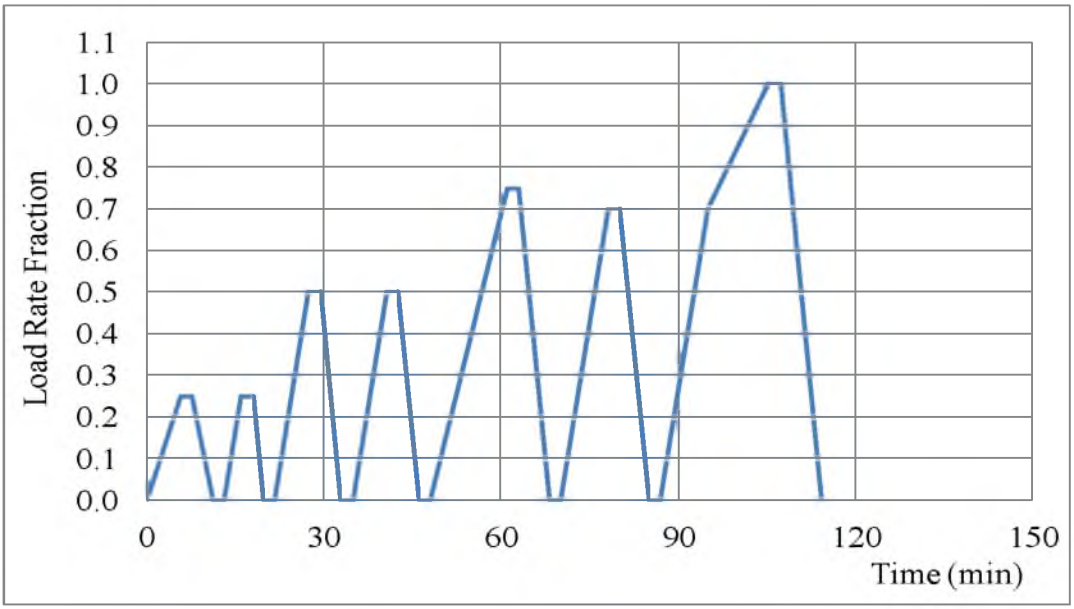

Fig 3.10: Cyclic Loading Protocol for Cast Connector 1

Table 3.4: LVDT Deflection Reading for Last Cycle of CC1-T2
Maximum Load = 2.5 P = 688 kips.

			On Cast Connector Leg			
Load (% 2.5P)	Load (kips)	LVDT # 1 (in.)	LVDT # 2 (in.)	LVDT # 3 (in.)	LVDT # 4 (in.)	LVDT # 5 (in.)
0%	0.0	0.00000	-	0.00000	0.00000	0.00000
20%	137.5	0.02169	-	0.00841	-0.01053	0.01886
40%	275.0	0.03801	-	0.01411	-0.02024	0.03524
60%	412.5	0.05274	-	0.02007	-0.03077	0.05233
80%	550.0	0.06739	-	0.02574	-0.04269	0.07159
100%	688.0	0.08408	-	0.03005	-0.11366	0.32184
0%	0.0	0.00107	-	-0.00285	-0.05627	0.22277
* LVDT # 2 was removed to prevent any damages in case of failure.						

Table 3.5: Strain Gage Reading (μ strain) for Last Cycle of CC1-T2 (Gages at Fork and Legs). Maximum Load = 2.5 P = 688 kips

		End of Legs		Fork Section		Saddle	
Load (% 2.5P)	Load (kips)	SG # 10 μ strain	SG # 11 μ strain	SG # 1 μ strain	SG # 2 μ strain	SG # 3 μ strain	SG # 13 μ strain
0%	0.0	0	0	0	0	0	0
20%	137.5	630	726	831	615	-591	-163
40%	275.0	1350	1319	1468	1193	-1082	-295
60%	412.5	2088	1903	2086	1769	-1564	-424
80%	550.0	2834	2484	2698	2343	-2040	-551
100%	688.0	3794	3102	3367	2958	-2494	-671
0%	0.0	222	23	-70	38	54	11

Table 3.6: Strain Gage Reading (μ strain) for Last Cycle of CC1-T2 Maximum Load = 2.5 P = 688 kips

Load (% 2.5P)	Load (kips)	SG # 4 μ strain	SG # 5 μ strain	SG # 6 μ strain	SG # 7 μ strain	SG # 8 μ strain	SG # 9 μ strain	SG # 12 μ strain
0%	0.0	0	0	-	0	0	0	0
20%	137.5	127	130	-	15	27	91	207
40%	275.0	213	226	-	47	50	163	356
60%	412.5	301	321	-	81	73	233	502
80%	550.0	388	414	-	116	97	304	646
100%	688.0	460	485	-	170	120	361	759
0%	0.0	-29	-27	-	25	0	-26	-42

is satisfied because the specimen was able to support a load equivalent to 2.5 times the superimposed load. The cast connector material exhibited linear performance under the maximum applied loads. Also, the strains and deformations on the cast connector after unloading the specimen were close to zero, indicating material linear behavior under the applied loading protocol. A visual inspection of the component after the test did not reveal cracks or permanent deformation of the cast connector. The test showed that the specimen can support several large loading cycles, but cumulative damage due to several

excursions into the nonlinear interval was not recorded because the yield stress of the cast connector material was larger than expected (see Section 3.3.).

Figure 3.11 and 3.12 show the maximum strain at each of the strain gage locations for cyclic test. It is evident that strains are concentrated around the fork sections and the legs of the connector. Strains around the base are an order of magnitude lower.

Figure 3.13 presents load-deformation/strain relationships, indicating a linear relationship. The sudden strain variations on this curve are caused by slip of the overall frame, as explained in Section 3.4.2.1.

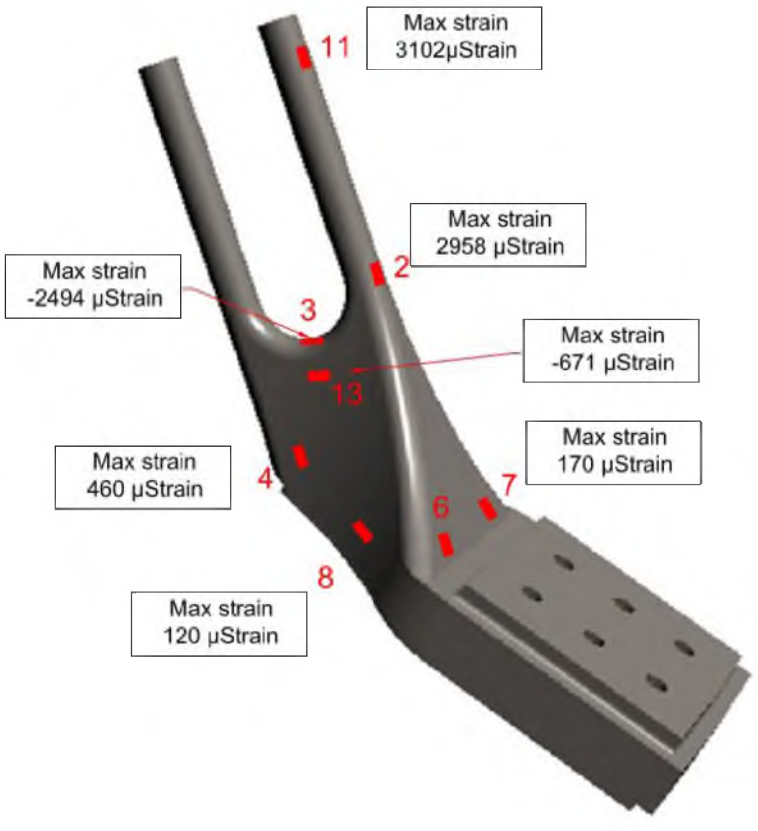

Fig 3.11: Maximum Strain for Cyclic Test of Cast Connector 1 (View I)

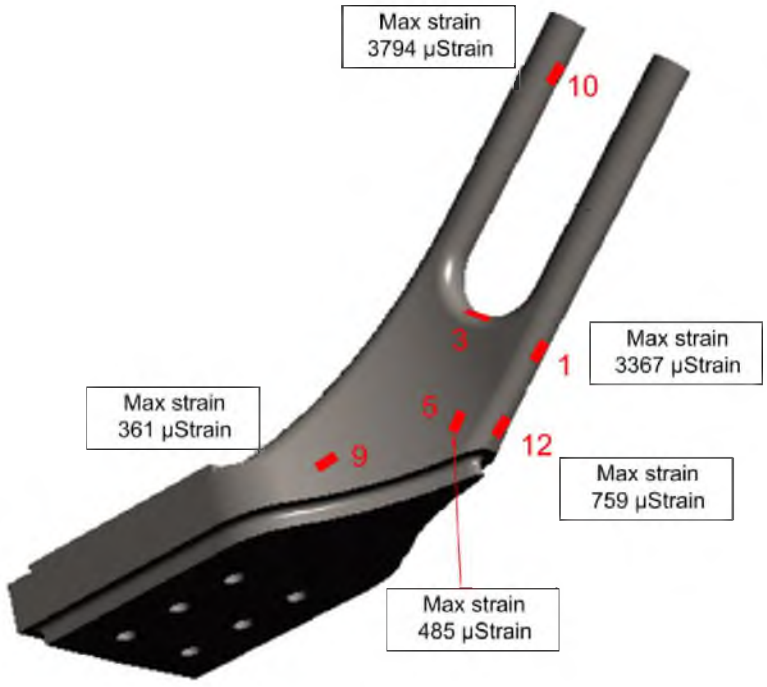

Fig 3.12: Maximum strain for cyclic test of Cast Connector 1 (View II)

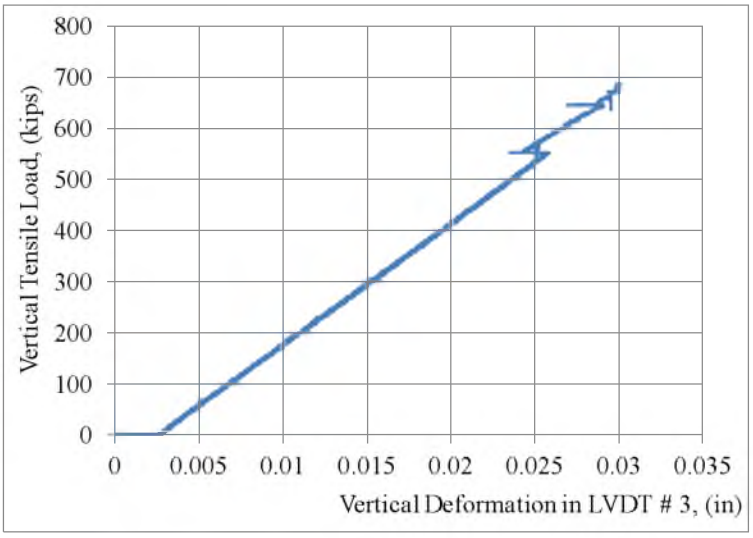

Fig 3.13: Deformation and Strains for Cast Connector 1 under Final Cycle.
Deformation at LVDT # 3

3.4.2.1 Slip of Column – Steel Box Connection

As observed in Figure 3.13, the load vs. vertical deflection curve for LVDT # 3 is linear but at a load of about 552 kips there is strain reversal, followed by a linear reloading path, and a couple of minor strain reversals. After each reversal the curve still follows a linear path with the same slope as that of original curve. This behavior was caused by slip of the subassembly column – steel reaction box connection (see Figure 3.4). Pretensioned bolts were used to connect the subassembly with the reaction box. Once the load exceeded the pretension capacity the entire subassembly slipped, but it did not affect the performance of the cast connector, which only experienced a sudden small loss of strain.

The slip effect can also be observed in Figure 3.14, which shows the strain increase at each time step for strain gage 1 with respect to time. As can be seen, the first jump in strain takes place at around 9300 seconds when the load reached 552 kips in the last cycle. That first jump is followed by few more jumps, which coincide with the curve irregularities of Figure 3.13.

3.4.2.2 Stress-Strain Behavior under Cyclic Loading

The strain variation with time under cyclic loading showed a linear relationship up to the maximum load 2.5P = 688 kips (Figure 3.15). The nominal yield stress of the material is f_y = 95 ksi, but North Star Casteel report (Appendix C) indicated that the yield overstrength is approximately 25%. The stress level at strain gage 10 was about 113.8 ksi (Figure 3.16), which is less than average f_y = 118.8 ksi. Hence, the connector material was in the linear interval.

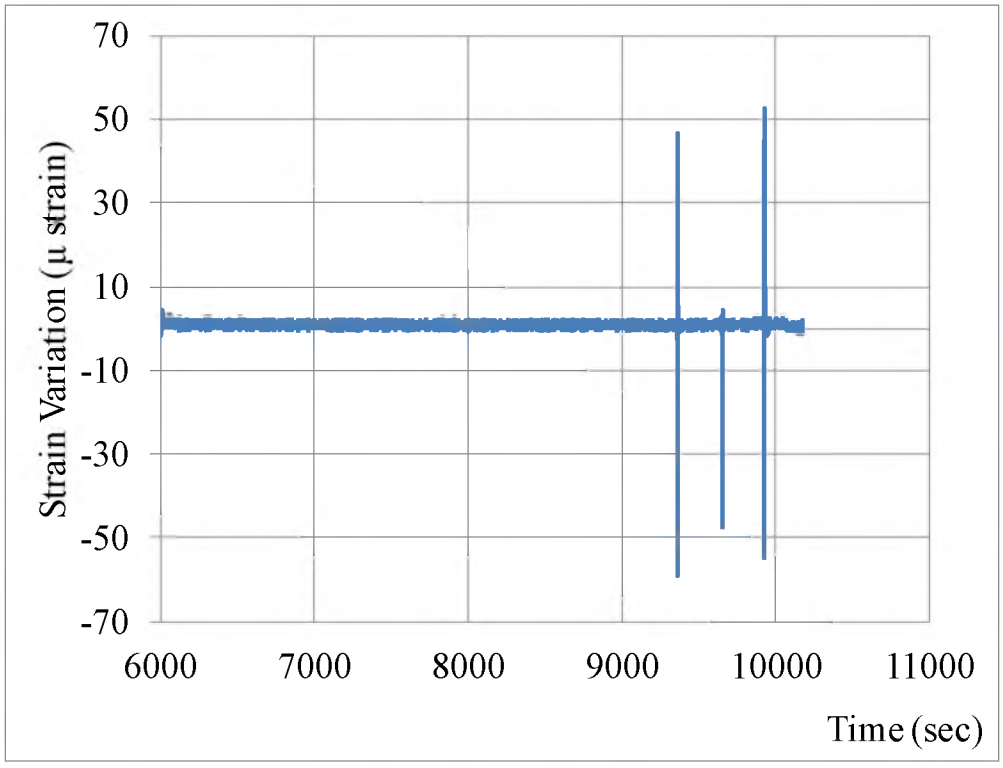

Fig 3.14: Differential Strain at Strain Gage # 1

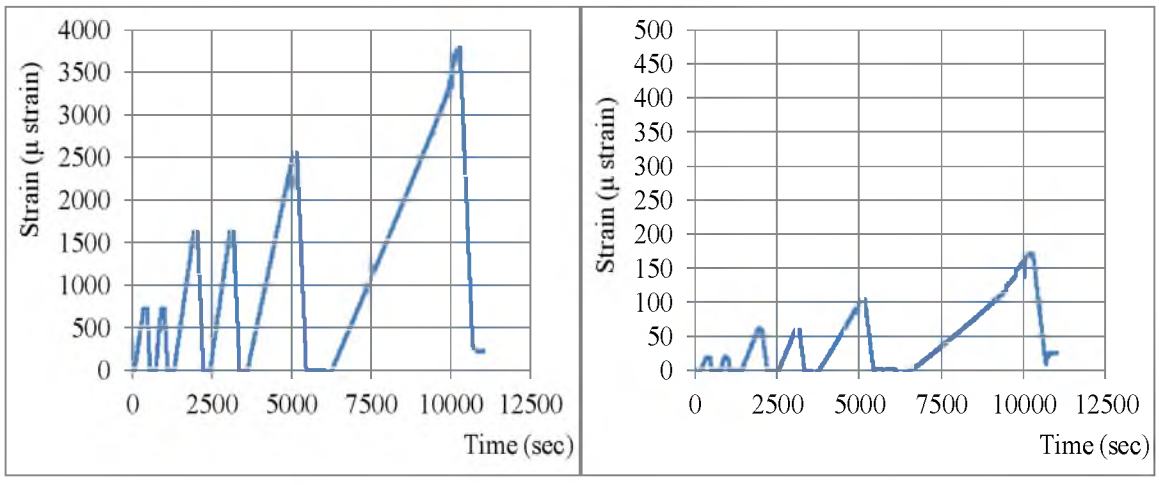

(a) (b)

Fig 3.15: Strain vs. Time Curves: (a) SG # 10; (b) SG # 7

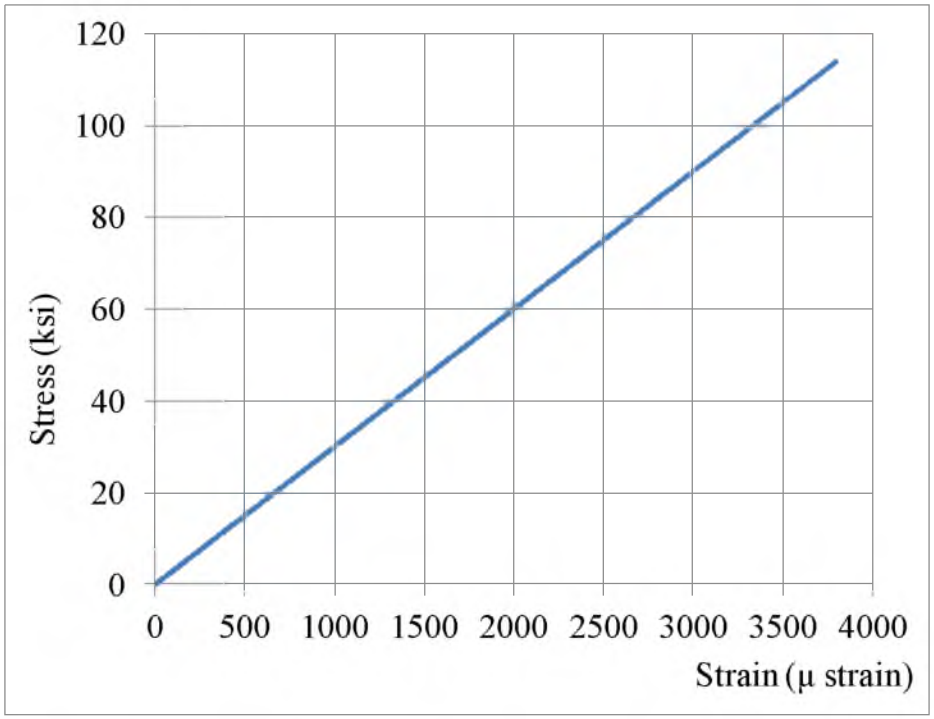

Fig 3.16: Cyclic Test Stress-Strain Curves for Strain Gage 10

3.5 Experimental Results for Cast Connector 2

The tests for Cast Connector 2 are similar to those for Cast Connector 1. Cast Connector 2 was also tested under monotonic and cyclic load, but the load was increased 3%. Therefore, the maximum load for the monotonic test was 1.03 (2P) = 567 kips, and for the cyclic load was 1.03 (2.5P) = 709 kips.

The location of strain gages and LVDTs for Cast Connector 2 tests is presented in Figure 3.17. For the monotonic load test, two LVDTs and fifteen strain gages were installed in the cast connector. For the cyclic load test, LVDT # 2 was removed to prevent damage to the equipment in case of failure, but strain gages were added to one of the connector legs (strain gages 16, 17, and 18), and to one of the rods (strain gages 19 and 20).

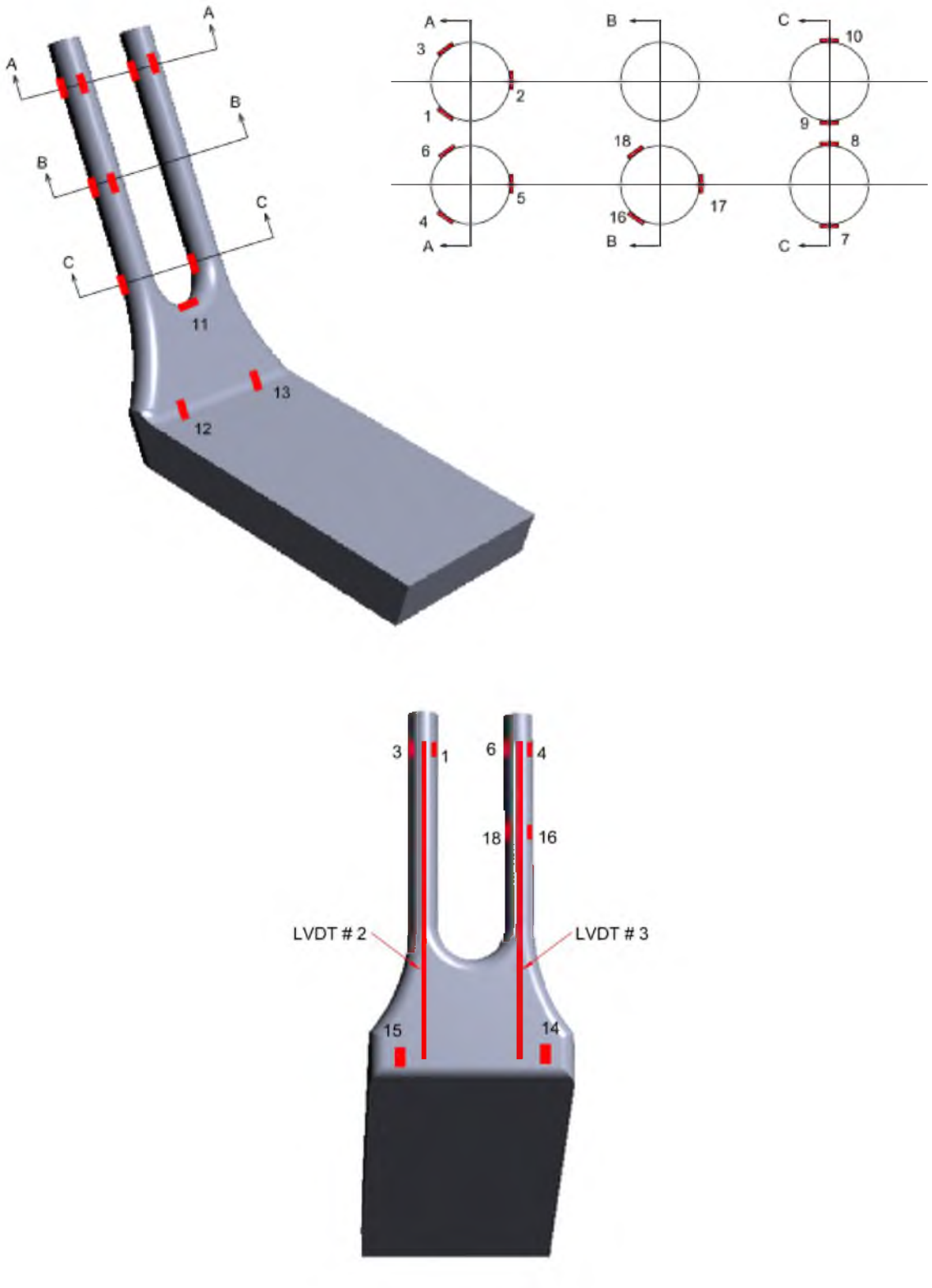

Fig 3.17: Strain Gages on Cast Connector 2 for Monotonic and Cyclic Tests.
(LVDT # 2 was used only for the monotonic tests. Strain Gages 16, 17 and 18 were used only for the cyclic test).

3.5.1 Monotonic Test (CC2-T1)

The load rate for this monotonic test was also 5 kips/min for Stage 2, 4 kips/min for Stages 3 and 4, and 3 kips/min for Stage 5. There were 10-minute pauses between different stages. The deformations and strains presented below follow these stages specified by BC Section 1714.3.1 (NYCBC, 2012). Table 3.7 provides LVDT deformations, including the two LVDTs placed in the cast connector (LVDTs 2 and 3). Note that the residual displacement of LVDT # 5 was caused by slip of the frame. Table 3.8 presents the strains at the end of legs (Strain Gage (SG) # 1, 2, 3, 4, 5 and 6), at the fork section (SG # 7, 8, 9 and 10), and at the saddle (SG # 11). Table 3.9 provides strain gage readings for the gages at the lower half of the connector (SG # 12, 13, 14 and 15)[1]. The largest strains were recorded at the legs and fork of the cast connector.

Table 3.7: LVDT Deflection Reading for CC2-T1
Maximum Load = 1.03 (2.0 P) = 567 kips.

				On Cast Connector Leg			
Stage	Load (% 2P)	Load (kips)	LVDT # 1 (in.)	LVDT # 2 (in.)	LVDT # 3 (in.)	LVDT # 4 (in.)	LVDT # 5 (in.)
1	0%	0.0	0.00000	0.00000	0.00000	0.00000	0.00000
2	25%	137.5	0.02596	0.00862	0.00733	-0.00633	0.01070
3	50%	275.0	0.04478	0.01175	0.01060	-0.02085	0.03332
4	75%	412.5	0.06095	0.01480	0.01430	-0.04470	0.06672
5	100%	550.0	0.07693	0.01863	0.02037	-0.09635	0.17868
5 †	103%	567.0	0.07892	0.01911	0.02076	-0.10175	0.18701
6 †	103%*	567.0	0.07940	0.01919	0.02066	-0.10320	0.18919
7	0%	0.0	0.00298	0.00586	0.00526	-0.05787	0.10948

† New stage for load of 1.03 x (2P)
* The second reading at 100% was taken 24 hours after the maximum load was reached.

[1] The parameters listed in Tables 3.7-3.9 were corrected to account for a delay of about 1300 seconds on the initial deformation and micro strain recording

Table 3.8: Strain Gage Reading (μ strain) for CC2-T1 (Fork and Leg Locations).
Maximum Load =1.03 (2.0 P) = 567 kips

			End of Legs						Fork Section				Saddle
Stage	Load (% 2P)	Load (kips)	SG # 1 μ strain	SG # 2 μ strain	SG # 3 μ strain	SG # 4 μ strain	SG # 5 μ strain	SG # 6 μ strain	SG # 7 μ strain	SG # 8 μ strain	SG # 9 μ strain	SG # 10 μ strain	SG # 11 μ strain
2	25%	137.5	792	522	802	815	444	494	145	460	498	171	-115
3	50%	275.0	1333	1217	1277	1465	1109	839	274	902	922	306	-209
4	75%	412.5	1852	1885	1759	2146	1765	1196	423	1330	1333	439	-308
5	100%	550.0	2396	2509	2209	2917	2432	1567	613	1747	1758	538	-406
5 †	103%	567.0	2459	2602	2281	2997	2518	1618	629	1803	1810	560	-418
6 †	103%*	567.0	2452	2608	2281	2987	2522	1618	624	1806	1803	562	-414
7	0%	0.0	256	-166	299	235	-154	196	23	57	77	16	-14

† New stage for load of 1.03 x (2P)
* The second reading at 100% was taken 24 hours after the maximum load was reached.

Table 3.9: Strain Gage Reading (μ strain) for CC2-T1 (Base Locations).
Maximum Load =1.03 (2.0 P) = 567 kips

			Base			
Stage	Load (% 2P)	Load (kips)	SG # 12 μ strain	SG # 13 μ strain	SG # 14 μ strain	SG # 15 μ strain
1	0%	0	0	0	0	0
2	25%	137.5	61	55	131	143
3	50%	275.0	178	216	238	245
4	75%	412.5	301	368	343	340
5	100%	550.0	430	492	463	435
5 †	103%	567.0	448	512	474	446
6†	103%*	567.0	448	529	474	447
7	0%	0.0	-37	-79	36	45

† New stage for load of 1.03 x (2P)
* The second reading at 100% was taken 24 hours after the maximum load was reached.

As observed in Figure 3.17, strain gages were placed at the same height in the cast connector legs for the second tests. For instance, SGs # 1, 2, and 3; and SGs # 4, 5, and 6 are placed at the same level. The average strains obtained from these gages is in agreement with the force applied at each stage, but significant variation among them is also observed. For instance, strain at SG # 6 is nearly half the strain at SG # 4. This discrepancy is partly attributed to the geometry of the specimen that is not perfectly circular. The main reason for this response is the restraining effect the rods had on the way that the connector deformed. Also note that the compressive strains recorded at the saddle of cast connector 2 (i.e., at the bottom of the fork) were approximately one-third of the strains recorded at the saddle of the first connector. The reason is that the fork of the second cast connector is more flexible because the lower part of this connector is thinner. Figure 3.18 shows the maximum stains at each strain gage location for monotonic load. The figure indicates that strains are concentrated around legs and fork section of the cast connector, in a similar fashion than the strain distribution of Cast Connector 1.

3.5.1.1 Stress-Strain Behavior under Monotonic Load

Figure 3.19 presents strain vs. time curves for SGs # 4 and 10, showing the maximum and minimum recorded strains, respectively. The overall linear behavior and flat plateau under sustained loading indicate that the specimen did not experience plastic deformations. Figure 3.20 shows the stress-strain curves for selected strain gages, which exhibit linearly elastic behavior up to a load 1.03(2P) = 567 kips. The maximum calculated stress for this test (SG # 4) is approximately 89.9 ksi, which is smaller than the average yield stress f_y = 118.8 ksi.

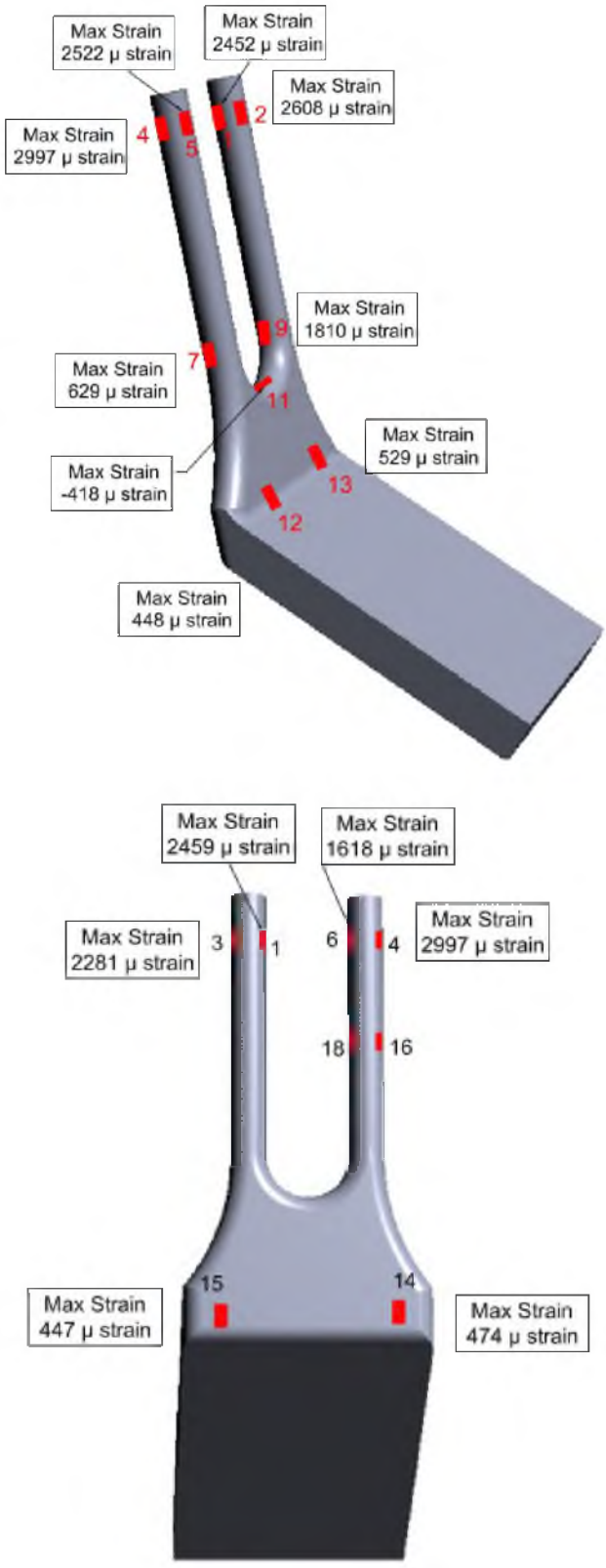

Fig 3.18: Maximum Strains for Monotonic Test of Cast Connector 2

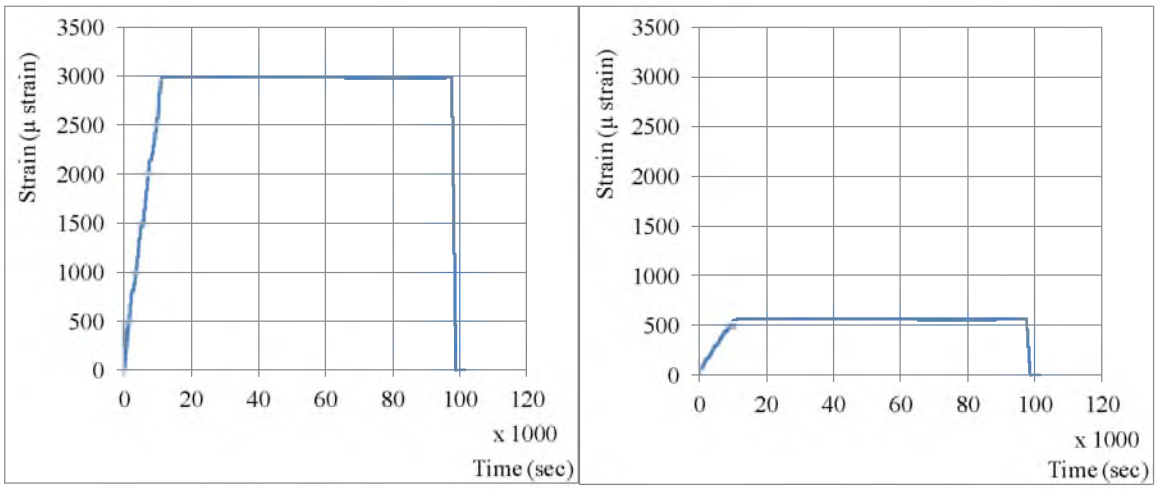

(a) (b)

Fig 3.19: Strain Variation with Time for: (a) SG # 4; (b) SG #10

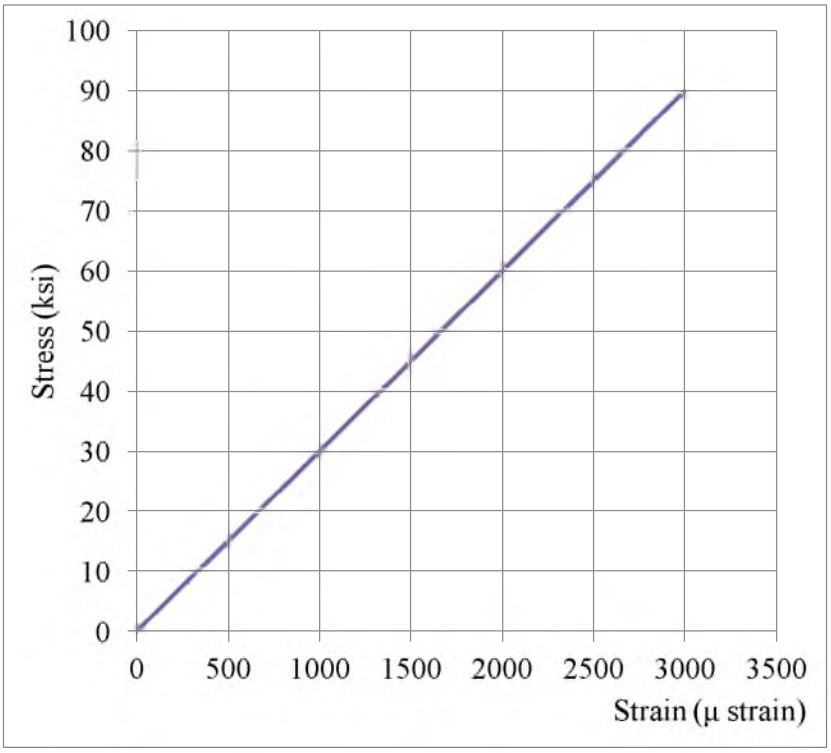

Fig 3.20: Stress-Strain Curves for Strain Gage 4

3.5.2 Cyclic Test (CC2-T2)

The cyclic loading protocol of Figure 3.21 was planned for the second cast connector. The seventh and ninth cycles were expected to reach a total load equivalent to 1.03 (2.5P) = 709 kips. However, a malfunctioning of the data acquisition system software interrupted the protocol several times. The cast connector was ultimately subjected to three cycles at 0.5 (2.5P) = 344 kips, one cycle at 0.7 (2.5P) = 482 kips, and a final cycle at 1.03 (2.5P) = 709 kips. The load rate for the first four cycles was 30 kips/min. For the final cycle the load rate was 30 kips/min up to 482 kips, and 10 kips/min thereafter.

The deformations recorded at the LVDTs for the final cycle of the loading protocol are presented in Table 3.10. The cast connector material exhibited linear performance under the applied load. The residual strains of LVDT # 5 were partly caused by slip of the frame connection. LVDT # 1 residual strains are the result of the plate and bolts interaction on the top plate connection.

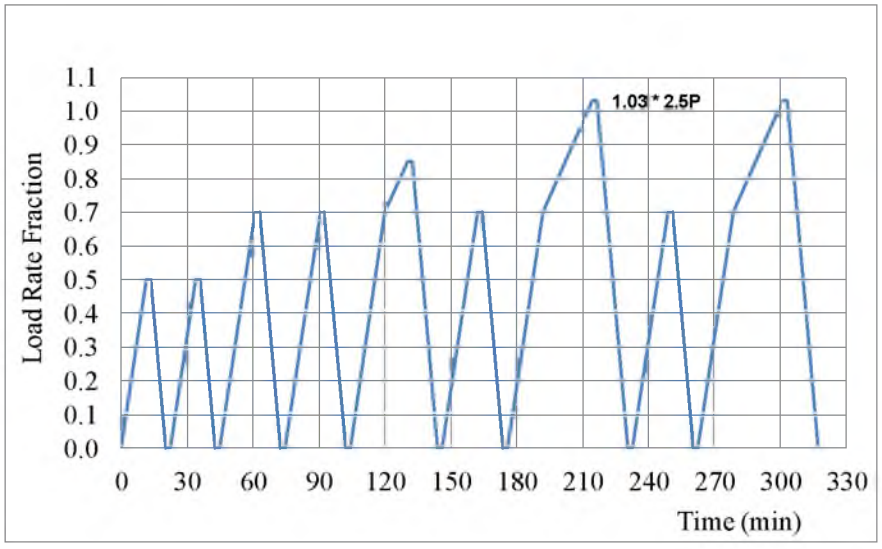

Fig 3.21: Original Cyclic Loading Protocol for Cast Connector 2

Table 3.10: LVDT Deflection Reading Last Cycle of CC2-T2.
Maximum Load = 1.03 (2.5 P) = 709 kips.

			On Cast Connector Leg			
Load (% 2.5P)	Load (kips)	LVDT # 1 (in.)	LVDT # 2 (in.)	LVDT # 3 (in.)	LVDT # 4 (in.)	LVDT # 5 (in.)
20%	137.5	0.02725	-	0.00875	-0.00705	0.01234
40%	275.0	0.04559	-	0.01198	-0.02157	0.03485
60%	412.5	0.06169	-	0.01608	-0.03817	0.05915
80%	550.0	0.07763	-	0.02040	-0.05113	0.08495
82%	567.0	0.07958	-	0.02098	-0.05331	0.08770
100%	688.0	0.09373	-	0.02537	-0.06783	0.16569
103%	709.0	0.09649	-	0.02617	-0.06845	0.18189
0%	0.0	0.02118	-	0.00632	-0.02821	0.10325
* LVDT # 2 was removed to prevent damages in case of failure						

Tables 3.11 and 3.12 show the readings for strain gages on the legs and fork of the connector, respectively. Table 3.13 shows the recorded strains at the base of the connector. The maximum applied load for the last cycle of the protocol was 1.03(2.5P) = 709 kips. The results are consistent with those of previous tests. The maximum strains are recorded at the legs of the connectors, and the cast connector exhibits linear behavior up to 1.03(2.5P) = 709 kips.

3.2.2.1 Stress-Strain Behavior under Cyclic Loading

The strain vs. time curves (Figure 3.22) show linear behavior up to the maximum load of 1.03 (2.5P). A series of small or interrupted cycles are recorded after the first three cycles, prior to the last cycle that reached the maximum load. These interrupted cycles and long pause before the last cycle were caused by a malfunctioning of the data acquisition system that interrupted the protocols several times. The recorded cycles, however, show that the cast connector exhibited linear behavior.

Table 3.11: Strain Gage Reading (μ strain) for Last Cycle of CC2-T2 (Leg Location).

		End of Legs			End of Legs			Midsection of Legs		
Load (% 2.5P)	Load (kips)	SG # 1 μ strain	SG # 2 μ strain	SG # 3 μ strain	SG # 4 μ strain	SG # 5 μ strain	SG # 6 μ strain	SG # 16 μ strain	SG # 17 μ strain	SG # 18 μ strain
20%	137.5	712	471	704	864	481	465	628	558	-
40%	275.0	1244	1155	1189	1516	1144	816	1032	1313	-
60%	412.5	1764	1818	1719	2171	1783	1191	1461	2035	-
80%	550.0	2301	2490	2303	2843	2423	1610	1919	2750	-
82%	567.0	2365	2571	2373	2922	2498	1661	1972	2835	-
100%	688.0	2819	3147	2882	3500	3044	2051	2374	3425	-
103%	709.0	2892	3253	2968	3595	3143	2121	2435	3532	-
0%	0.0	189	-151	220	166	-123	177	158	-127	-
Strains for strain gage 18 could not be recorded due to a bad soldered wire.										

Table 3.12: Strain Gage Reading (μ strain) for Last Cycle of CC2-T2 (Fork and Saddle Location).

		Fork Section				Saddle
Load (% 2.5P)	Load (kips)	SG # 7 μ strain	SG # 8 μ strain	SG # 9 μ strain	SG # 10 μ strain	SG # 11 μ strain
20%	137.5	166	446	452	137	-99
40%	275.0	306	880	878	267	-198
60%	412.5	450	1305	1292	411	-298
80%	550.0	599	1742	1711	572	-402
82%	567.0	615	1794	1760	592	-414
100%	688.0	729	2187	2129	739	-498
103%	709.0	744	2259	2206	767	-512
0%	0.0	-2	56	101	1	1

Table 3.13: Strain Gage Reading (μ strain) for Last Cycle of CC2-T2 (Base Location).

		Base		Base	
Load (% 2.5P)	Load (kips)	SG # 12 μ strain	SG # 13 μ strain	SG # 14 μ strain	SG # 15 μ strain
20%	137.5	81	138	138	129
40%	275.0	200	292	244	227
60%	412.5	317	428	349	326
80%	550.0	438	577	459	431
82%	567.0	452	592	472	444
100%	688.0	550	691	567	542
103%	709.0	568	704	582	557
0%	0.0	-26	-33	26	33

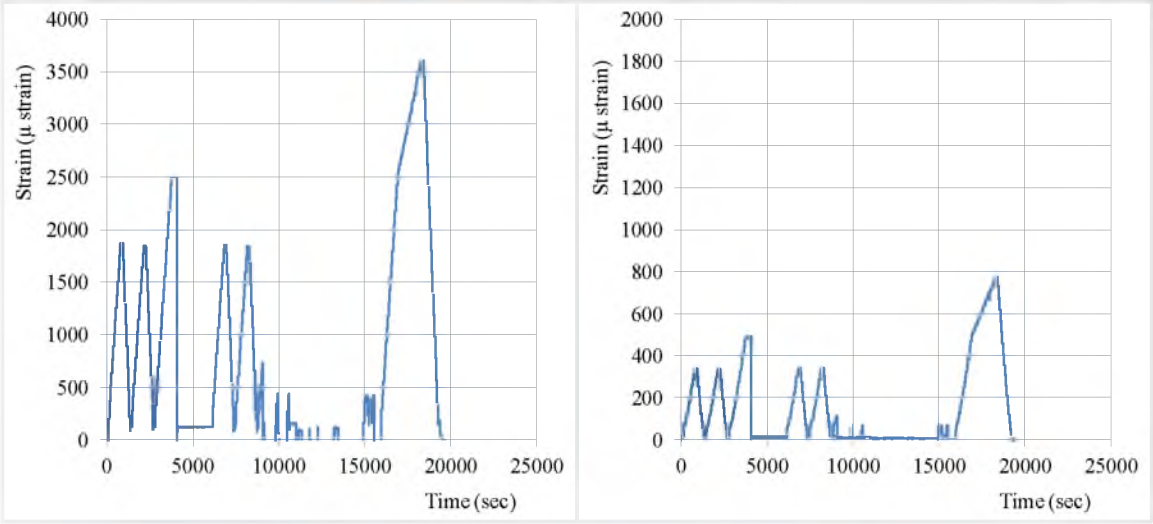

(a) (b)

Fig 3.22: Strain vs. Time Curves for: (a) SG # 4; (b) SG # 10

Figure 3.23 shows the maximum strains at each strain gage location for the last cycle of the cyclic test. Maximum strains were developed around the fork and the legs of the connector. Figure 3.24 shows the stress-strain curve for stain gage 4. Figure 3.24 shows that the maximum stress was still below the average yield stress obtained from the heat tests ($f_y = 118.8$ ksi, Appendix C).

3.6 Additional Test Performed on Cast Connector 2

To study the nonlinear performance of the connector and the material, Cast Connector 2 was subjected to additional tests. Five more tests were performed on the connector specimen, each test with a targeted maximum load higher than that of the previous test. In the first tests the specimen was subjected to a maximum load of 826 kips (3P). The second test performed reached a maximum load of 894 kips (3.3P).

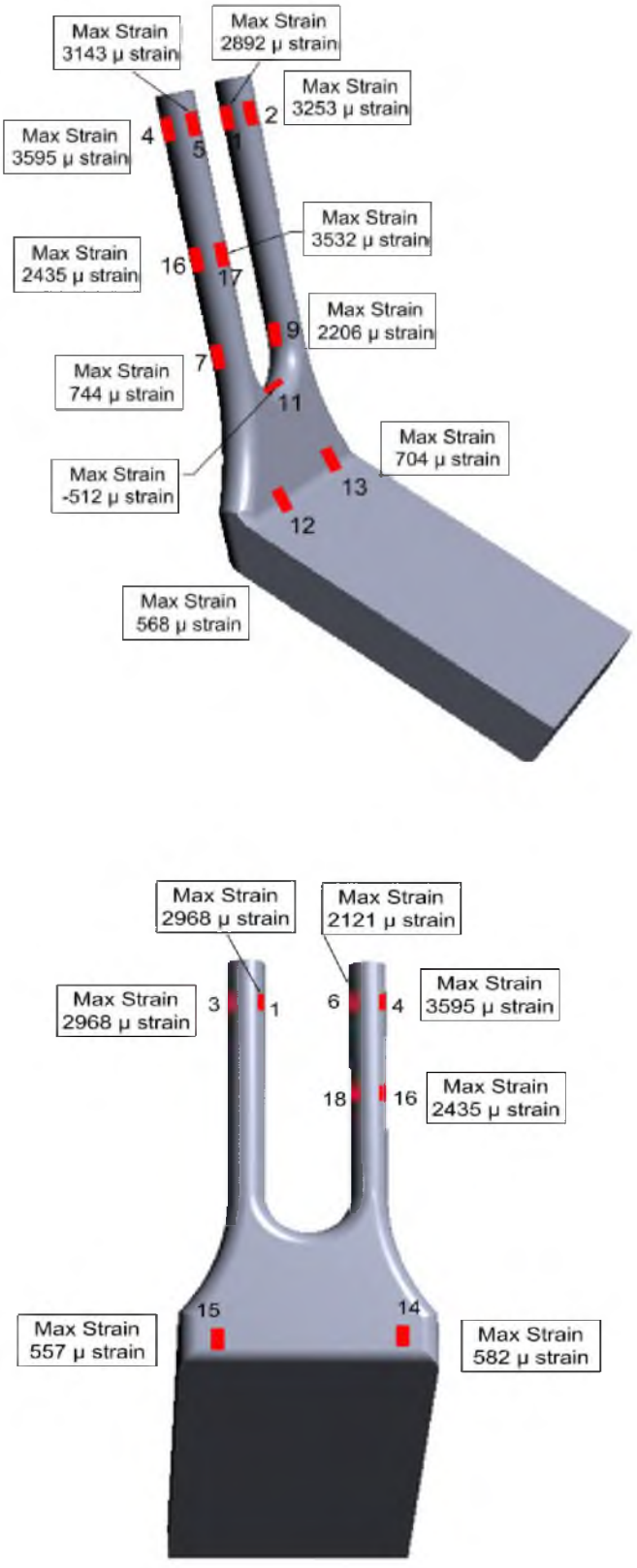

Fig 3.23: Maximum Strains for Cyclic Test of Cast Connector 2 (CC2-T2)

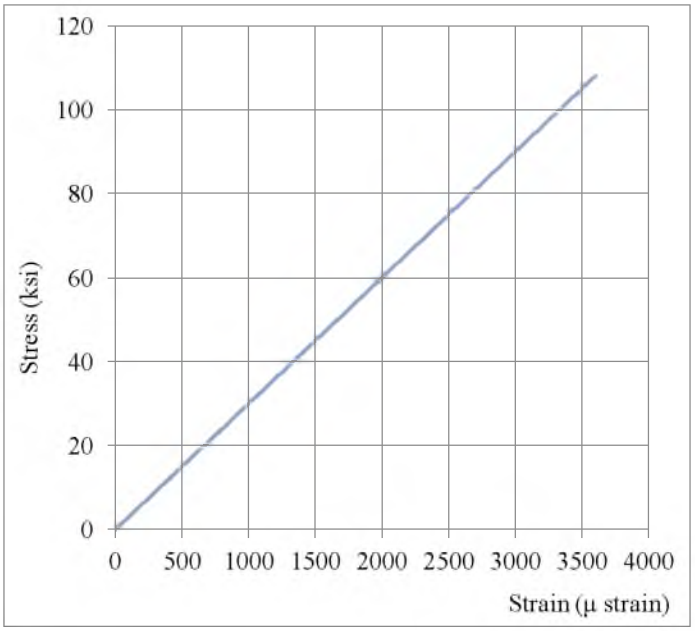

Fig 3.24: Stress-Strain Curves for Strain Gage 4

The third test targeted 1000 kips as the maximum load but a nut connecting one of the stainless steel rods to the top assembly plate failed at a load of about 888 kips. The next two tests were performed on only one leg of the connector, partly because of the failed nut and partly to prevent failure of the subassembly. In these tests the targeted maximum loads were halved because only one leg was loaded. The first of these two tests, was performed on the west leg with targeted maximum load of 570 kips (equivalent to 1040 kips for both legs). However, at a load of 482 kips another nut connecting the steel rod and top assembly plate failed. The second test was performed on the east leg. This time the loading protocol was the same as the first one-legged test. This test, however, resulted in failure of the connector itself at load of about 475 kips (equivalent to 950 kips for both legs).

3.6.1 Additional Test 1: Maximum Load 826 kips (1.2 × 2.5P = 3P)

The first additional test on Cast Connector 2 was performed by loading the specimen under the loading protocol shown in Figure 3.25. The load rate was 30 kips/min until the load reached 482 kips. After 482 kips the loading rate was 10 kips/min until the load reached 709 kips and 4 kips/min for the final loading stage. Figures 3.26 and 3.27 show the load vs. strain and strain vs. time plot for SG # 4, respectively.

3.6.2 Additional Test 2: Maximum Load 894 kips (1.3 × 2.5P = 3.25P)

The second additional test on Cast Connector 2 followed a loading protocol similar to that of the first additional test. The difference being that the maximum load applied was 894 kips. Figure 3.28 shows the loading protocol followed for this test.

In this test the cast connector showed clear nonlinear behavior for first time. Figure 3.29 shows the load vs. strain curve for SG # 17. The nonlinear portion of the curve started around 842 kips. Figure 3.29 shows that the curve began incursion into nonlinear interval at a strain of around 0.429% for SG # 17. The corresponding load was 848 kips and stress 124.4 ksi, which are close to the values of observed yield stress of the material (see Section 3.3). Figure 3.30 shows the stress-strain curve for the connector specimen at the location of SG # 17. The curve shows that the material started yielding at stress of 128 ksi.

3.6.3 Additional Test 3: Maximum Load 888 kips

The target load for this test was 1000 kips (1.45 × 2.5P = 3.63P). Figure 3.31 shows the loading protocol used for the test. The objective of this test was to record cast

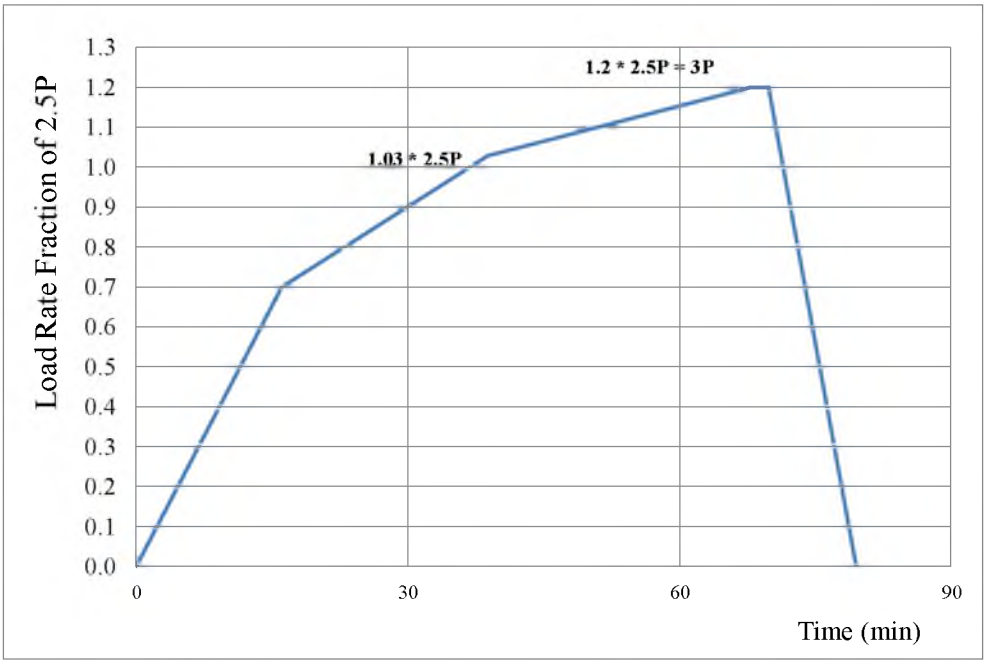

Fig 3.25: Loading Protocol for Additional Test 1

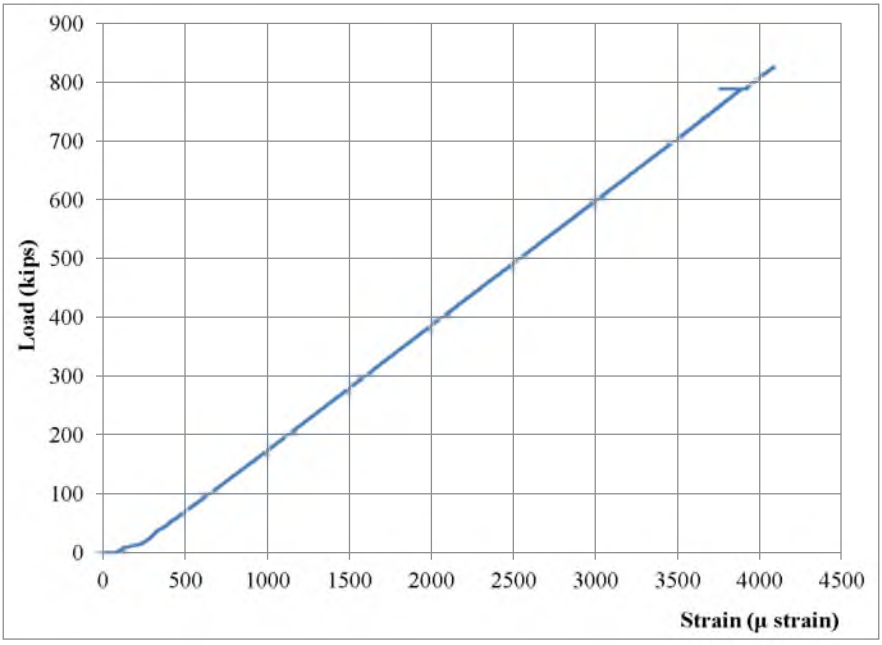

Fig 3.26: Load vs. Strain Curve for SG # 4

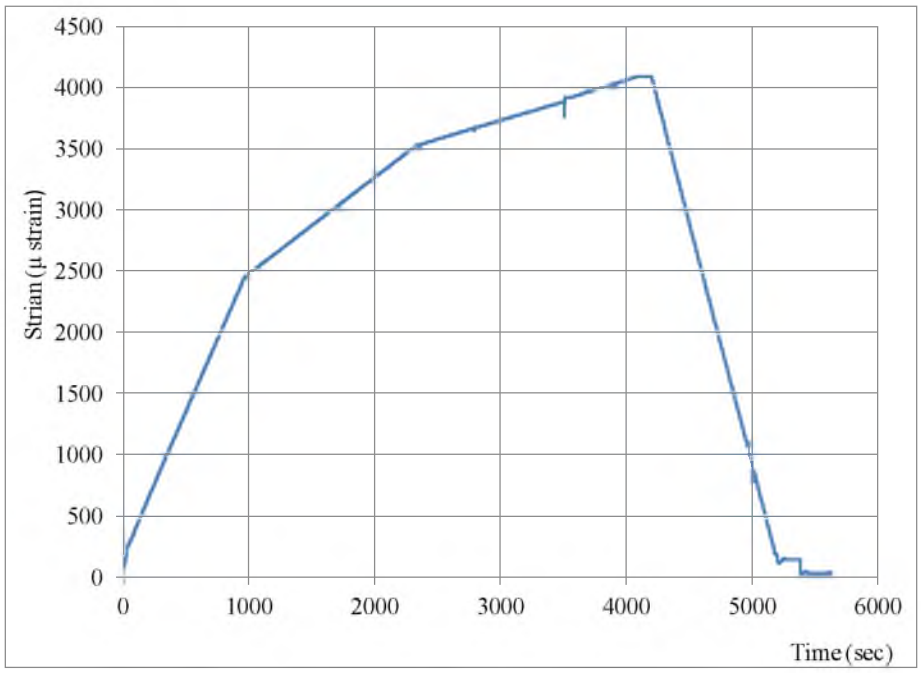

Fig 3.27: Strain vs. Time Curve for SG # 4

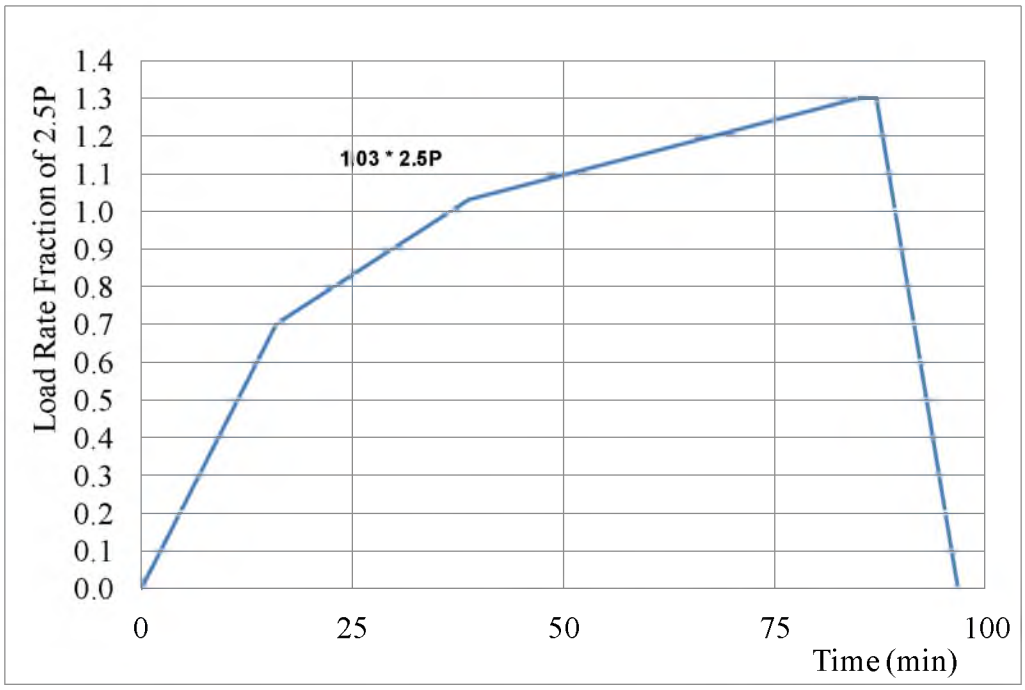

Fig 3.28: Loading Protocol for Additional Test 2

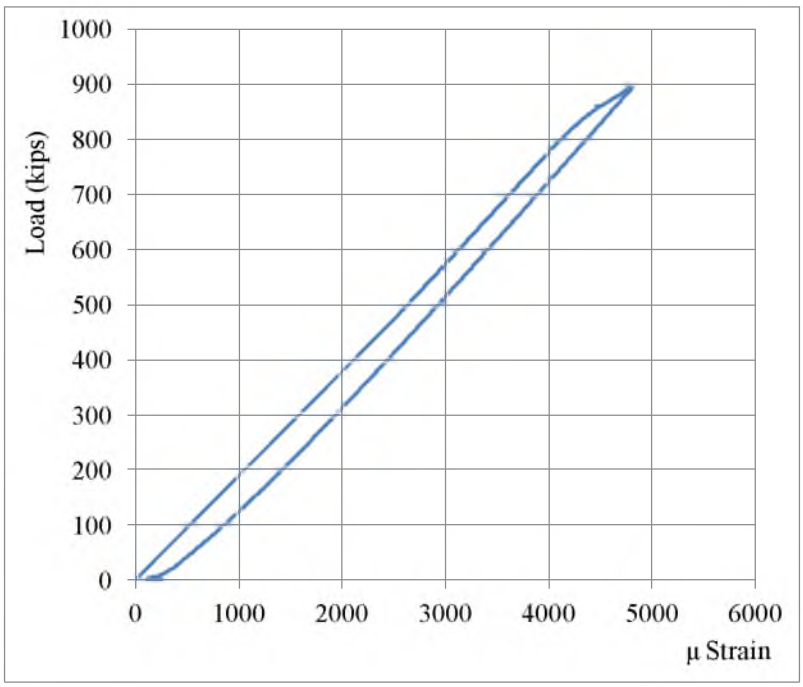

Fig 3.29: Load vs. Strain Curves for SG # 17

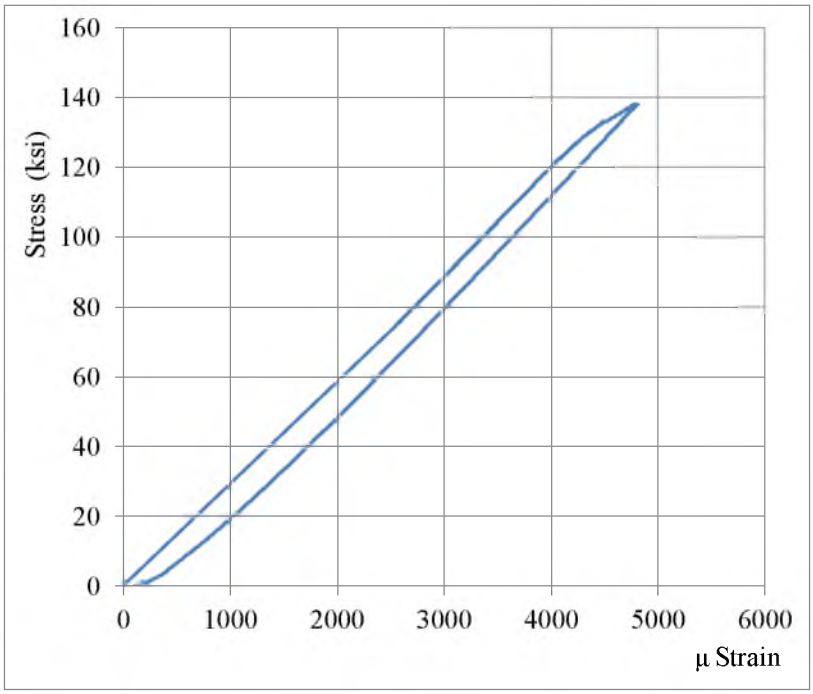

Fig 3.30: Stress-Strain Curve for SG # 17

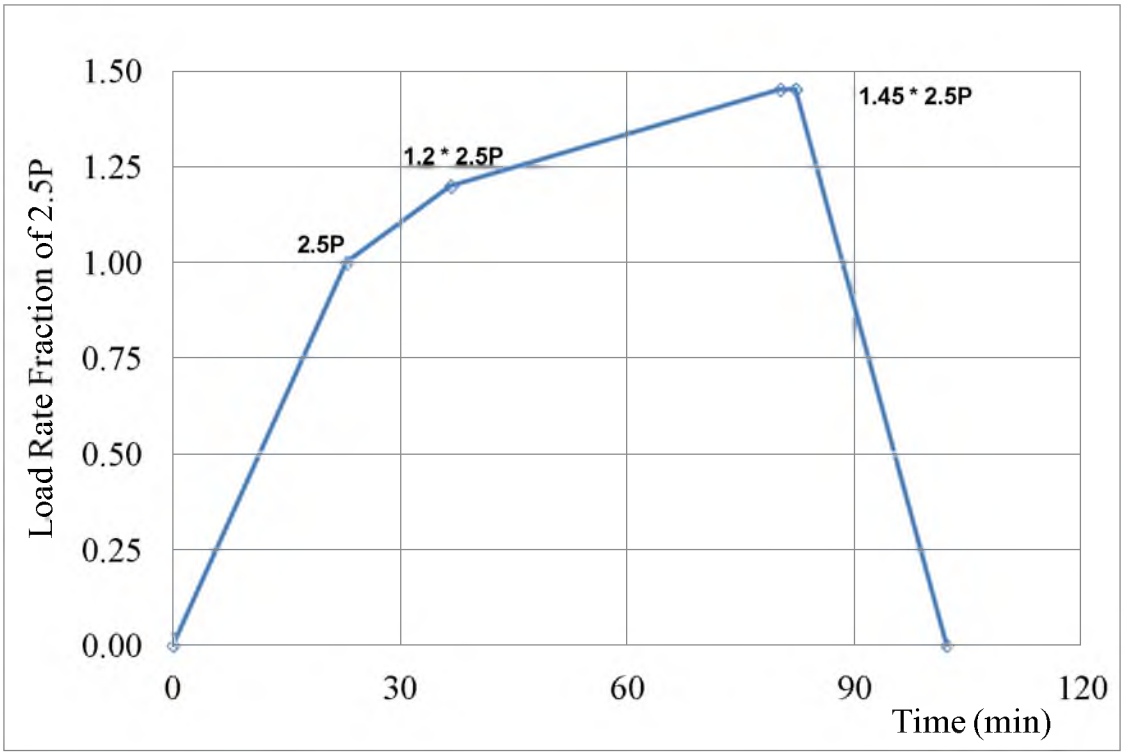

Fig 3.31: Loading Protocol for Additional Test 3

connector high nonlinear behavior. Unfortunately, as the load reached around 888 kips the nut connecting one of the stainless steel rods and the top assembly plate failed and the test had to be stopped. Load vs. strain curve obtained for this was similar to the additional test 2. Figure 3.32 shows the load vs. strain and strain vs. time plot for SG # 17.

3.6.4 Additional Test 4: Single Leg Loaded, Maximum Load 482 kips

This test was carried out after the failure of the nut connecting one of the rods and the top assembly plate (test of Section 3.6.3), and consequently, only one leg was loaded in this test. Unfortunately, the same failure occurred as in additional test three. The failure of the nut resulted in lack of reliable data.

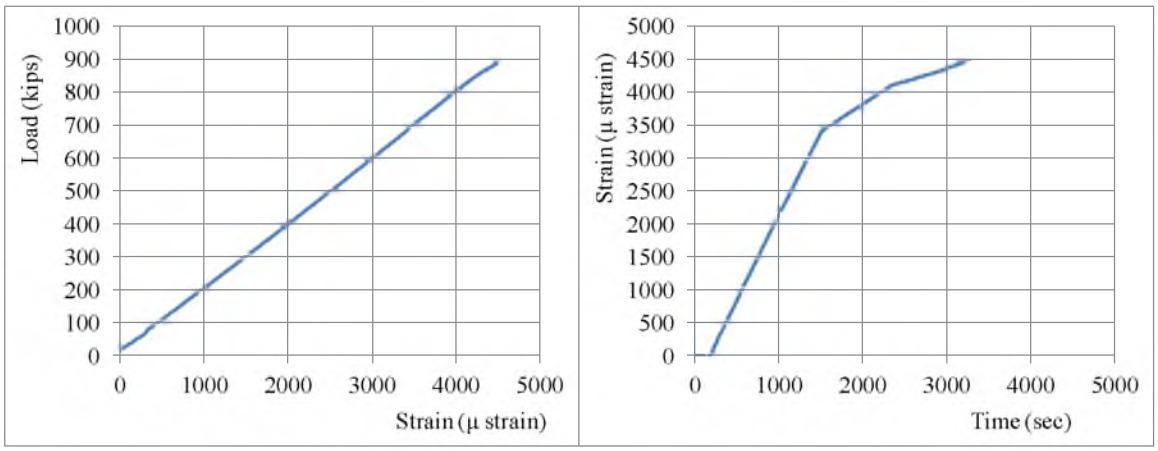

(a) (b)

Fig 3.32: (a) Load vs. Strain for SG # 17; (b) Strain vs. Time SG # 17*

* Change in the slope of line in Figure 3.26 (b) is due the change in the rate of loading.

3.6.5 Additional Test 5: Single Leg Loaded, Maximum Load 475 kips

This was the final test performed on Cast Connector 2 specimen. Like additional test four, only one leg was loaded. Failure was observed at a load of 475 kips, equivalent to 950 kips (1.38 × 2.5P = 3.45P) if both the legs were loaded. The loading protocol of Figure 3.33 was used for the test. The protocol is similar to the test presented in Section 3.6.3, but the load at each stage is halved.

Figure 3.34 shows the load vs. strain curve for SG # 5. The curve shows some nonlinearity. The nonlinear portion of the curves is still not very prominent due to the position of the strain gages relative to the fracture point. The strain gage was considerably distant from the fracture point to be greatly influenced by the failure. Strain gages # 7 and 8 were closer to the failure location but they were not greatly influenced either. This was due to increase in the cross section. This can be attributed to the geometry of the connector. The varying width of the connector legs significantly affected how the connector responded to the applied load and ultimately how the strain gages

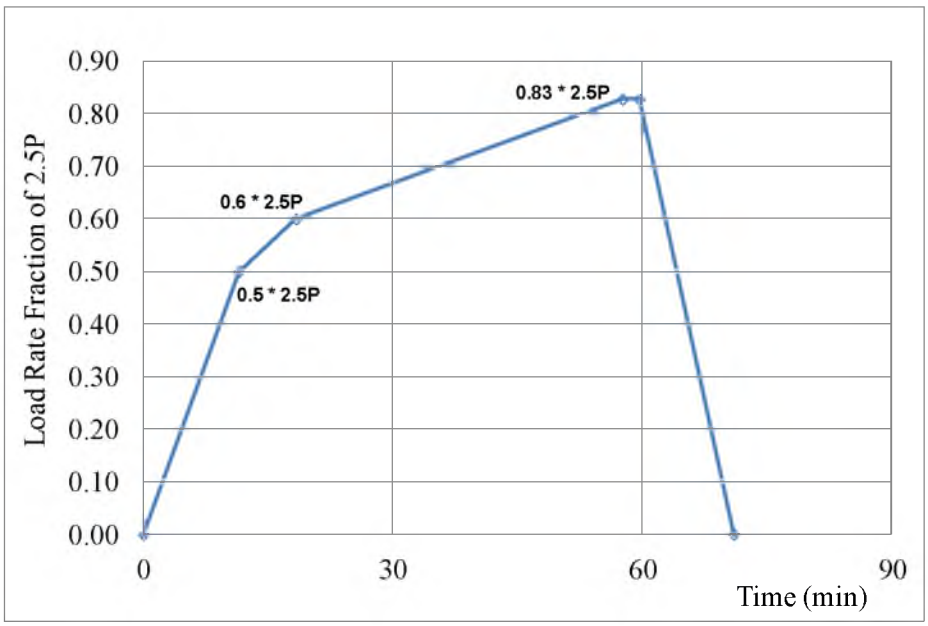

Fig 3.33: Loading Protocol for Additional Test 5

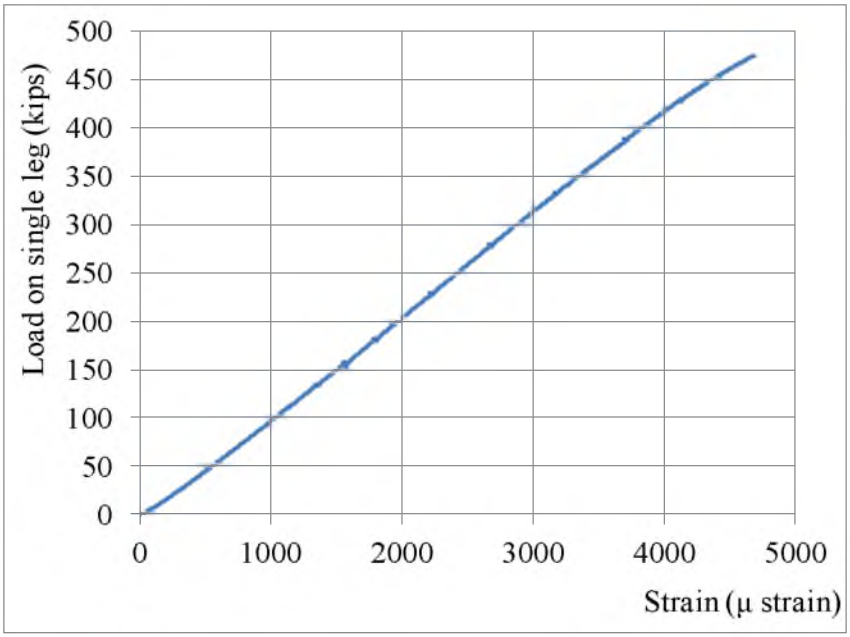

Fig 3.34: Load vs. Strain for SG # 5

responded. Figure 3.35 shows the stress-strain curves for SG # 5. The figure shows similar characteristics as observed for other cases. The yielding appears to start around 127.5 ksi.

3.7 Summary of Experimental Tests

The experimental tests performed on cast connectors 1 and 2 demonstrate their ability to sustain large loads. Although Cast Connector 1 was not tested up to failure load, the final test on Cast Connector 2 showed the failure load was 475 kips for one leg. If both the legs were loaded the failure load would be much higher than that. To simulate and verify the experimental test and find the failure load, finite element (FE) analyses were performed (Chapter 4).

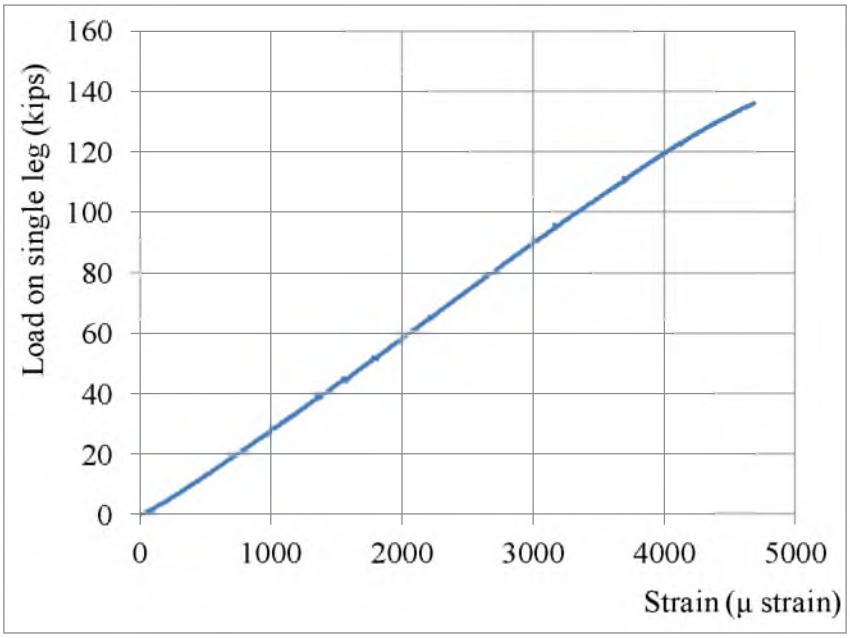

Fig 3.35: Stress-Strain Curve for SG # 5

CHAPTER 4

FINITE ELEMENT MODELING

The cast connectors were modeled in the finite element (FE) program ANSYS to simulate the specimens' linear and nonlinear behavior, ultimately determining the response controlling parameters. The models' results were compared to experimental data results. Once the models were sufficiently calibrated, a parametric study was carried out with the expected relevant parameters to investigate their effect on the connectors' response.

This chapter includes the description of the FE model created for each connector and the results obtained from the analysis. Stress and strain distributions at different load levels obtained from the FE analysis were compared to experimental test results. Normal stress and von Mises stress for these simulations are similar (apart from fact that von Mises stress distribution does not show negative sign)

4.1. FE Modeling of Cast Connector 1

The three dimensional (3D) geometry was created in a preprocessing software (SolidWorks, Dassault Systèmes) using the dimensions from drawings and actual sample measurements. This geometry was imported to ANSYS. The entire geometry of the connector was modeled as a solid element and SOLID95 was used as element type.

Modulus of elasticity was defined as 30000 ksi as calculated from the material stress-strain curve for the material, Section 3.3. Yield strength was defined as 116 ksi and the ultimate strength was provided as 130.8 ksi. Poisson's ratio of 0.3 was used, which is a standard value for steel. Most steels when used within their design limit exhibit a stable Poisson's ratio of 0.3.

The connector was constrained at its base in three directions, and monotonically increasing tensile load was applied to the cast connector model's legs. The results from this analysis were compared to the actual laboratory results. Figures 4.1 and 4.2 illustrate the von Mises stress distribution in cast connector 1 for a total tensile load of 688 kips. At this load level, the FE model exhibited linear performance with maximum stress of approximately 91.3 ksi, which is below the average measured yield strength of 118.8 ksi.

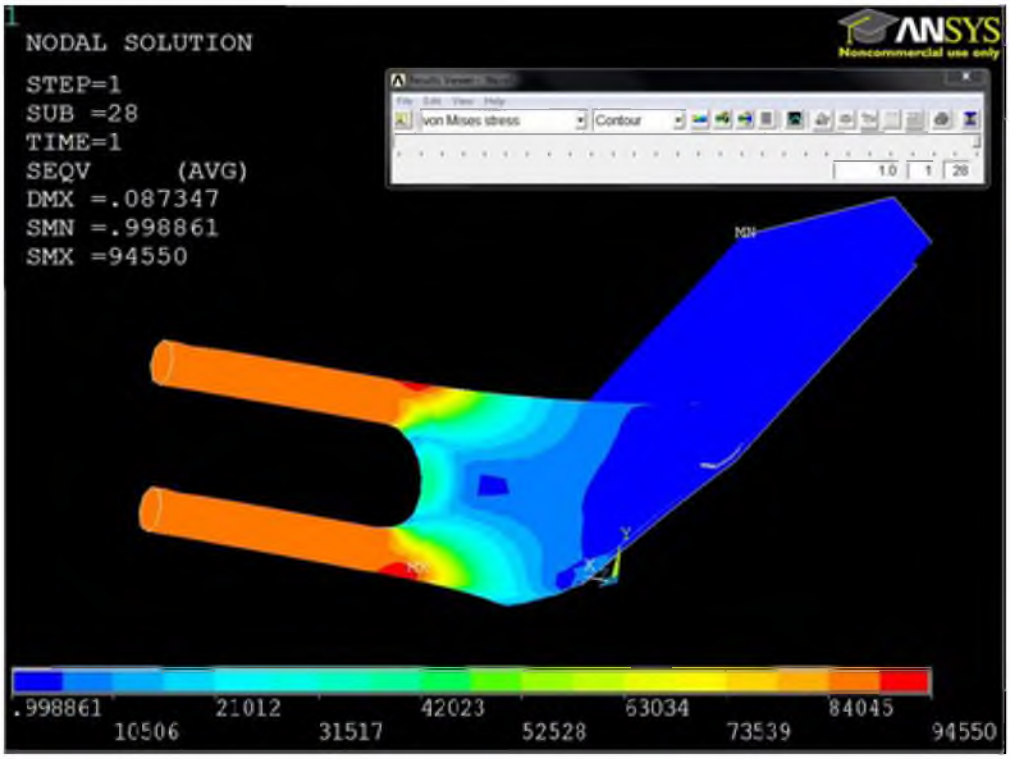

Fig 4.1: von Mises Stress Distribution in Cast Connector 1 at 688 kips (View I)

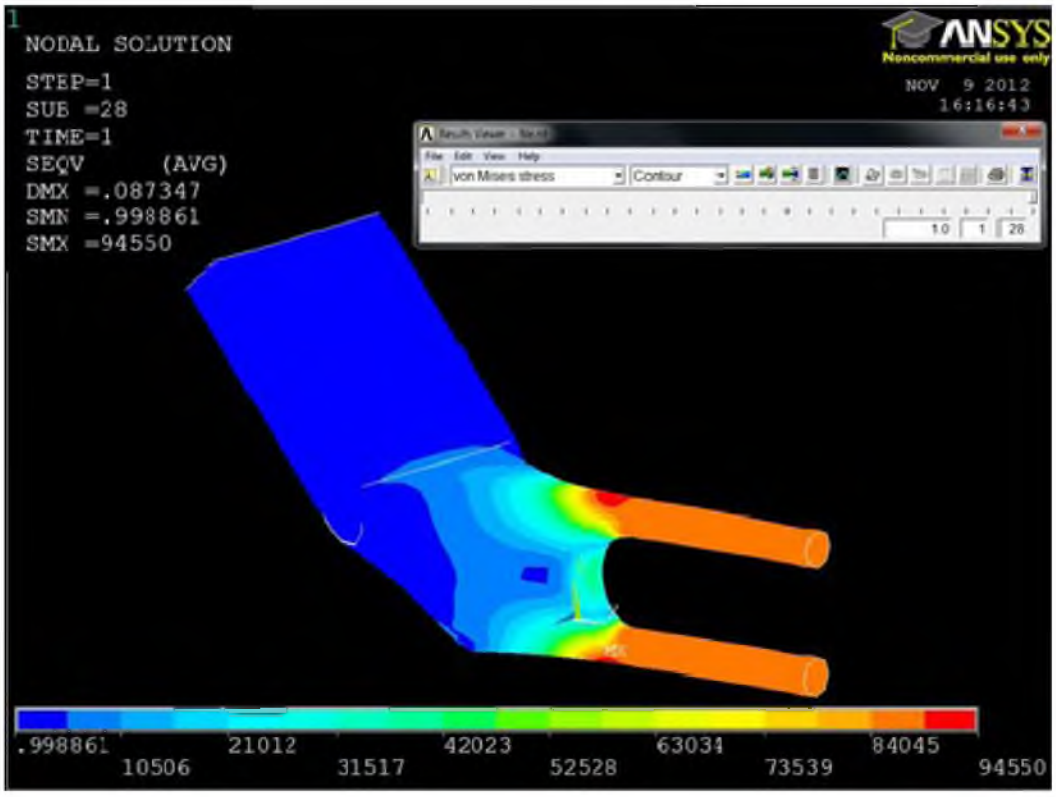

Fig 4.2: von Mises Stress Distribution in Cast Connector 1 at 688 kips (View II)

Figure 4.3 shows comparison of load vs. stress curves for SG # 1 obtained from laboratory tests and FE analysis. The figure shows that the curves tend to agree with each other to some extent with a maximum error of 9.6%.

Regarding Cast Connector 1's strain, lab tests show that for monotonic load of 550 kips (CC1-T1), the maximum strain is 2653 μstrain with a corresponding stress of 79.6 ksi. For this test and load level, ANSYS analysis stress was 73 ksi, rendering an error of 8.3%. For the cyclic test with a maximum load of 688 kip (CC1-T2) the maximum strain is 3367 μstrain with a corresponding stress of 101 ksi. The corresponding stress in ANSYS was 91.3 ksi, a 9.6% difference. As observed, lab test results and ANSYS analysis show reasonable agreement.

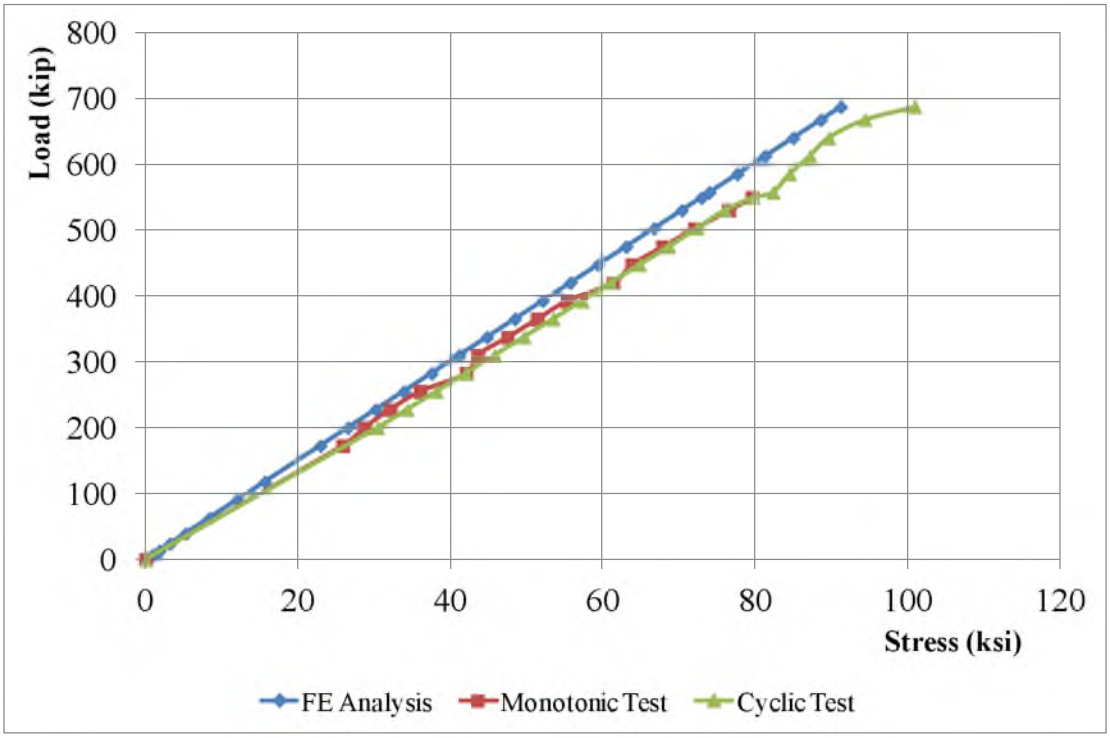

Fig. 4.3: Comparison of Load-Stress Curves from Lab Tests and FE Analysis (Cast Connector 1)

After verifying that the FE model agrees with lab results (which also validates the model), the load on the FE model was increased to evaluate the connector's nonlinear behavior. The material properties for this simulation were not changed from those used for previous simulation. The failure load criterion for the simulation was defined as the load when elements reached the provided ultimate stress.

The analysis revealed that Cast Connector 1 would fail at a load of 1044 kips. Figure 4.4 show von Mises stress distribution on the connector at a load of 1044 kips. The FE model showed that the connector would fail at the legs, close to the transition, to form a forked section.

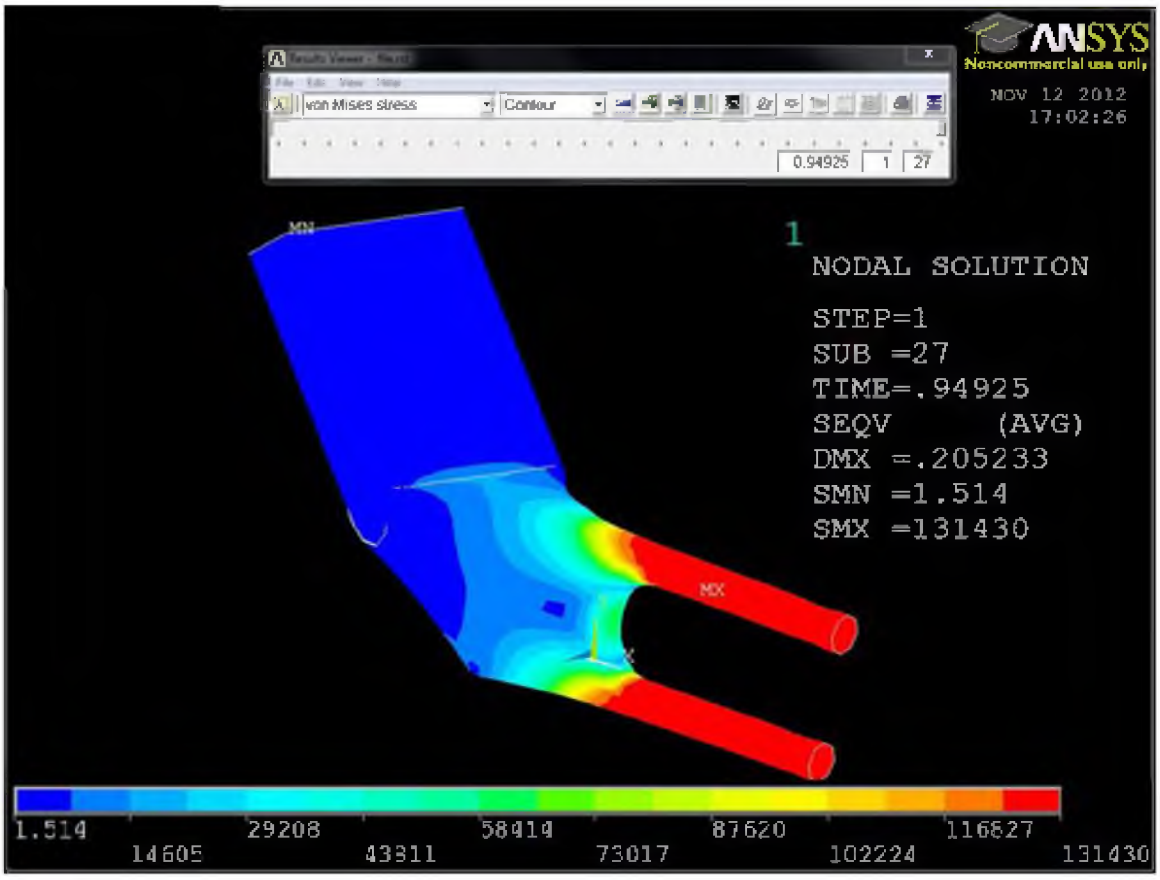

Fig 4.4: von Mises Stress Distribution for Cast Connector 1 at 1044 kips

4.1.1 Verification of the Model in a Different FE Program

A different FE program (ABAQUS; Dassault Systèmes, 2011) was also used to verify the model in addition to ANSYS. The ABAQUS model provided a verification of FE results, and the opportunity to perform a convergence study by refining the model mesh, a difficult task in ANSYS due to memory constraints.

ABAQUS results for Cast Connector 1 analyses were similar to those obtained from ANSYS. The latter model predicted a failure load of 1044 kips, while ABAQUS showed the failure load at 1045 kip.

4.1.2 Mesh Refinement Study (Convergence Study):

ABAQUS results at SG location one, and for a load of 688 kips, were compared to those obtained from experimental tests on Cast Connector 1 by refining the mesh size. Table 4.1 shows the stress comparison at SG # 1 for the initial model with an average element size on 1 in. and for four additional models in which the average element size was reduced. Table 4.1 also shows the relative error for each case. It is clear that as the number of elements increases, the error decreases up to case four. The difference in results stabilizes at an element size of 0.4 in. or lower.

The model created in ANSYS was similar to case one of Table 4.1, and the error was 9.6%. This value is close to 10.1% error obtained from the ABAQUS simulation. Figure 4.5 represents the plot of convergence study shown in Table 4.1.

4.2 FE Modeling of Cast Connector 2

Procedures similar to those used for Cast Connector 1 were implemented on Cast Connector 2. To gain sufficient confidence with the model, the FE analysis was run to simulate laboratory tests and match or compare the results. Figure 4.6 show the stress distribution on Cast Connector 2 for 709 kips (1.03*2.5P).

Comparison of the FE analysis results with the experimental data showed that the model was able to predict the stress distribution on the connector within reasonable accuracy with a maximum error of 12%. Stresses at SG # 8 and SG # 17 were compared (Figure 4.7) as the FE model showed that they were closer to the critical location (shown in red in Figure 4.6).

Table 4.1: Results from Convergence Study with Relative Error.
Experimental Stress at Location 1 = 101.01 ksi

Case No.	Element Size (in.)	Number of Elements	Average von Mises Stress (ksi)	Relative Error
1	1	12747	90.7742	-0.10133
2	0.8	22035	91.7611	-0.09156
3	0.6	50910	93.3958	-0.07538
4	0.4	146357	95.8536	-0.05105
5	0.3	316894	95.8394	-0.05119

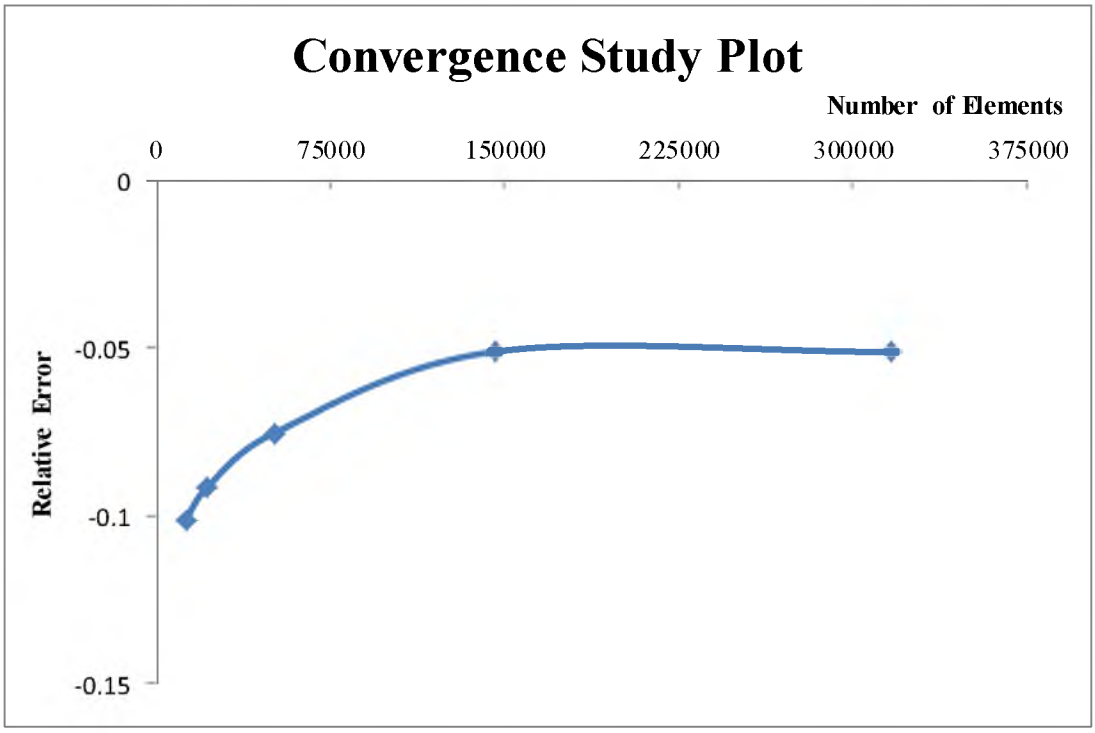

Fig 4.5: Plot of Relative Error with Respect to Number of Elements

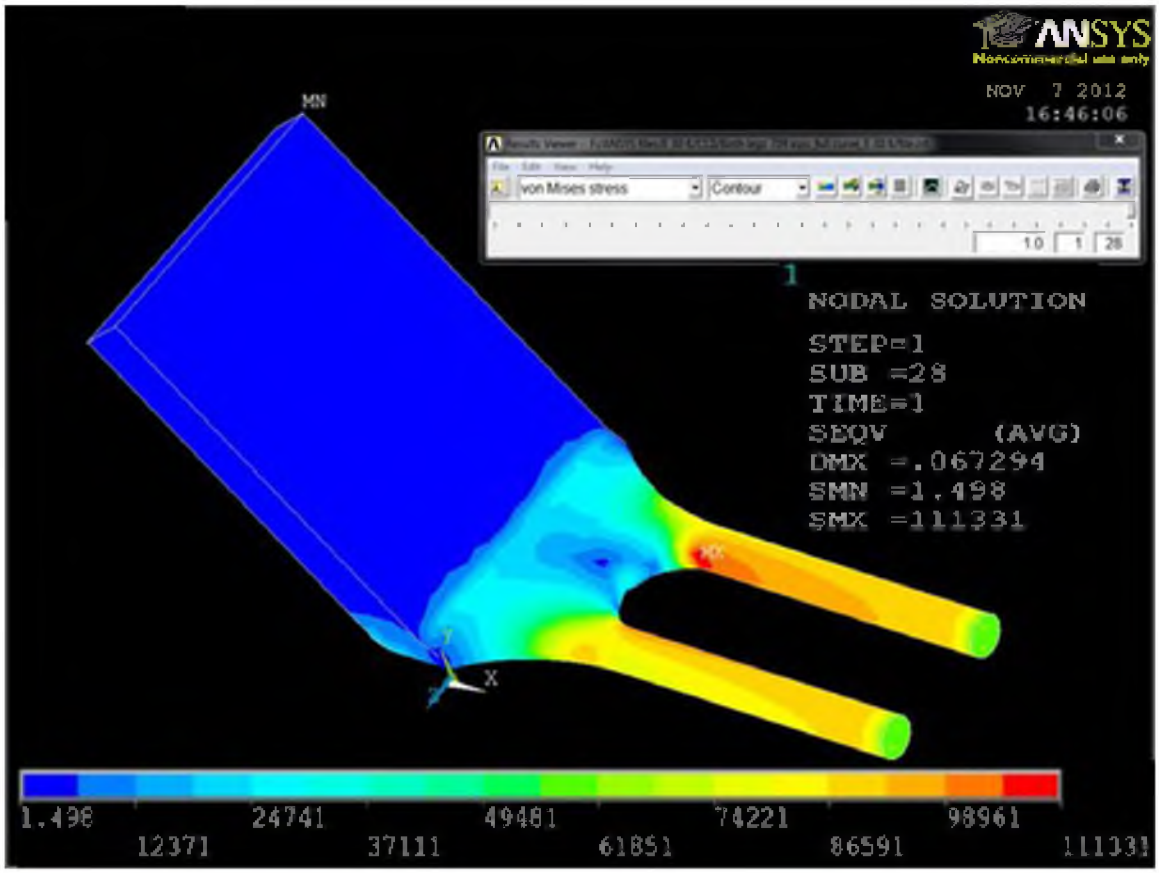

Fig 4.6: von Mises Stress Distribution on Cast Connector 2 at 709 kips

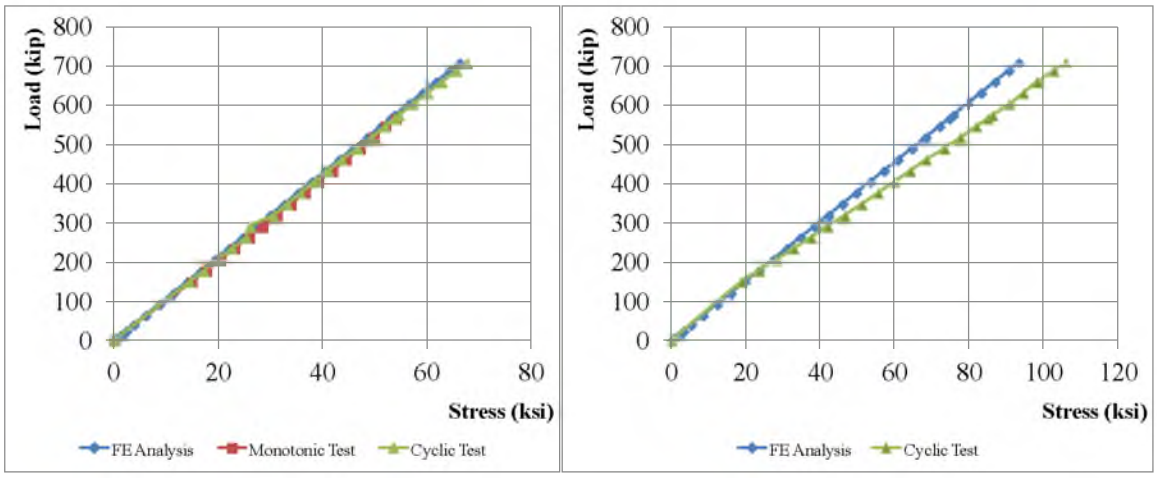

(a) (b)

Fig 4.7: Comparison of Load-Stress Curves from Lab Tests and FE Analysis (709 kips).
(a) SG # 8; (b) SG # 17 (SG #17 was not used for monotonic test)

As more test data were available for cast connector 2, comparisons were also made with results obtained from simulating each test (894 kip and 888 kip). Figures 4.8 and 4.9 show load vs. stress curves for SGs # 4, 8 and 17 obtained from experimental tests and FE analysis.

All the curves show reasonable agreement (with a maximum difference of 19% at maximum load of 894 kips). This difference is reduced by increasing the number of elements in the model as done for cast connector 1 (see Section 4.1.1).

After the above validations, the FE model was subjected to tensile loads only on one leg as the additional test 5 (Section 3.6.5). The failure load observed in FE analysis was 516.6 kip and that observed in experimental tests was 475 kip. The FE model's prediction was 8.8% higher than the experimental failure load. Figure 4.10 shows the stress distribution on cast connector 2 as predicted by FE analysis at a failure load of 516.6 kips. Figure 4.11 compares the load vs. stress curves for SGs # 4, 8 and 17.

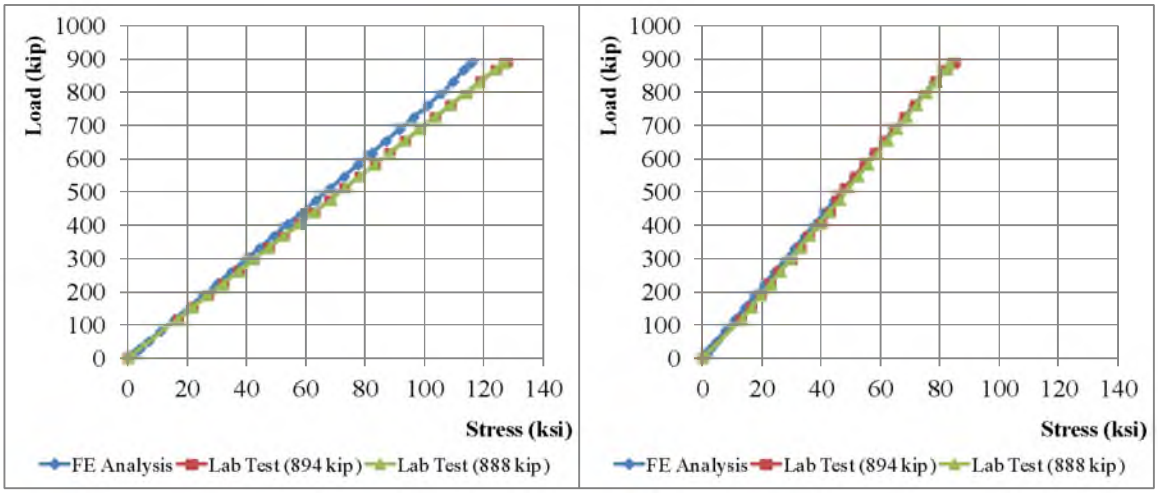

(a) (b)

Fig 4.8: Comparison of Load-Stress Curves: (a) SG # 4; (b) SG # 17

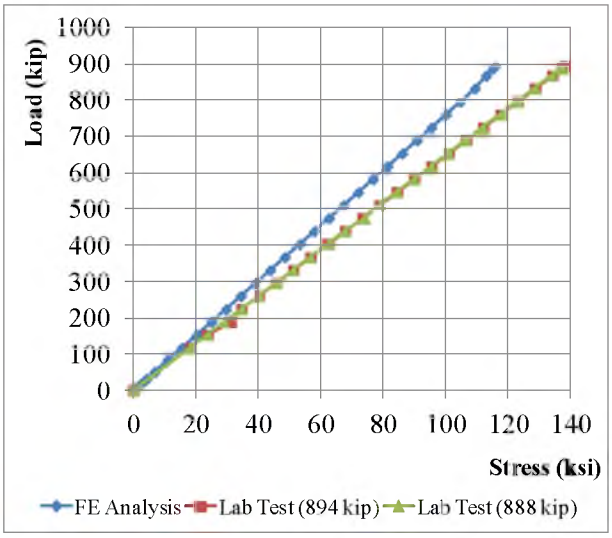

Fig 4.9: Comparison of Load-Stress Curves from Lab Tests and FE Analysis (SG #17)

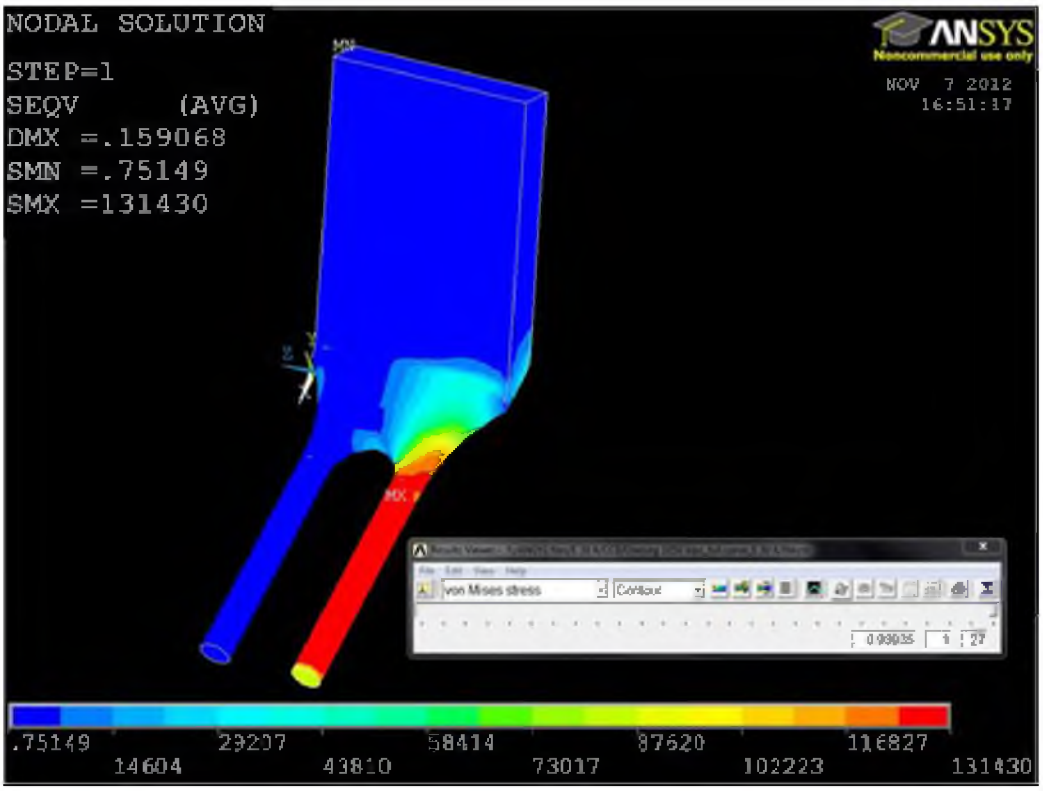

Fig: 4.10: von Mises Stress Distribution on Cast Connector 2 at 516.6 kip

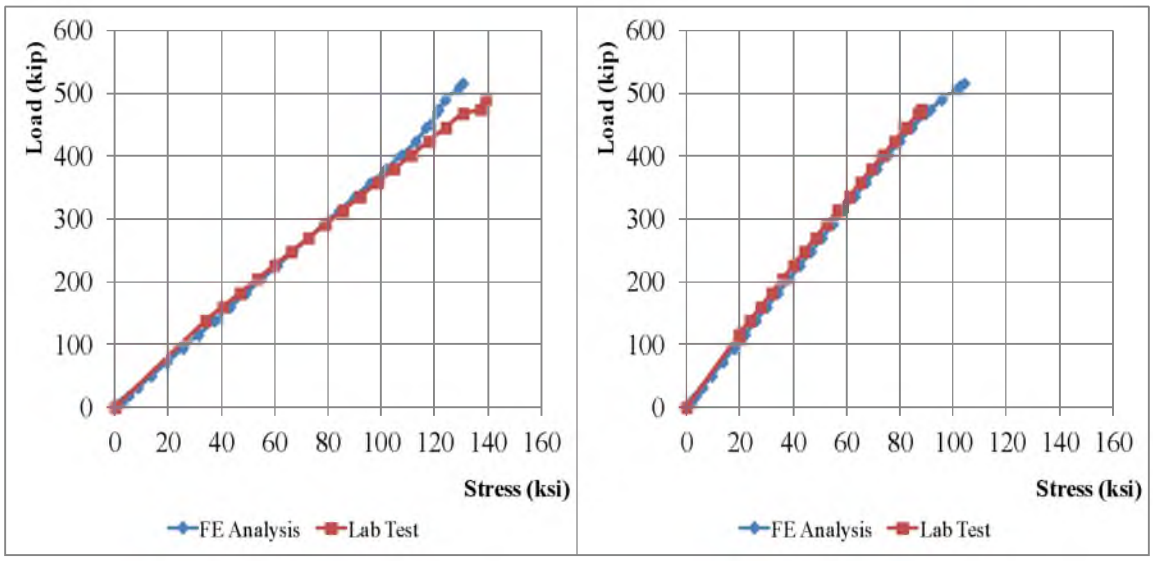

(a) (b)

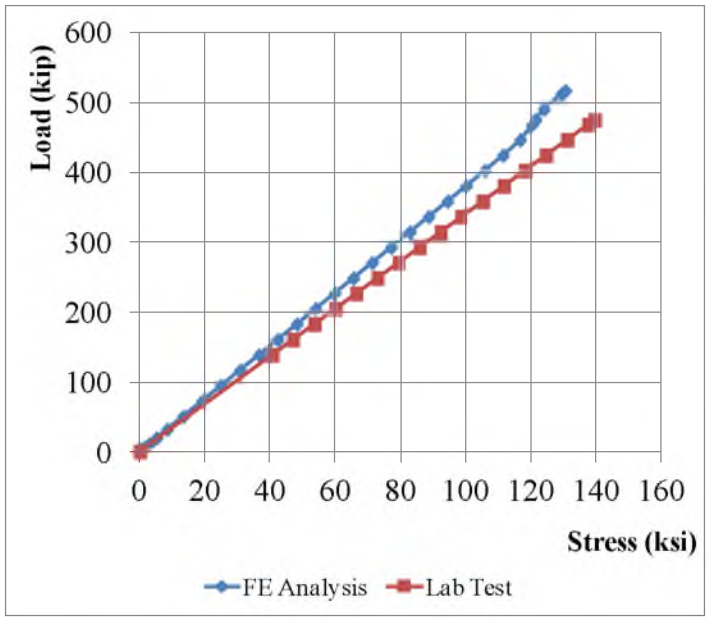

(c)

Fig 4.11: Load-Stress Curves from Lab Tests and FE Analysis at Failure Load (a) SG # 4; (b) SG # 8; (c) SG #17

4.3 Parametric Study

A parametric study was performed based on the model used for verification and validation, to find those parameters affecting the response of casted connectors. Geometry, material property, casting process and other parameters affect the response of such connectors. In this parametric study, material properties are considered. The parametric study is used to evaluate cases that are not viable during the experimental phase. The material properties investigated in this section are the modulus of elasticity, postyielding slope and yield stress.

4.3.1 Modulus of Elasticity (E)

For the first parametric study, three modulus of elasticity were considered: 29000 ksi, 30000 ksi and 32000 ksi. The tangential slope (postyielding slope) kept constant at 6% of initial slope (as obtained from the stress strain curve for the material, see Section 3.3). The stress-strain curve for each case was idealized as bilinear curve (Figure 4.12).

Ultimate failure load was compared for each case to evaluate if modifications to the modulus of elasticity would have a significant impact on the response of the connectors. Table 4.2 presents a comparison of each case for both connectors. The table shows that although the modulus of elasticity of the material has some effect on the response of the connectors, the impact is not as significant. The results for base case (which utilizes the full stress-strain curve for simulation) and 30000 ksi case (which idealizes the stress-strain curve as bilinear) show good agreement. It shows that idealization of the curve as bilinear does not alter the results significantly.

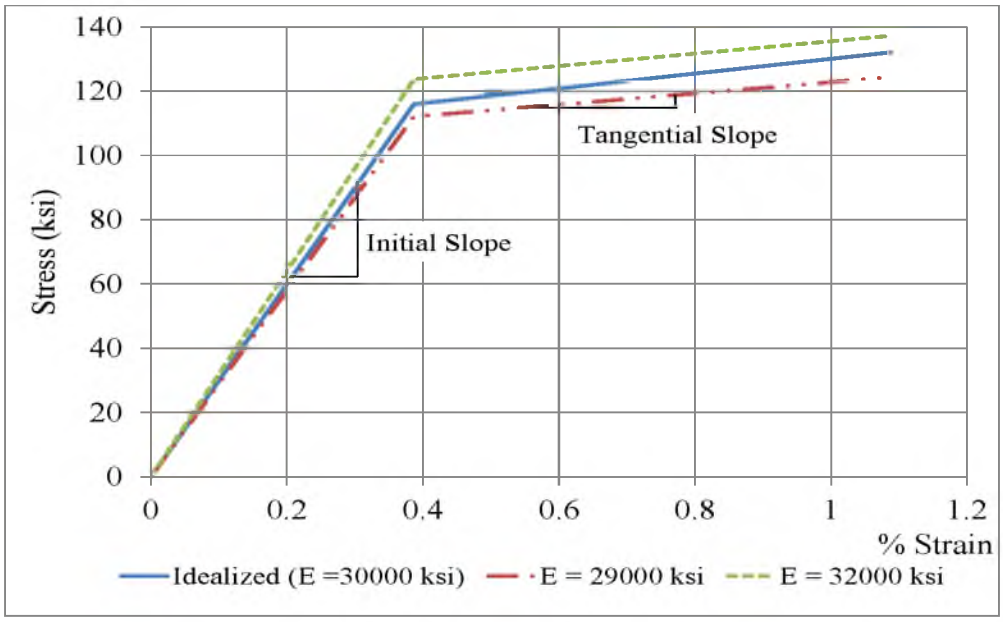

Fig 4.12: Idealized Bilinear Stress-Strain Curves

Table 4.2: Comparison of Failure Load for Different Modulus of Elasticity

Modulus of Elasticity E (ksi)	**Maximum Load at Failure (kip)**	
	Cast Connector 1	**Cast Connector 2**
Base Case*	1042.0	1035.4
29000	1024.4	1024.4
30000	1046.4	1035.4
32000	1093.5	1069.5

* Note: Base case refers to the simulation in which actual stress-strain curve was used.

Figure 4.13 presents load vs. stress curves for SG # 1 of Cast Connector 1, for three modulus of elasticity used for the study. Figure 4.14 shows similar comparison for SG # 4, 8 and 17 of Cast Connector 2. Figures 4.14 (a)-(b) and 4.15 show that there is a small effect on Cast Connector 2 as modulus of elasticity (E) changes; specifically when E changes from 30000 ksi to 32000 ksi. However, there is a small difference between the curves for 30000 ksi and 32000 ksi. One of the reasons for the small effect of change in E could be nonuniform change in stiffness or rigidity of different parts of the connectors.

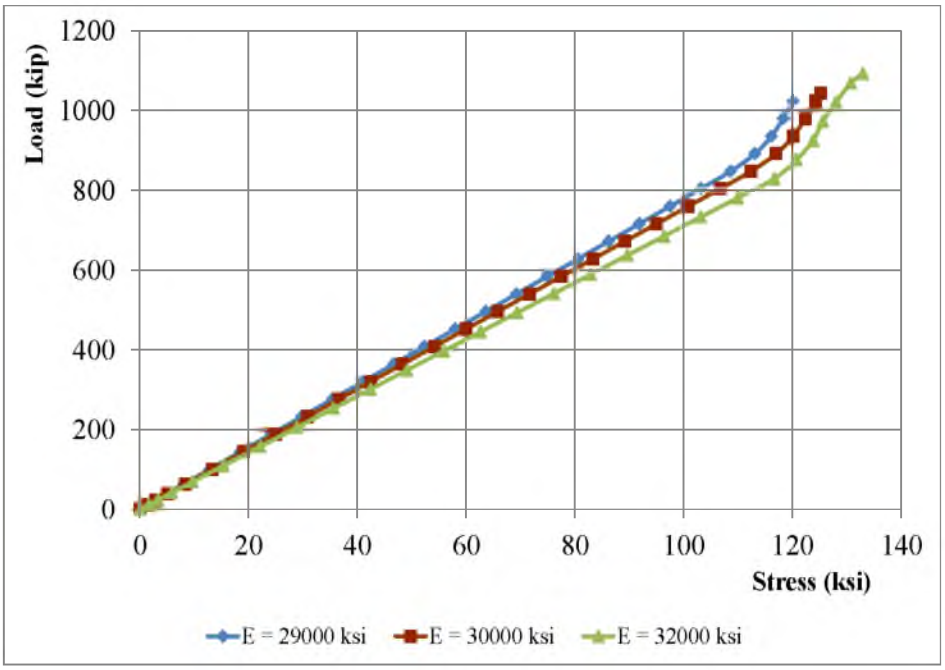

Fig 4.13: Load vs. Stress Curves for Three Different Modulus of Elasticity
(SG #1, Cast Connector 1)

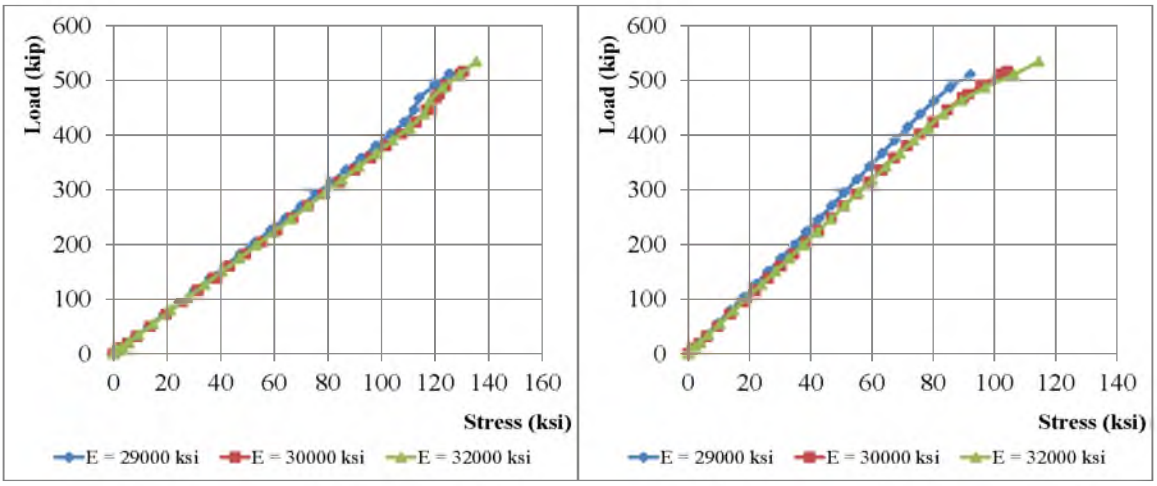

(a) (b)

Fig 4.14: Load vs. Stress Curves for Different Modulus of Elasticity (Cast Connector 2)
(a) SG #4; (b) SG # 8

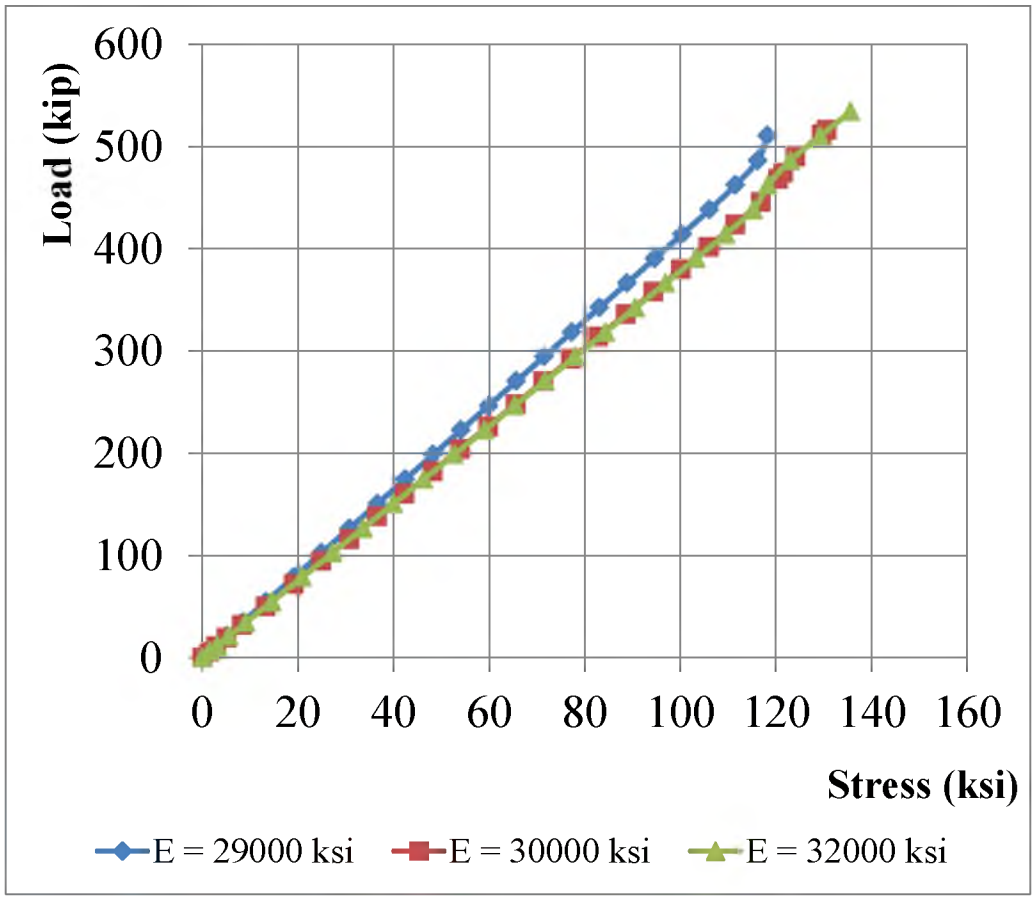

Fig 4.15: Load vs. Stress Curves for Different Modulus of Elasticity (Cast Connector 2) SG # 17

The legs of Cast Connector 2 are more flexible compared to its base and Cast Connector 1 due to the difference in geometry. Hence, the change in E has varying degree of effect on legs and other parts of the connector. Figure 4.16 shows the load vs. stress curves for the three modulus of elasticity for a location (A) away from the inner part of the legs, as shown in the figure. The figure shows that the effect of change in E is much greater for this location than that for locations shown in Figures 4.14 (a)-(b) and 4.15.

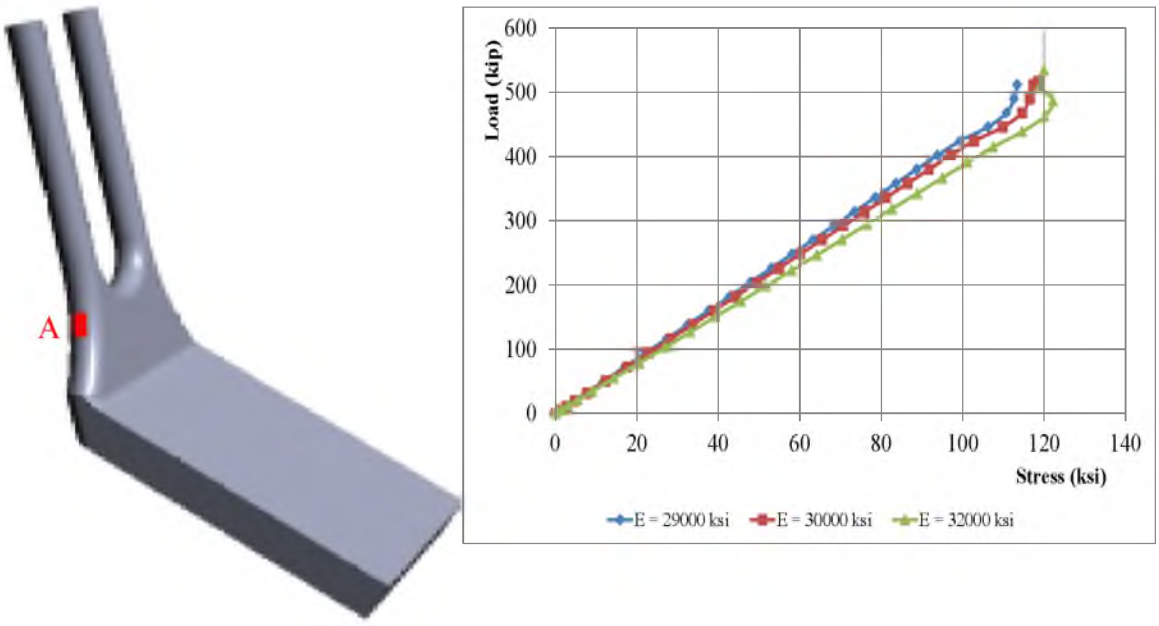

Fig 4.16: Location A (left); Load vs. Stress Curve for Location A (right)

4.3.2 Postyielding Slope

For the second parametric study, tangential slope (postyielding modulus) was changed keeping the initial modulus, yield stress and the ultimate strain constant. The stress strain curve is still idealized as bilinear curve. Figure 4.17 shows the curves used for this parametric study. The tangential slope was varied as 2%, 4%, 6%, 8% and 10% of the initial slope.

Ultimate failure load was chosen as the comparison criteria for this case also. Table 4.3 summarizes the findings from this parametric study. The results show that for tangential slope less than 6%, the effect on connectors' response is significant. However, for tangential slope greater than 6%, the response is affected but to a lesser degree.

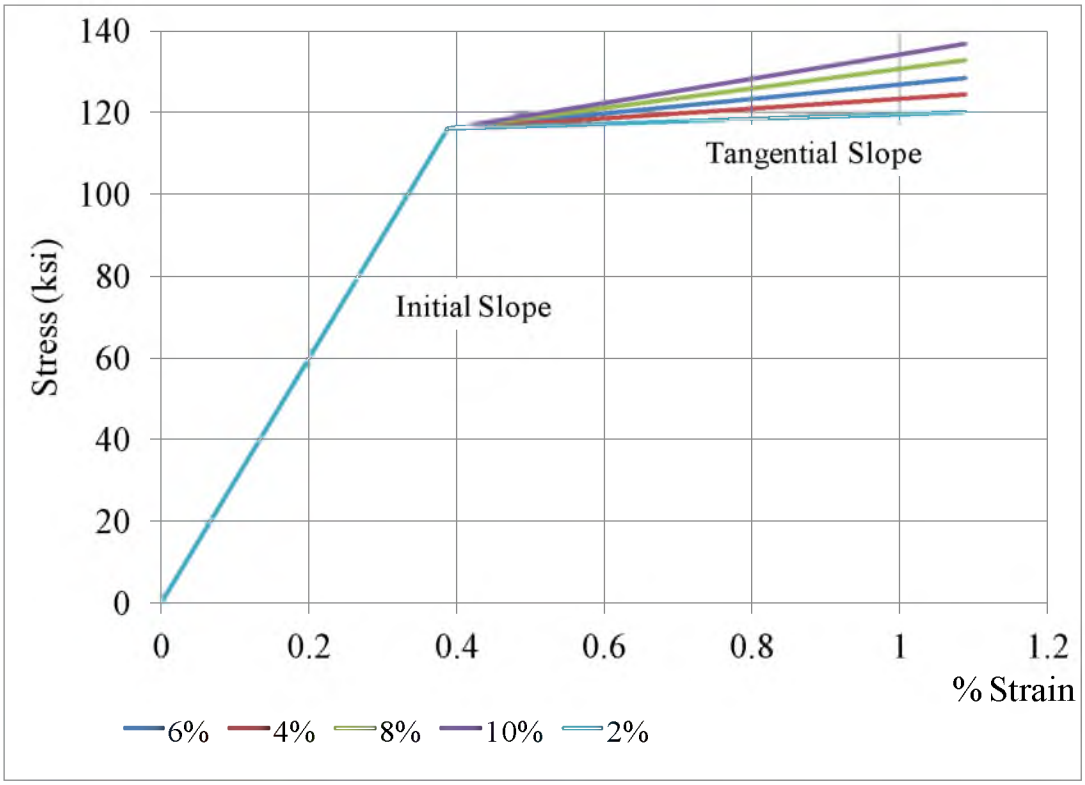

Fig 4.17: Idealized Stress-Strain Curves with Different Tangential Slopes.
(Initial Slope = 30,000 ksi)

Table 4.3: Comparison of Failure Load for Different Tangential Slopes

Tangential Slope	**Maximum Load at Failure (kip)**	
	Cast Connector 1	**Cast Connector 2**
2%	936.7	936.7
4%	980.4	980.4
6%	1046.4	1035.4
8%	1057.5	1047.5
10%	1083.5	1079.2

4.3.3 Yield Stress

Yield stress was the third parameter studied in this study. Yield stress of a material is one of the most varying parameters. Hess et al. (2002) and Mansour et al. (1993) investigated the variance of yield stress of high strength steels. They found the coefficient of variance (COV) for the yield stress to be 0.07-0.11.

Using the minimum COV, (i.e., 0.07), yield stress of the cast material was varied to see its effect on cast connectors' behavior. New yield stresses used for this study were $f_y \pm (\text{COV})\, f_y$. Yield stress for first case was taken as 107.88 ksi with corresponding ultimate strength of 124.23 ksi. Ultimate strength was computed from strain maintaining constant ductility. Second case refers to the case with the actual yield stress (116 ksi). Yield stress and ultimate stress for third case was 124.18 ksi and 143.09 ksi, respectively. Table 4.4 compares the ultimate load for each case for Cast Connectors 1 and 2. Table 4.4 shows a wider range of failure load compared to that for different modulus of elasticity and different postyielding slopes. It can be concluded that of the three parameters investigated in this study, yield stress has the largest influence.

These results show that material property selection affects the casted connector's performance. However, the effect is secondary to the influence of geometric configuration.

Table 4.4: Comparison of Failure Load for Different Yield Stress

Case	**New Yield Stress**	**Maximum Load at Failure (kip)**	
		Cast Connector 1	**Cast Connector 2**
I	$f_y - (\text{COV})\, f_y$	967.8	967.8
II	f_y	1042.0	1035.4
III	$f_y + (\text{COV})\, f_y$	1135.8	1104.95

CHAPTER 5

DISCUSSION

5.1 Evaluation of Laboratory Tests

The tests performed on cast connectors 1 and 2, show that the connectors are capable of sustaining the design load. The initial monotonic and cyclic tests on the connectors helped establish the high strength capability of the connector. The legs were identified as the critical sections of the connectors. Tensile loads of 688 kips (2.5P) and 709 kips (1.03× 2.5P) were supported by the connectors within linear regime. The study of additional tests on cast connector 2 indicated that under tensile loads as high as 848 kips (3.1P) the connectors behave linearly.

The overall connector's nonlinear performance was very close to expectations based on the material characteristics. The connectors exhibited large elastic capacity, but the stress-strain curve for the material (A148 GR. 115/95 (ASTM A958, 2006) show that the cast connector material is less ductile than other structural steels, a conclusion supported by the tests carried out to the failure limit state. Thus, the experimental tests performed in this study support the use of cast connectors to demand solicitations expected under wind loading conditions. Further tests are required prior to using cast

connectors under seismic demands. On the other hand, the cast connector's high strength results in a more efficient bracing system.

5.2 Evaluation of FE Analysis

FE analyses were performed to verify the experimental test results and to perform a parametric study. FE analysis techniques accurately predicted the stress distribution over the complex cast connectors' geometry.

FE analyses highlighted the complex stress distribution over the uneven geometry of the connectors, and showed good agreement with the findings from the experimental tests. The parametric study showed that effect of variation of the material properties is not as significant. Complex geometrical configuration of the connectors governs its overall response.

5.3 Limitations of the Study

The goals of the study are the cast connectors' performance evaluation subjected to quasi-static loading, and identification of the parameters most affecting their performance. Experimental tests performed and FE analyses results show that the connectors should perform satisfactorily for the application of design quasi-static load of 275 kips. Results of the parametric study show that the material properties affect the connectors' performance. However, the factors that affect the material properties have not been investigated in this study.

The results from experimental tests and FE analyses show that the elongation or the ultimate strain at failure was less than the ultimate strain of around 1.1%. The FE

analysis shows that at the most critical location the ultimate strain was 24.2% lower. This could be attributed to the **size effect** (effect of test-piece dimension). This means that the results, like the ultimate load capacity and ultimate strain, are limited to test specimens having dimensions similar to that of the tested connectors. Effect of test-piece dimension can be expressed by the Bertella-Oliver equation:

$$e = e_o(L/A^{1/2})^{-a}$$

where e_o is the specific elongation constant; $L/A^{1/2}$ is the slimness ratio of gage length (L) and cross-sectional area (A), a is another material constant. Graphical form of the Bertella-Oliver equation is shown in Figure 5.1.

The graph shows that the elongation decreases as the slimness ratio increases. This explains the reduction of strain for same stress as the dimension of cast connector was greater than the specimen used to obtain the stress-strain curve (which was 0.5 in. diameter). Also, the performance of the connectors is evaluated only for quasi-static load. Performance of such connectors under dynamic loads could render different conclusions.

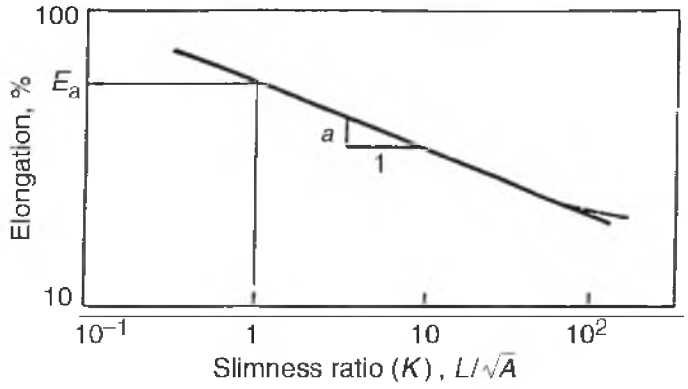

Fig 5.1: Graphical Form of the Bertella-Oliver Equaiton

CHAPTER 6

CONCLUSIONS AND RECOMMENDATIONS

6.1 Conclusions

This study addresses the performance of high strength alloy steel cast connectors under quasi-static tensile loading, as well as the parameters controlling the structural response. Tension tests were performed on both connectors, and FE simulations were used to validate the experimental results and predict stress distributions. The main findings are:

- The cast connectors are capable of withstanding the design load, P, of 275 kips. NYCBC requires connectors to be used in bracing systems to be able to safely support 2 and 2.5 times the design load. Tests revealed that both connectors met the requirement. The only test taken to failure had a safety factor of 3.5.
- Experimental tests show a failure load of 475 kip (for single leg test) for cast connector 2. FE analysis showed that to be 516.6 kip (single leg) for the same case, a difference of 8.8%. FE analysis for two legs loaded case showed that the failure load was about 1035.4 kips. Hence, for

experimental tests it would be expected to have an ultimate load of at least 950 kips.

- Although cast connector 1 was not tested up to failure, the FE analysis showed a maximum load of 1044 kips.
- Stress distributions in the connectors were largely governed by their complex geometric shapes. Apart from geometry, material properties also affect their response, but to a lesser degree.
- Brittle failure was observed for Cast Connector 2 at 3.5 times the design load. This brittle behavior appears to be triggered by the cast connector legs dimensions.

In conclusion, cast connectors under quasi-static load performed better than expected. The connector was able to support 846 kips, which is 3.07 times more than the design load (P = 275 kips) and 1.23 times more than 2.5P, while still exhibiting elastic behavior. Hence, using such connectors in bracing systems, subjected to lateral loads like wind load, is justified provided that the connection designed to perform within linear range for expected loading.

6.2 Recommendations

It is recommended for future research to perform a more detailed exploration into factors affecting the material properties supplemented by sufficient laboratory tests and testing the connectors under dynamic or seismic load.

Because of the limited number of laboratory tests, it was difficult to create a complete picture of factors affecting the material properties and performance of such

connectors. Further research is necessary to fully investigate and understand the extent of impact these factors have on the connectors' responses. Some considerations could be taken towards improving the ductility of the material, such as, altering the heat treatment and cooling rate of the material.

This study involved evaluation of performance of cast connectors under quasi-static load. As the cast connectors are a part of lateral bracing system, it is of interest to understand the performance of the connectors under dynamic or seismic loading. These experimental tests are needed to determine the feasibility of high strength connectors in seismic regions.

APPENDIX A

ANALYSIS OF DIFFERENT STRUCTURAL COMPONENTS

The subassembly and its different components, including the connections, were analyzed using SAP 2000. The structural components strength capacity and deflection limits were evaluated for a maximum load 2.5P = 688 kips. The subassembly had to safely sustain the applied loads. Deflection of the subassembly also had to be checked as there was small (3/8 in.) clearance between the subassembly and the load frame.

The top assembly plate (i.e., the plate connecting the steel rods and the actuator) was also analyzed. A simplistic finite element model was prepared in SAP 2000 to check if the plate was capable of transferring the load safely.

A.1 Analysis and Check for the Subassembly

The subassembly designed for the tests was analyzed in SAP 2000 to verify the demand capacity ratio of each element, deflection of the entire subassembly, and connection design (Figures A.1, A.2 and A.3). The joint reactions, axial force and shear force on each member are presented in Figures A.4, A.5 and A.6, respectively.

Fig A.1: Frame Label and Load Assignment

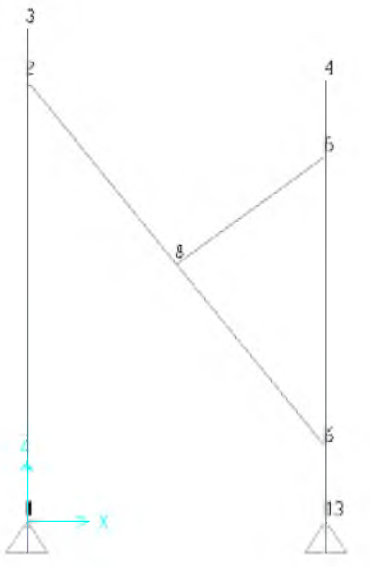

Fig A.2: Joint Assignment

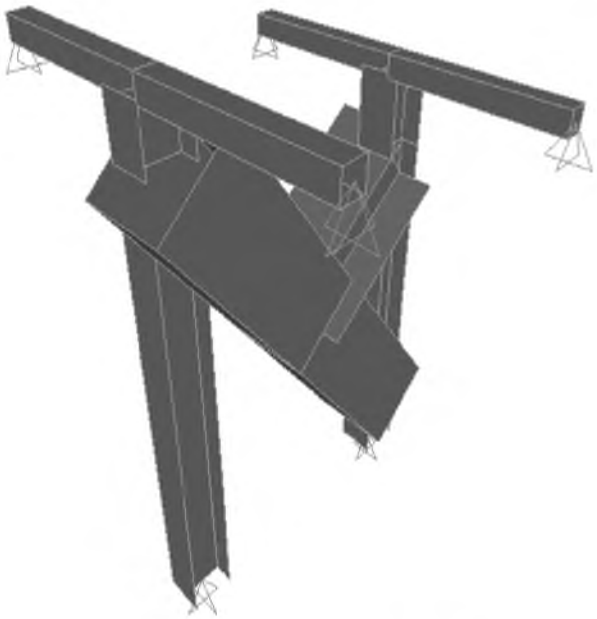

Fig A.3: Extruded View of the Subassembly Modeled in SAP 2000

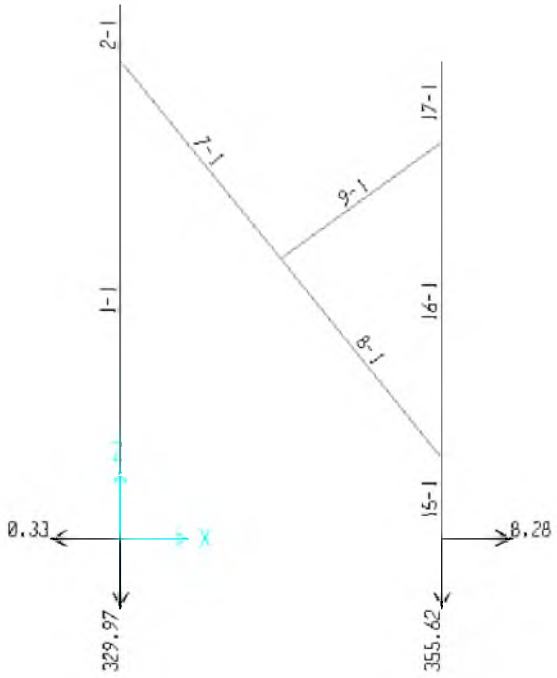

Fig A.4: Joint Reactions (Force in kips)

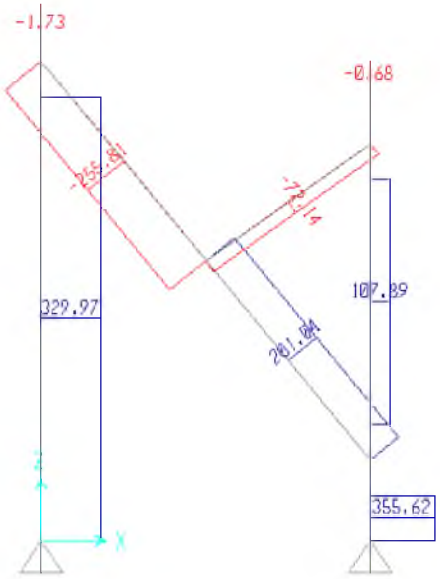

Fig A.5: Axial Force on the Members
(Force in kips)

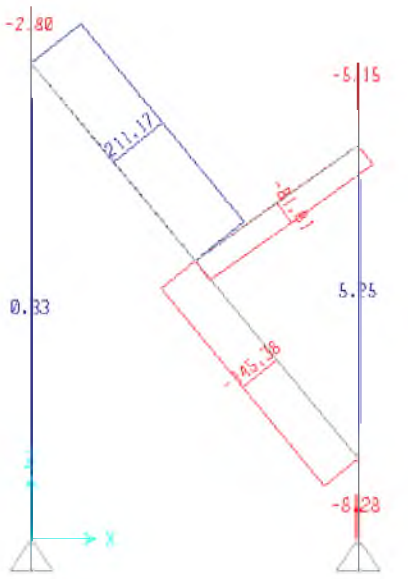

Fig A.6: Shear Force on the Members
(Force in kips)

Table A.1 shows that demand/capacity ratios of all members are less than unity for a tensile applied load of 688 kips. Along with the members, all the joint connections were designed in accordance with AISC design code (Part 7, 8, 9 and 10).

The analysis was also used to verify that the deflection of the subassembly did not exceed the clearance of the load frame and the subassembly. Table A.2 presents the deflection of all the joints. U1, U2 and U3 represent the deflection in X, Y and Z direction, respectively. Deflection of joint number 5 along X direction (U1 in the table) was the most crucial one as its deflection had to be smaller than the clearance of 3/8 in.

A.2 Analysis of Top Assembly Plate

A steel plate was used to tie the rods connecting the cast connectors to the actuator. Force was applied to the rod and ultimately to the connector via this plate. The top plate was modeled in SAP 2000 under the expected loading conditions.

Table A.1: Demand/Capacity Ratio of Each Member of the Subassembly for a Load of 688 kips

TABLE: Steel Design 1-Summary Data-AISC-LRFD93				
Frame	**Design Sect**	**Design Type**	**Status**	**Ratio**
1	W8X58	Column	No Messages	0.699171
2	W8X58	Column	No Messages	0.037151
7	Col 18	Brace	No Messages	0.807028
8	Col 18	Brace	No Messages	0.558839
9	W14X211	Brace	No Messages	0.315086
11	4x4	Beam	No Messages	0.707654
12	4x4	Beam	No Messages	0.707654
13	4x4	Beam	No Messages	0.548118
14	4x4	Beam	No Messages	0.548118
15	W8X58	Column	No Messages	0.772691
16	W8X58	Column	No Messages	0.296337
17	W8X58	Column	No Messages	0.068452

Table A.2: Joint Displacements

Joint	**OutputCase**	**CaseType**	**U1**	**U2**	**U3**
Text	Text	Text	in	in	in
1	live	LinStatic	0	0	0
2	live	LinStatic	0.07961	0	0.05383
3	live	LinStatic	0.08723	0	0.05380
4	live	LinStatic	0.16073	0	0.02135
5	live	LinStatic	0.13843	0	0.02137
6	live	LinStatic	0.02347	0	0.00975
8	live	LinStatic	0.09996	0	0.07674
9	live	LinStatic	0	0	0
10	live	LinStatic	0	0	0
11	live	LinStatic	0	0	0
12	live	LinStatic	0	0	0
13	live	LinStatic	0	0	0

A 3 in. plate was reinforced with 1 in. central plate at the top and bottom to withstand the maximum tensile force of 2.5P. To reduce load concentration around bolt holes, 1 in. thick washers were used to distribute the load on the plate.

Figure A.7 and Figure A.8 show the FEM model in SAP 2000 and von Mises stress contour for the top plate. The central green portion in Figure A.7 is the 1 in. thick reinforcement plate welded on top and bottom of the 3 in. thick plate (represented in blue). The green elements at the sides and the yellow elements at the center of the plate represent the washers. Load was applied on the two central washers.

A.3 Connection Design Check

Calculations were made to find out capacity of each connection. Connections at joints numbered 1, 2, 5, 6, 8 and 13 (refer Figure A.2) were investigated. Calculations showed that the capacity of connections were as follows

- Joint 1 and 13: 557 kip (each),
- Joint 8 (welded connection): 664 kip
- Joint 2 and 6 : 329 kip (each)
- Joint 5 (bolted connection, with prying considered): 338 kip

The capacity of each connection was greater than the forces acting on these connections shown in Figures A.5 and A.6. Sample calculations for finding out the capacity of some connections are provided. All the calculations, presented in sample calculations, are based on AISC Steel Construction Manual.

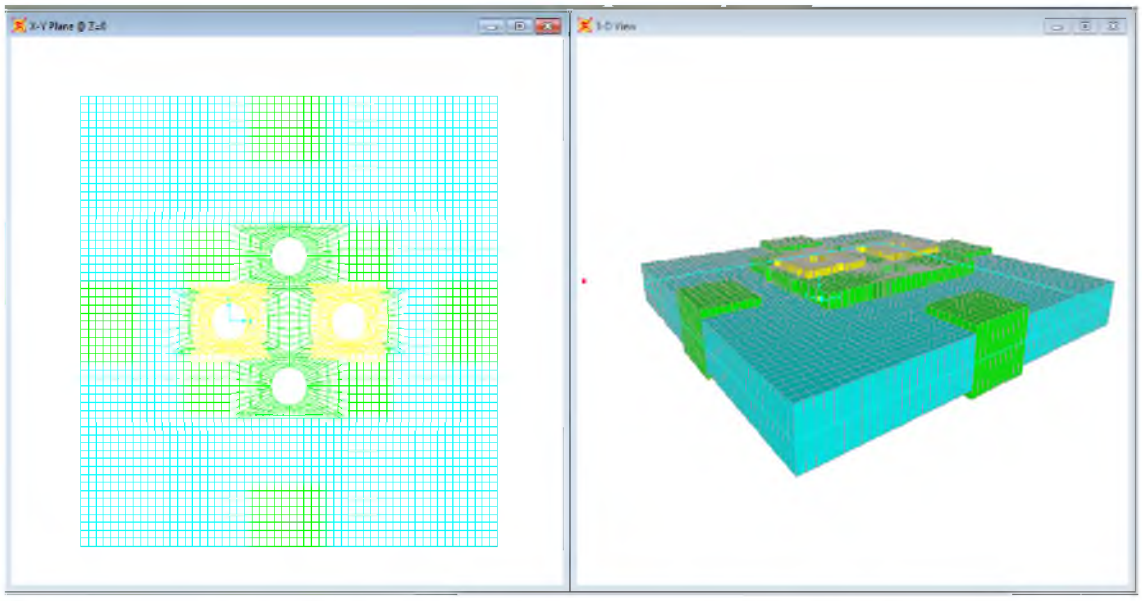

Fig A.7: Finite Element of Top Assembly Plate in SAP 2000

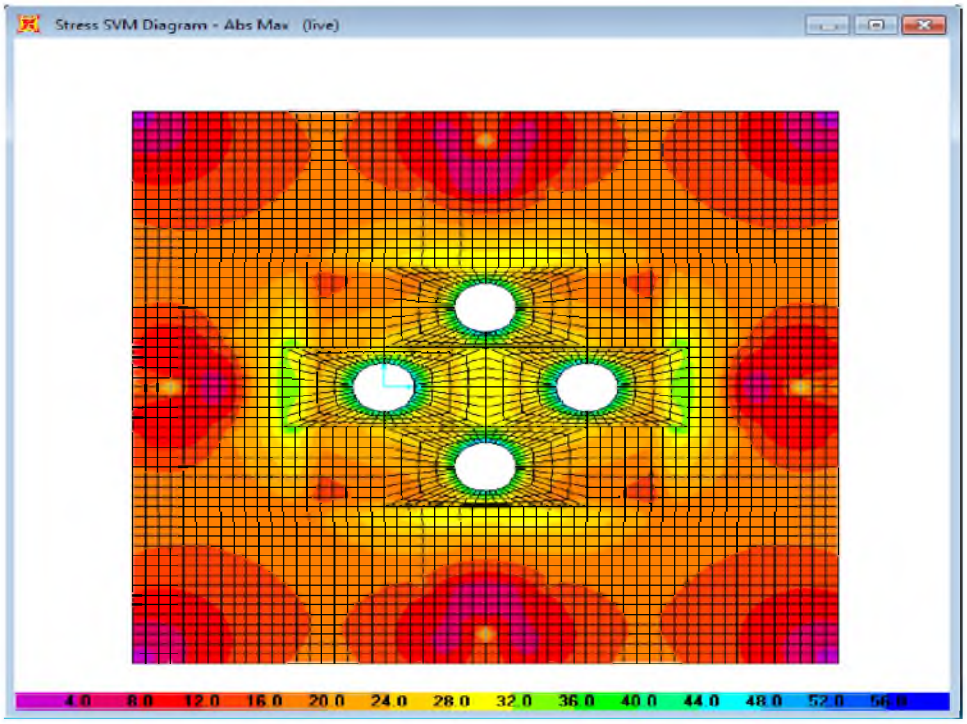

Fig A.8: von Mises Stress Distribution Contour

A.3.1 Sample Calculations

A.3.1.1 Joints 1 and 13

Connections given by joint number 1 and 13 each have two separate connections with six-1 ¼ in. diameter bolts arranged in two columns separated by 8 in. spacing. Each separate connection is subjected to eccentric shear force. The capacity of these connections can be found out by "Instantaneous Center of Rotation Method" (ICR method) described in part 7 of the AISC Steel Construction Manual. Table A.3 provides the calculations for finding the capacity of a connection.

The table shows that capacity of each six bolt connection is 278.5 kip. Hence, the capacity of joint 1 and 13 is equal to twice the capacity of a single six bolt connection (= 557 kip). This capacity is greater than the force acting on these connections.

Table A.3: Calculations of Joint Capacity using ICR Method

For A 325 X type bolt 1 1/4"

Instantaneous Center Distance (E) = 2.5364 in. Shear strength of bolts ϕr_n = 62.7 kips

Spacing of columns= 8 in.

Distance of load from last bolt line (Lp) = 7 in. moment arm : 9.536 in

Bolt No	x_i	y_i	L_i	r_i	$r_i/\varphi r_n$	$(X_i/L_i)*(r_i/\varphi_{r\,n})$	$L_i(r_i/\varphi_{rn})$	r_y (Reaction)
1	2.54	4	4.74	34.41	0.86	0.461	4.07	18.42
2	10.54	4	11.27	39.26	0.98	0.918	11.06	36.70
3	2.54	0	2.54	28.35	0.71	0.709	1.80	28.35
4	10.54	0	10.54	39.08	0.98	0.977	10.29	39.08
5	2.54	4	4.74	34.41	0.86	0.461	4.07	18.42
6	10.54	4	11.27	39.26	0.98	0.918	11.06	36.70
				Pu allowable =		278.5	kips	

A.3.1.2 Joint 2 and 6

Joint 2 and 6 each, have two-five bolt connections as shown in Figure A.9. They are concentrically loaded in shear and tension. The computations for finding out the capacity of the connection are presented in the following.

A.3.1.2.1 Members Properties

A 572 Gr. 50

F_y = 50 ksi, F_u = 65 ksi

Thickness of plate (t) = 3/8”

a = 2 ¾” ≤ 3.5” (OK)

L_{eh} = 2*d = 2(1) = 2” < 2¼” (OK)

n < 6

A.3.1.2.2 Shear Strength

φ_{rn} = 40 kips (p. 7-22 of AISC manual)

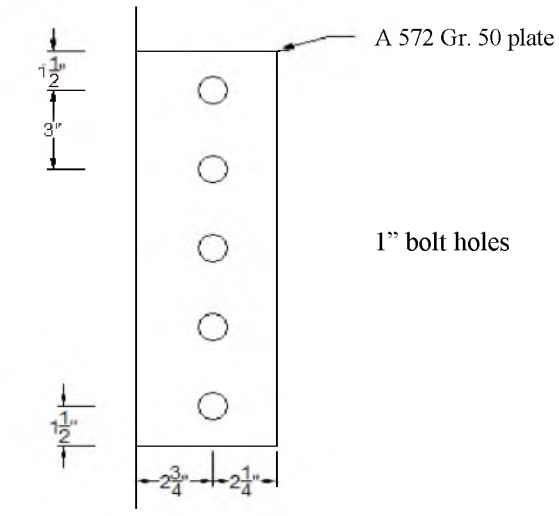

Fig A.9: Connection Detail of Joint 2 and 6

Shear deformation, $\varphi_{rn} = 0.75\ (2.4)\ d\ t\ F_u$

$= 0.75\ (2.4)\ (1)\ (3/8)\ 65 = 43.88$ kip

Tear out:

$\varphi R_n = 0.75\ (1.2)\ L_c\ t\ F_u = 0.75\ (1.2)\ (1.5 - 17/32)\ (3/8)\ 65$

$= 26.57$ kip

Tear trough:

$\varphi_{rn} = 0.75\ (1.2)\ (3\text{-}17/16)\ (3/8)\ 65 = 42.5$ kip

Therefore, $\varphi R_n = 4*40 + 26.57 = 186.57$ kip

A.3.1.2.3 Weld Strength

$w_{min} = 1/4$" but, w = 5/16" (OK)

$100*w = 100\ (5/16) = 31.25 > (3 \times 5 + 2 \times 1½) = 18$ in.

therefore, $L_e = 18$ in.

$\varphi R_n = 0.75\ (0.6)\ Fe_{XX}\ t_e\ L_e = 0.75\ (0.6)\ (70)\ (0.707)\ (5/16)\ 2\ (18)$

$= 250.54$ kip

A.3.1.2.4 Shear Yield on Plate

$\varphi R_n = 0.6\ A_g\ F_y = 0.6\ (18)\ (3/8)\ 50 = 202.5$ kip

A.3.1.2.5 Shear Fracture (Rupture) on Plate

$\varphi R_n = 0.75\ (0.6)\ [15\text{-}5(1 + 1/8)]\ 3/8\ (65) = 102.83$ kip

A.3.1.2.6 Block Shear of Plate

φR_n = 123.4 kip

A.3.1.2.7 Plate Bending

φR_n =0.9 F_y S/(2¾) = 0.9 (50) (3/8) $(15)^2$ /(6 * 2.75) = 127.84 kip > 102.83 kip

hence, V_u = 102.83 kip

Therefore, $P_u = V_u/\cos(39)$ = 164.75kip

2 x P_u = 329 kip

Similar calculations can be done for the strength of connection in tension. However, the tensile strength is more than the shear strength, hence the shear strength governs. Hence, capacity of the joint = **329 kips.**

APPENDIX B

STRAIN RATE COMPUTATION

Table B.1: Strain Rate Calculation for Cast Connector 1

Cast Connector I

LVDT L_0 = 13.25 in.

Monotonic

Load	Load rate	Time	LVDT 2			LVDT 3			SG 10	SG 11	Avg	Rate
(kip)	(kip/min)	(min)	Deflection	Strain	rate (in/in/min)	Deflection	Strain	rate (in/in/min)	(in/in)	(in/in)	(in/in)	(in/in/min)
137.5	5	27.5	0.0062	0.0005	1.688E-05	0.0064	0.0005	1.756E-05	0.00075	0.00059	0.00067	2.427E-05
275.0	4	34.4	0.0108	0.0008	1.028E-05	0.0115	0.0009	1.124E-05	0.00136	0.00111	0.00124	1.660E-05
412.5	4	34.4	0.0181	0.0014	1.601E-05	0.0184	0.0014	1.508E-05	0.00228	0.00181	0.00204	2.343E-05
550.0	3	45.8	0.0225	0.0017	7.278E-06	0.0230	0.0017	7.591E-06	0.00291	0.00219	0.00255	1.111E-05

Cyclic

Load	Load rate	Time	LVDT 2			LVDT 3			SG 10	SG 11	Avg	Rate
(kip)	(kip/min)	(min)	Deflection	Strain	rate (in/in/min)	Deflection	Strain	rate (in/in/min)	(in/in)	(in/in)	(in/in)	(in/in/min)
137.5	30	4.6		0	0.000E+00	0.00841	0.00063	1.385E-04	0.00063	0.000726	0.00068	1.479E-04
275.0	30	4.6		0	0.000E+00	0.01411	0.00106	9.386E-05	0.00135	0.001319	0.00133	1.432E-04
412.5	30	4.6		0	0.000E+00	0.02007	0.00151	9.814E-05	0.002088	0.001903	0.002	1.442E-04
550.0	10	9.1		0	0.000E+00	0.02574	0.00194	4.694E-05	0.002834	0.002484	0.00266	7.278E-05
688.0	10	13.8		0	0.000E+00	0.03005	0.00227	2.357E-05	0.003794	0.003102	0.00345	5.717E-05

*Note: LVDT 2 was not used in cyclic test.

Table B.2: Strain Rate Calculation for Cast Connector 2 (Monotonic Test)

Cast Connector II

LVDT L_0 = 19.375 in.

Monotonic

Load (kip)	Load rate (kip/min)	Time (min)	LVDT 2 Deflection	Strain	rate (in/in/min)	LVDT 3 Deflection	Strain	rate (in/in/min)
137.5	5	27.5	0.00862	0.000445	1.618E-05	0.00733	0.00038	1.376E-05
275.0	4	34.4	0.01175	0.000606	4.700E-06	0.01060	0.00055	4.910E-06
412.5	4	34.4	0.01480	0.000764	4.579E-06	0.01430	0.00074	5.555E-06
550.0	3	45.8	0.01863	0.000962	4.313E-06	0.02037	0.00105	6.835E-06
557.0	3	2.3	0.01911	0.000986	1.062E-05	0.02076	0.00107	8.627E-06

Load (kip)	SG 1 (in/in)	SG 2 (in/in)	SG 3 (in/in)	Avg (in/in)	Rate (in/in/min)	SG 4 (in/in)	SG 5 (in/in)	SG 6 (in/in)	Avg (in/in)	Rate (in/in/min)
137.5	0.00079	0.000522	0.000802	0.000705	2.565E-05	0.000815	0.00044	0.000494	0.0005843	2.125E-05
275.0	0.00133	0.001217	0.001277	0.001276	1.659E-05	0.001465	0.00111	0.000839	0.0011377	1.610E-05
412.5	0.00185	0.001885	0.001759	0.001832	1.618E-05	0.002146	0.00177	0.001196	0.0017023	1.643E-05
550.0	0.0024	0.002509	0.002209	0.002371	1.177E-05	0.002917	0.00243	0.001567	0.0023053	1.316E-05
557.0	0.00246	0.002602	0.002281	0.002447	3.257E-05	0.002997	0.00252	0.001618	0.0023777	3.100E-05

Table B.3: Strain Rate Calculation for Cast Connector 2 (Cyclic Test)

Cyclic

Load	Load rate	Time	LVDT 2			LVDT 3		
(kip)	(kip/min)	(min)	Deflection	Strain	rate (in/in/min)	Deflection	Strain	rate (in/in/min)
137.5	30	4.6		0	0.000E+00	0.00875	0.00045	9.853E-05
275.0	30	4.6		0	0.000E+00	0.01198	0.00062	3.637E-05
412.5	30	4.6		0	0.000E+00	0.01608	0.00083	4.617E-05
550.0	10	9.1		0	0.000E+00	0.02040	0.00105	2.446E-05
557.0	10	0.7		0	0.000E+00	0.02098	0.00108	4.276E-05
688.0	10	13.1		0	0.000E+00	0.02537	0.00131	1.730E-05
709.0	10	2.1		0	0.000E+00	0.02617	0.00135	1.966E-05

*Note: LVDT 2 was not used in cyclic test.

Load	SG 1	SG 2	SG 3	Avg	Rate	SG 4	SG 5	SG 6	Avg	Rate
(kip)	(in/in)	(in/in)	(in/in)	(in/in)	(in/in/min)	(in/in)	(in/in)	(in/in)	(in/in)	(in/in/min)
137.5	0.00071	0.00047	0.00070	0.00063	1.372E-04	0.00086	0.00048	0.00047	0.00060	1.316E-04
275.0	0.00124	0.00116	0.00119	0.00120	1.237E-04	0.00152	0.00114	0.00082	0.00116	1.212E-04
412.5	0.00176	0.00182	0.00172	0.00177	1.246E-04	0.00217	0.00178	0.00119	0.00172	1.214E-04
550.0	0.0023	0.00249	0.00230	0.00236	6.556E-05	0.00284	0.00242	0.00161	0.00229	6.329E-05
557.0	0.00237	0.00257	0.00237	0.00244	1.024E-04	0.00292	0.00250	0.00166	0.00236	9.762E-05
688.0	0.00282	0.00315	0.00288	0.00295	3.916E-05	0.00350	0.00304	0.00205	0.00287	3.852E-05
709.0	0.00289	0.00325	0.00297	0.00304	4.206E-05	0.00360	0.00314	0.00212	0.00295	4.190E-05

APPENDIX C

NORTH STAR CASTEEL REPORT

NORTH STAR CASTEEL

STEEL CAST CONNECTIONS LLC

Customer:	2658 Walnut Ave SW Seattle WA 98116
Date:	March 20, 2012
Re PO #:	

Parts:

Number:	Type:	Date
2	SCC-WBF4VE	03/20/2012

	Heat #	Heat #	Heat #	Heat #	Heat #	Specification
	20781	20781				ASTM A958 8620 115/95
Julian #	**04921**	04922				
Carbon	0.203	0.203				0.18 – 0.23 %
Silicon	0.55	0.55				0.30 – 0.60 %
Manganese	0.81	0.81				0.60 – 1.00 %
Sulfur	0.005	0.005				0.04 % max
Phosphorous	0.01	0.01				0.035 % Max
Chromium	0.486	0.486				0.40 – 0.60 %
Nickel	0.496	0.496				0.40 – 0.70 %
Molybdenum	0.198	0.198				0.15 -0.20 %

Tensile Strength	130.8	130.8	115 KSI Minimum
Yield Strength	115.2	115.2	95 KSI Minimum
Elongation	16	16	14 % Minimum
Reduction of Area	43	43	30 % Minimum

	Heat #	Heat #	Heat #	Heat #	Heat #	Specification
	20781	20781				A-370
Ft-Lbs	47.0	47.0				-20F
	42.0	42.0				Average 35 Ft-Lbs
Ft-Lbs	42.0	42.0				
Average	43.5	43.6				

Certified By: Laurer Ridgdon

Metallurgist

820 South Bradford Street•Seattle, Washington 98108
Phone 206/622•0068 • Fax 206/622•0115

NORTH STAR CASTEEL

STEEL CAST CONNECTIONS LLC

Customer:	2658 Walnut Ave SW Seattle WA 98116
Date:	March 20, 2012
Re PO #:	

Parts:

Number:	Type:	Date
1	SCC-WBF5HE	03/20/2012

	Heat #	Heat #	Heat #	Heat #	Heat #	Specification
	20795					ASTM A958 8620 115/95
Julian #	**05321**					
Carbon	0.225					0.18 – 0.23 %
Silicon	0.38					0.30 – 0.60 %
Manganese	0.72					0.60 – 1.00 %
Sulfur	0.007					0.04 % max
Phosphorous	0.01					0.035 % Max
Chromium	0.58					0.40 – 0.60 %
Nickel	0.54					0.40 – 0.70 %
Molybdenum	0.20					0.15 -0.20 %

Tensile Strength	137.3	115 KSI Minimum
Yield Strength	121.8	95 KSI Minimum
Elongation	15	14 % Minimum
Reduction of Area	45	30 % Minimum

	Heat #	Heat #	Heat #	Heat #	Heat #	Specification
	20795					A-370
Ft-Lbs	40					-20F
	44					Average 35 Ft-Lbs
Ft-Lbs	41					
Average	40.5					

Certified By: Xavier Delgado R

Metallurgist

820 South Bradford Street•Seattle, Washington 98108
Phone 206/622•0068 • Fax 206/622•0115

APPENDIX D

LVDT AND STRAIN GAGE CHARACTERISTICS

LVDTs:

No. 1: LVDT located between the actuator plate and the subassembly's top plates.

Model: MVL7C Range: ± 0.500 inch

Part No: 060-5654-01

S/N: L6931600

No. 2: (On the cast connector, behind the visible side)

Model: MVL7C Range: ± 0.500 inch

Part No: 060-5654-01

S/N: L6931200

No. 3: (On the cast connector, visible side)

Model: MVL7C Range: ± 0.500 inch

Part No: 060-5654-01

S/N: L6931300

No. 4: (for the lateral deflection of entire assembly)

Model: MVL7C Range: ± 0.500 inch

Part No: 060-5654-01

S/N: L6931800

No. 5: (bottom of the frame)

Model: MVL7C Range: ± 0.500 inch

Part No: 060-5654-01

S/N: L6931500

Strain Gages

	Grid Resistance in Ohms	TC of Gage Factor, % / 100°C
	350.0 ± 0.3%	(+1.3 ± 0.2)
Grid	Gage Factor @ 24°C	Transverse Sensitivity
1	2.120 ± 0.5%	+0.1 ± 0.2%

Calculation of Thermal Output for Strain Gages:

$a_0 + a_1*T + a_2*T^2 + a_3*T^3 + a_4*T^4$

where, a_0, a_1,.... a_4 are coefficients as given below and T^N is temperature raised to the power N.

Order	Fahrenheit	Celsius
0	-2.26 E+2	-8.83 E+1
1	+5.46 E+0	+5.84 E+0
2	-3.87 E-2	-9.91 E-2
3	+8.80 E-5	+4.71 E-4
4	-5.62 E-8	-5.90 E-7

Foil Lot Number	Batch Number
A65AD853	CF531872
Item Code	**Code**
3204	223113

REFERENCES

ABAQUS/CAE 6 version 12.2 [computer software]; 3D Simulia Dassault Systèmes: Waltham, Massachusetts, 2012.

SolidWorks [computer software]; 3D Simulia Dassault Systèmes: Waltham, Massachusetts, 2012.

American Institute of Steel Construction. Part 7, 8, 9 and 10. In *Steel Construction Manual* (14th ed.): Chicago, Illinois, 2011.

ANSYS version 14.5 [computer software]; ANSYS, Inc.: Canonsburg, Pennsylvania, 2012.

ASM International. *Tensile Testing* (2nd ed.); Davis, J.R., Eds.; ASM International: Materials Park, Ohio, 2004.

American Society for Testing Materials. *A370-05 Standard Test Methods and Definitions for Mechanical Testing of Steel Products*; ASTM International: West Conshohocken, Pennsylvania, 2006.

American Society for Testing Materials. *A958-00 Standard Specification for Steel Castings, Carbon and Alloy, with Tensile Requirements, Chemical Requirements Similar to Standard Wrought Grades*; ASTM International: West Conshohocken, Pennsylvania, 2006.

American Society for Testing Materials. *A488/A488M-06 Standard Practice for Steel Castings, Welding, Qualifications of Procedures and Personnel*; ASTM International: West Conshohocken, Pennsylvania, 2006.

Bao, W.; Xing, W.; Qiu, J. The Use of Cast Steel in Steel Structure. *Advanced Material Research*. 2011, 183-185.

Bjorhovde, R. Performance and Design Issues for High Strength Steel in Structures. *Advances in Structural Engineering*. 2010, Vol. 13, No. 3.

Brockenbrough, R.L.; Merritt, F.S. (2006). Properties of Structural Steels and Effects of Steelmaking and Fabrication. In *Structural Steel Designer's Handbook: AISC, AASHTO, AISI, ASTM, AREMA, and ASCE-07Design Standards* (4th ed.); McGraw-Hill: New York, 1999; pp 1.1-1.40.

Chen, Y.Y.; Zhao, X.Z.; Tong, L.W. Research and Application of Connections of Structural Steel Casting. *Advances in Structural Engineering*. 2010, Vol. 13 No. 3.

Coelho, A.M.G.; Bijlaard, F. High Strength Steel in Buildings and Civil Engineering Structures: Design of Connections. *Advances in Structural Engineering*. 2010, Vol. 13, No. 3.

SAP2000 version 14.1.0 [computer software]; Computers and Structures, Inc.: Berkeley, California, 2009.

Edlund L. In *Coefficients of Variation for the Yield Strength of Steel*, 2nd Colloquium on Stability of Steel Structures, Liege, Belgium, 1977.

Hess, P.E.; Barchman, D.; Assakkaf, I.A.; Ayyub, B.M. Uncertainties in Material Strength, Geometric, and Load Variables. *Naval Engineers Journal*. 2002, Vol. 114, Issue 2.

Krawinkler, H; Parisi, F.; Ibarra L.; Ayoub, A; Medina, R. Development of a Testing Protocol for Woodframe Structures. In *The CUREE-Caltech Woodframe Project*; CUREE Publication: Richmond, CA, 2001; W-02.

Mansour, A. E.; Lin, M.; Hovem, L; Thayamballi, A. Probability-based ShipDesign Procedures; A Demonstration. In *SSC-368*. U.S. Coast Guard: Washington, DC, 1993.

Monroe, R; and Poweleit, D. Scraping the Sky with Steel Castings. *Engineered Casting Solutions*. 2004, Vol. 6, Issue 2.

NYC Buildings. Structural Tests and Special Inspections. In *New York City Building Code*, NYC Buildings: New York, 2012; Chapter 17. http://www.nyc.gov/html/dob/downloads/pdf/cc_chapter17.pdf.

Oliveira, J.-C. de; Gray, M.G.; Packer, J. A.; Christopoulos, C. In *Standardized Cast Steel Connectors for Tubular Hollow Structural Sections*, Proceedings of the CSCE Annual Conference, Quebec, Canada, 2008.

RPBW. In *Typical Truss Details 3. S-432.00*; Renzo Piano Building Workshop: Genova, Italy, 2010.

Tectonic Engineering. In *Procedure for Testing Notch Bracing Casting Connection Assembly*; Rev. 2011: Long Island City, New York, 2011.